


UNIVERSITY OF
BIRMINGHAM

# ALTERNATIVE FUELS AND AFTERTREATMENT SYSTEMS FOR LOW EMISSIONS ENGINES

by

**OMID DOUSTDAR**

A thesis submitted to
The University of Birmingham
for the degree of

**DOCTOR OF PHILOSOPHY**

Department of Mechanical Engineering
The University of Birmingham
May 2019

UNIVERSITY OF
BIRMINGHAM

## University of Birmingham Research Archive

### e-theses repository

This unpublished thesis/dissertation is copyright of the author and/or third parties. The intellectual property rights of the author or third parties in respect of this work are as defined by The Copyright Designs and Patents Act 1988 or as modified by any successor legislation.

Any use made of information contained in this thesis/dissertation must be in accordance with that legislation and must be properly acknowledged. Further distribution or reproduction in any format is prohibited without the permission of the copyright holder.

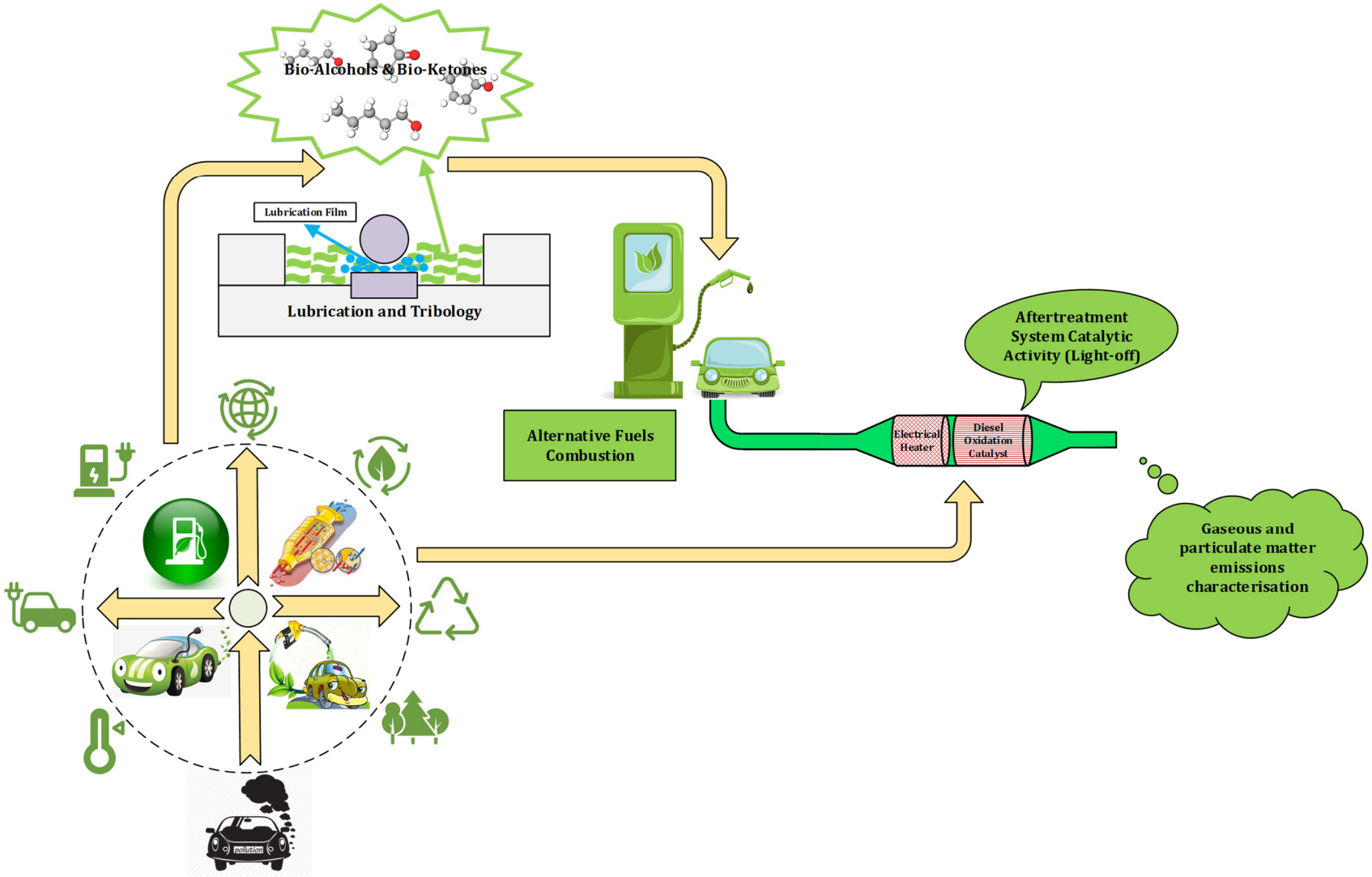
# ABSTRACT

This research provides an understanding of the synergies between the combustion of bio-oxygenated fuels and thermal management of the aftertreatment systems for the control of diesel gaseous and particulate matter emissions.

Blends of diesel with bio-alcohols and a bio-ketone with different molecular structure including butanol, pentanol, cyclopentanol and cyclopentanone proved to be promising alternative fuels in terms of energy density, viscosity, lubricity, tribological mechanisms, combustion behaviour and emissions reduction. Using bio-oxygenated fuels with a higher polarity (mainly cyclic compounds) resulted in lower wear scar size by up to 38%, compared to the diesel baseline, during the lubricity test. Engine-out hydrocarbons and particulate matter emissions were lower by up to 37% and 91%, respectively. The modified exhaust gas composition from the combustion of the aforementioned oxygenated fuel blends, improved the catalyst oxidation reactions, and light-off was achieved at lower exhaust gas temperatures.

Furthermore, an active control strategy of heating the aftertreatment system was studied. Due to reduced catalyst light-off temperature when using the alternative fuels for combustion, e.g. by up to 26 °C for CO, a lower heater energy input was required for the catalytic light-off when compared to diesel combustion only. Importantly, modifying the exhaust gas composition of the diesel baseline by adding 500 ppm of $H_2$ gas upstream of the catalyst decreased the CO light-off temperature by approximately 50 °C.

# GRAPHICAL ABSTRACT



*Dedicated to my beloved family*

*Raziyeh, Akbar and Amir*

# ACKNOWLEDGEMENTS

I would like to gratefully acknowledge all the people who helped me during my PhD. Firstly, I would like to express my sincerest gratitude towards my lead supervisor, Professor Athanasios (Thanos) Tsolakis, for his invaluable supervision, technical comments and generous support. He welcomed me to his highly equipped ''Future Fuel and Engine'' laboratory. My co-supervisor, Professor Miroslaw Lech (Mirek) Wyszynski is greatly acknowledged for his endless support, as a father, during my undergraduate and PhD, which cannot be described by words. I would like also to thank my PhD progress internal assessor, Dr Karl Dearn for all scientific comments.

I would like to especially thank Dr Jose Martin Herreros for his kind support and for monitoring my progress and providing constructive comments during my PhD. I will never forget his encouragement even during experiments in the lab. Notably, Dr Soheil Zeraati Rezaei is acknowledged as a colleague, mentor, advisor and my close friend. His endless kind support and guidance are greatly appreciated. He has always motivated me and was cooperative in different stages of this research.

I would like to thank my best close friend during PhD, Dr Hessam Jahangiri, for all of his endless supports, helps and advices. He always motivated me and providing me welcoming social environment. Special appreciation to all my friends, particularly, Dr Hamid Mahmoudi for encouraging me to do PhD and Dr Mohammadreza Hamedi not only for his scientific support but also providing me friendly social environment.

I would like to thank my colleagues, Dr Hadi Nozari, Dr Maria Bogarra Macias, Dr Manju Tanwar, Dr Mohammed Fayad, Dr Vahid Nasrollahi, Mr Jun Chan, Mr Sak Sittichompoo, Mr Ammar Wahbi, Dr Ali Al Qahtani, Mr Lewis Parry, Dr Yasser Al Qahtani

and Mr Aawishkar Dharmadhikari, for their help and support during these years. Thanks also go to technicians at the University, Mr Jack Garrod, Mr Kevan Charlesworth, Mr Peter Thornton and Mr Lee Gauntlett for their help in manufacturing new test facilities. Also, Special thanks to Birmingham Automobile Division Centre of IMechE committee members, particularly, Professor Clive Neal-Sturgess and Mr Fred Walker.

Many thanks to undergraduate students in Mechanical Engineering from Year 2015 to 2019, especially, Mr David Childs, Miss Susan Fraser, Mr Harry Bennell, Mr Barnaby Hawthorn, Mr Abdul Ifham, Miss Gabrielle Chester, Miss Laura Green, Mr Matthew Woodward, and Miss Jaymisha Panchal for their help and encouragement during my PhD.

Thanks to the University of Birmingham and European Union's Horizon 2020-research and innovation programme (grant agreement No 691232-Knocky-H2020-MSCA-RISE-2015) for the PhD scholarship and financial support. Also, special appreciation to EPSRC for funding FACE project (Ref: EP/P03117X/1) which supported part of this research. Many thanks to Dr Reinhard Tatschl from AVL Graz, Austria for providing the AVL software tools within the frame of the AVL-UoB Partnership Program and to DI Christian Roelver and Dr Ivo Pah for their continuous support and technical exchange opportunity on all related topics.

I would like to thank all my friends, especially Dr Ata Jalili, Mr Amir Rabet Ghannadi, Dr Siavash Esfahani, Dr Mohsen Moslemin, Dr Saber Mousavi, Mr Behrouz Sadri, Dr Sahand Faraji, Dr Farzad Shokrollahi, Dr Shahriar Parisouz, Mr Saadat Zeraati Rezaei, Dr Yasin Kabiri, Dr Mahdi Jelodari, Mr Arash Izadpanah, Dr Hassan Vafamehr, Dr Salman Rouhanifar, and Mr Riyaz Aziz from Al-Dar Co. in Dubai.

Many sincere thanks also go to my uncle, Mostafa, for his unconditional supports and helps during my undergraduate and PhD studies. He provides me a welcoming warm social environment during my stay in UK, far from my family in IRAN.

Finally and most importantly, I would like to thank my mother and father, Raziyeh and Akbar, for their unconditional love, patience and support. Very special thanks to my brother, Amir, for his unconditional support during my studies which cannot be described by words. This appreciation also include my beloved grandmother whom I lost during the course of this PhD, may she rest in peace.

This thesis was proofread for conventions of language, spelling and grammar by "Janet's Proofreading Service".

Omid Doustdar

May 2019

# TABLE OF CONTENTS

**CHAPTER 1. INTRODUCTION ..... 1**

1.1. Overview ..... 1

1.2. Research Aim and Objectives ..... 5

1.3. Contributions to the New Knowledge ..... 6

1.4. Thesis Outline ..... 7

**CHAPTER 2. LITERATURE REVIEW ..... 10**

2.1. Emissions from Road Transport ..... 10

2.2. Diesel Engines ..... 12

2.3. Alternative Fuels ..... 13

2.3.1. Alternative Fuel Properties and Behaviour in Engines ..... 16

2.3.2. Alcohols ..... 20

2.3.3. Ketones ..... 25

2.4. The Way Forward to Sustainable Transport ..... 26

2.5. Diesel Exhaust Gas Aftertreatment Technologies ..... 27

2.6. Summary ..... 30

**CHAPTER 3. METHODOLOGY ..... 32**

3.1. Fuel Characterisation ..... 32

3.1.1. Kinematic Viscosity ..... 35

3.1.2. Surface Tension ..... 36

3.1.3. Calorific Value ..... 37

3.2. Analysis of Lubrication Mechanisms ..... 37

3.3. Engine Test Bed and Instrumentation ..... 44

3.3.1. Engine Laboratory ..... 44

3.3.2. Single Cylinder Research Diesel Engine ..... 46

3.3.3. Aftertreatment System and Instrumentation ..... 50

3.3.4. Emission Analysers ..... 53

3.4. Experimental Errors and Repeatablity ..... 55

3.5. Summary ..... 56

**CHAPTER 4. INVESTIGATION OF LUBRICATION PROPERTIES AND TRIBOLOGICAL BEHAVIOUR OF BIO-ALCOHOLS AND BIO-KETONES ..... 57**

4.1. Introduction ..... 57

4.2. Fuel Properties ..... 58

4.3. Lubricating Properties of Alternative Fuels ..... 64

4.3.1. Wear Resistance of Alternative Fuels ..... 66

4.3.2. Wear and Lubrication Mechanisms ..... 70

4.3.3. Surface Topography ..... 76

4.4. Summary ..... 79

**CHAPTER 5. IMPACT OF ALTERNATIVE FUELS ON COMBUSTION, GASEOUS AND PARTICULATE MATTER EMISSIONS' CHARACTERISTICS ..... 81**

5.1. Introduction ..... 81

5.2. Results and Discussion ..... 82

5.2.1. Combustion Analysis ..... 82

5.2.2. Gaseous Emissions ..... 85

5.2.2.1. THC Emissions ..... 85

5.2.2.2. CO and $CO_2$ Emissions ..... 88

5.2.2.3. $NO_x$ Emissions ..... 90

5.2.3. Particulate Matter ..... 92

5.3. Summary ..... 95

**CHAPTER 6. ENHANCING THE LOW TEMPERATURE ACTIVITY OF DIESEL OXIDATION CATALYST BY USING ELECTRICAL HEATING AND ALTERNATIVE FUELS 98**

6.1. Introduction ..... 98

6.2. Results and Discussion ..... 100

6.2.1. Impact of Alternative Fuels' Combustion on the DOC's Catalytic Activity. 100

6.2.2. Effects of Alternative Fuels' Combustion on DOC Light-off ..... 103

6.2.2.1. CO Conversion in the DOC ..... 103

6.2.2.2. THC Conversion in the DOC ..... 109

6.2.2.3. NO to $NO_2$ Oxidation in the DOC ..... 112

6.2.3. Interaction between Efficient Heating Strategy and DOC Activity ..... 117

6.2.4. Effects of Alternative Fuels' Combustion and an Efficiently Heated DOC on Particulate Matter ..... 120

6.3. Summary ..... 127

**CHAPTER 7. CONCLUSIONS ..... 128**

7.1. Investigation of Lubrication Properties and Tribological Behaviour of Bio-alcohols and Bio-ketones ..... 129

7.2. Impact of Alternative Fuels on Combustion, Gaseous and Particulate Matter Emissions' Characteristics ..... 130

7.3. Enhancing the Low Temperature Activity of a Diesel Oxidation Catalyst by Using Electrical Heating and Alternative Fuels ..... 131

7.4. Concluding Remarks ..... 132

7.5. Future Work ..... 132

**References ..... 134**

# LIST OF FIGURES

Figure 1-1: Thesis outline ..... 7

Figure 2-1: The evolution of transport energy (modified) [2] ..... 10

Figure 2-2: Alternative fuels performance and emissions ..... 17

Figure 2-3: Distribution on energy losses produced from vehicles (modified) [45] 18

Figure 3-1: Molecular structure of the neat tested fuels ..... 33

Figure 3-2: The Sita T15 surface tension meter method [109] ..... 36

Figure 3-3: The HFRR experimental set-up ..... 38

Figure 3-4: The HFRR acceptable test condition (ISO 12156 -1) [111] ..... 40

Figure 3-5: The example of a wear scar (ISO 12156-1) ..... 42

Figure 3-6: Methodology for Lubrication and tribology experiments ..... 44

Figure 3-7: The engine laboratory ..... 45

Figure 3-8: Single cylinder research diesel engine test bed ..... 46

Figure 3-9: Experimental set-up diagram ..... 47

Figure 3-10: Aftertreatment reactor set-up ..... 52

Figure 4-1: Density of fuels ..... 61

Figure 4-2: Surface tension of fuels ..... 62

Figure 4-3: Viscosity of fuels ..... 62

Figure 4-4: Lower heating value of fuels ..... 63

Figure 4-5: Friction coefficient of tested fuels and their blends with diesel ..... 65

Figure 4-6: Wear scar diameter of tested fuels and their blends with diesel ..... 67

Figure 4-7: SEM and topography micrographs of disc tested in different fuels ..... 74

Figure 4-8: Wear scar depth of tested fuels and their blends with diesel ..... 77

Figure 4-9: Surface roughness of tested fuels and their blends with diesel ..... 78

Figure 5-1: In-cylinder pressure and heat release rate ..... 83

Figure 5-2: Total hydrocarbon emissions at 2 bar IMEP and 4 bar IMEP ..... 86

Figure 5-3: Hydrocarbon emissions' speciation ..... 87

Figure 5-4: Carbon monoxide emissions at 2 bar IMEP and 4 bar IMEP ..... 89

Figure 5-5: Carbon dioxide emissions at 2 bar IMEP and 4 bar IMEP ..... 89

Figure 5-6: Nitrogen oxides' emissions at 2 bar IMEP and 4 bar IMEP ..... 91

Figure 5-7: Particle size distribution at (a) 2 bar IMEP; (b) 4 bar IMEP ..... 93

Figure 6-1: Heater OFF-Gaseous emissions' concentration at 2 bar IMEP, bDOC and aDOC ..... 101

Figure 6-2: Heater OFF-Gaseous emissions' concentration at 4 bar IMEP, bDOC and aDOC ..... 102

Figure 6-3: Change of aDOC composition in D100L during light-off test ..... 105

Figure 6-4: Change of aDOC composition in D100L+$H_2$ during light-off test ..... 105

Figure 6-5: Change of aDOC composition in B20L during light-off test ..... 106

Figure 6-6: Change of aDOC composition in P20L during light-off test ..... 106

Figure 6-7: Change of aDOC composition in CP20L during light-off test ..... 107

Figure 6-8: Change of aDOC composition in CPK20L during light-off test ..... 107

Figure 6-9: CO light-off of the DOC from alternative fuels' combustion ..... 108

Figure 6-10: THC light-off of the DOC from alternative fuels' combustion ..... 111

Figure 6-11: DOC inlet temperature required for 25%, 50%, 75% and maximum conversion ..... 112

Figure 6-12: $NO_2/NO_x$ ratio in light-off study of alternative fuels' combustion ..... 113

Figure 6-13: $N_2O$ production over the DOC in the exhaust of alternative fuels' combustion ..... 116

Figure 6-14: Heater ON-Gaseous emissions' concentration at 2 bar IMEP, bDOC and aDOC ..... 118
Figure 6-15: Heater ON-Gaseous emissions' concentration at 4 bar IMEP, bDOC and aDOC ..... 119
Figure 6-16: Heater OFF-particle size distribution in bDOC and aDOC at 2 bar IMEP ..... 122
Figure 6-17: Heater OFF-particle size distribution in bDOC and aDOC at 4 bar IMEP ..... 123
Figure 6-18: Heater ON-Particle size distribution in bDOC and aDOC at 2 bar IMEP ..... 124
Figure 6-19: Heater ON-particle size distribution in bDOC and aDOC at 4 bar IMEP ..... 125

# LIST OF TABLES

Table 2-1: EU's emissions' standards for category M1 passenger cars ..... 12

Table 3-1: The HFRR technical data ..... 38

Table 3-2: HFRR ISO 12156-1 test condition ..... 41

Table 3-3: Test engine specifications ..... 47

Table 3-4: Engine test conditions abbreviations and colour codes ..... 50

Table 3-5: Random error experiment to monitor repeatability ..... 56

Table 4-1: Physical and chemical properties of neat tested fuels ..... 59

Table 4-2: Properties of 20%vol blending of fuels ..... 60

Table 4-3: Properties of 40%vol blending of fuels ..... 60

Table 4-4: Properties of gasoline-diesel blends ..... 60

Table 5-1: Summarised combustion analysis for test conditions ..... 82

Table 5-2: Particle size distribution for tested fuels ..... 92

Table 6-1: Engine and aftertreatment operating conditions ..... 99

Table 6-2: Effects of the DOC on particle size distribution for tested fuels ..... 126

# LIST OF NOTATIONS

| Symbol | Unit | Description |
|---|---|---|
| $C_p$ | J/(kg.K) | Specific heat capacity at constant pressure |
| $C_v$ | J/(kg.K) | Specific heat capacity at constant volume |
| $L$ | J/kg | Latent heat |
| $m$ | | Mass fraction |
| $\dot{m}_{Fuel}$ | kg/s | Mass flow rate of the fuel |
| $nm$ | | Nano meter |
| $p$ | Pa | Pressure |
| $P_{Ind}$ | kW | Indicated power of the engine |
| $Q_n$ | $MJ.kg^{-1}$ | Net heat of combustion |
| $Q_g$ | $MJ.kg^{-1}$ | Gross heat of combustion |
| $t$ | s | Time |
| $T$ | K | Temperature |
| $v$ | m/s | Velocity |
| V | $m^3$ | Volume |
| $v_f$ | | Volume fraction |
| $\mu m$ | | Micro meter |
| $\gamma$ | | Ratio of specific heat |
| $\theta$ | deg | Crank angle |
| $\lambda$ | | Specific (relative) air-fuel ratio |
| $\rho$ | $kg/m^3$ | Density |

# LIST OF ABBREVIATIONS

| | |
|---|---|
| AC | Alternating current |
| aDOC | After Diesel Oxidation Catalyst |
| $Al_2O_3$ | Alumina |
| AP | Accumulation mode Particles |
| ASTM | American Society for Testing and Materials Standard |
| AVP | Absolute vapour pressure |
| B | Butanol |
| bDOC | Before Diesel Oxidation Catalyst |
| C | Atomic carbon |
| CFD | Computational fluid dynamics |
| CFPP | Cold filter plugging point |
| $CH_2O$ | Formaldehyde |
| $CH_3OH$ | Methanol |
| $CH_3CHO$ | Acetaldehyde |
| $CH_4$ | Methane |
| $C_2H_2$ | Acetylene |
| $C_2H_4$ | Ethylene |
| $C_2H_5OH$ | Ethanol |
| $C_2H_6$ | Ethane |
| $C_3H_6$ | Propylene |
| $C_3H_7OH$ | Propanol |
| $C_3H_8$ | Propane |
| $C_4H_9OH$ | Butanol |
| $C_5H_{11}OH$ | Pentanol |

| | |
|---|---|
| CI | Compression ignition |
| CO | Carbon monoxide |
| $CO_2$ | Carbon dioxide |
| COV | Coefficient of variation |
| CP | Cyclopentanol |
| CPK | Cyclopentanone |
| cpsi | Cells per square inch |
| CRT | Continuously regenerating trap |
| DOC | Diesel oxidation catalyst |
| DPF | Diesel particulate filter |
| DR | Dilution Ratio |
| EDS | Energy dispersive spectrometer |
| EGR | Exhaust gas recirculation |
| EHC | Electrically heated catalyst |
| EN | European Standards |
| EU | European Union |
| FTIR | Fourier transform infrared |
| GHSV | Gas hourly space velocity |
| H | Atomic hydrogen |
| $H_2$ | Hydrogen |
| $H_2O$ | Water |
| HC | Hydrocarbon |
| HCF | Humidity correction factor |
| HEPA | High efficiency particle arrestance |
| HEV | Hybrid electric vehicles |
| HFRR | High Frequency Reciprocating Rig |
| HHV | Higher heating value |

| | |
|---|---|
| HRR | Heat release rate |
| IC | Internal combustion |
| IMEP | Indicated mean effective pressure |
| IEA | International Energy Agency |
| ISFC | Indicated specific fuel consumption |
| ISO | International Standard Organization |
| ITE | Indicated thermal efficiency |
| LHV | Lower heating value |
| LNT | Lean $NO_x$ trap |
| Mil | Milli-inch |
| MNC | Maximum number concentration |
| MND | Median diameter |
| MWSD | Mean wear scar diameter |
| $N_2$ | Nitrogen |
| $N_2O$ | Nitrous oxide |
| NCR | $NO_x$ storage reduction catalyst |
| NEDC | New European driving cycle |
| $NH_3$ | Ammonia |
| NMHC | Non-methane hydrocarbons |
| NO | Nitric oxide |
| $NO_2$ | Nitrogen dioxide |
| $NO_x$ | Nitrogen oxides |
| NP | Nucleation mode Particles |
| O | Atomic oxygen |
| $O_2$ | Oxygen |
| OH | Hydroxyl radicals |
| Pd | Palladium |

| | |
|---|---|
| PCM | Phase change material |
| PGM | Platinum-group metals |
| PM | Particulate matter |
| PN | Particulate number |
| ppm | Parts per million |
| Pt | Platinum |
| PTFE | Polytetrafluoroethylene, Teflon |
| RH | Relative humidity |
| Rh | Rhodium |
| RPM | Revolutions per minute |
| SCR | Selective catalytic reduction |
| SEM | Scanning electronic microscope |
| SI | Spark ignition |
| SMPS | Scanning Mobility Particle Sizer |
| $SO_2$ | Sulphur dioxide |
| SOC | Start of combustion |
| SOF | Soluble organic fraction |
| SOI | Start of injection |
| TDC | Top dead centre |
| TES | Thermal energy storage |
| THC | Total hydrocarbons |
| $TiO_2$ | Titanium dioxide |
| TNC | Total number concentration |
| TWC | Three-way catalyst |
| USV | Ultra Shear Viscometer |
| ULSD | Ultra-low sulphur diesel |

# CHAPTER 1. INTRODUCTION

## 1.1. Overview

The impact of emissions from conventional road vehicles on the environment and human health has led to the introduction of stringent emissions legislations, such as the EUROs in the European Union. Various technologies have been developed for reducing fuel consumption, gaseous (including $CO_2$) and particulate matter emissions. Optimised engine calibration, alternative fuels, aftertreatment systems and vehicle electrification are some of these technologies.

Currently, there are around 1.2 billion passenger cars and 380 million commercial vehicles in the world and these numbers are increasing daily; so it is essential to investigate the possibilities to reduce their emissions [1]. These cars are mostly running with liquid fuels due to their high energy density and ease of transport and storage. Based on the predictions, even by 2040 around 90% of transport energy will come from liquid petroleum fuels powering internal combustion engines [2-5]. Any alternatives to the internal combustion engines such as battery electric vehicles or hydrogen fuel cell vehicles can be significantly expensive and also environmentally damaging, if challenges associated with their primary energy source and battery production process are not completely or partially decarbonized and toxicity effects associated with the battery supply are not properly addressed [2]. The demand for batteries to be used in electric and hybrid vehicles is increasing rapidly. These battery vehicles are not necessarily zero-emission vehicles as sometimes the emissions point is just shifted from roads to somewhere else. Electricity generators on a large scale produce more particulates, $NO_x$

and $SO_2$ than conventional automotive engines. Also, environmental problems associated to mining of the metals needed for batteries is another issue in battery production [2]. So, the greenhouse gas emissions impact of electric vehicles batteries can be worse than that of internal combustion engines depending on the method of manufacturing and application [2].

As a short/medium term plan, using alternative fuels such as biofuels, natural gas and hydrogen can be a potential solution. It seems that to mitigate emissions and their environmental impacts, the efficient integration of alternative fuels, aftertreatment systems and propulsion systems (including electrified powertrains) is one of the feasible solutions [2].

One of the objectives of this research is to investigate alternative diesel fuels that can be produced from renewable sources. Bio-alcohols and a bio-ketone as oxygenated fuels such as, butanol, pentanol, cyclopentanol and cyclopentanone seems promising alternative replacements for conventional fuels in compression ignition engines. Their favourable and close physico-chemical properties to conventional fuels and adequate blending stability, higher energy density and high cetane number of them compared to common bio-alcohols (e.g. ethanol) prove their advantages for further investigations. The presence of these fuels as blend with diesel can affect the lubrication and tribological mechanisms. The performance of fuel injection component is dependent on the tribological performance of tested fuels lubricity. Differences in molecular structure and composition of fuels lead to differences in fuel lubricity and tribology results. Longer carbon chain length of chosen bio-alcohols and bio-ketones show advantages in properties compared to well-known bio-alcohols such as ethanol.

Also, this research aims at improving the combustion process in compression ignition engines by the use of these alternative fuels, in order to reduce emissions that have a harmful environmental impact on public health. The efficiency and performance of the engine by using these fuels are studied. In addition, gaseous and particle emissions need to be removed from exhaust gas by using different technologies. Currently, there are various aftertreatment systems for diesel engines, which include a combination of a diesel oxidation catalyst (DOC), selective catalytic reduction (SCR) and diesel particulate filter (DPF). All of these systems are used in the engines to reduce carbon monoxide (CO), total hydrocarbon (THC), nitrogen oxides ($NO_x$) and particulate matter (PM).

In the aftertreatment system, catalysts reduce the required activation energy for the chemical reactions of emissions conversion, which affects oxidation and reduction of emissions in the vehicle's exhaust gas. The temperature inside catalytic aftertreatment systems is a key parameter of the efficiency of the emissions' conversion process. Also, engine's cold-start, where the exhaust gas temperature is low to activate the catalytic emissions' conversion reactions, is a very challenging stage for investigation of improving conversion efficiency. In addition to gaseous emissions, particulate matter is harmful, with a risk of causing cancer. The effect of new alternative fuels on particles' emissions needs to be considered to fulfil the legislation requirements.

In the automotive industry, engines with higher fuel economy and lower emissions are in demand to fulfil customers' requests and legislative emissions' requirements. Turbocharging, fuel injection strategies, and exhaust gas recirculation are some of the technologies for improving an engine's efficiency. Some of these technologies will decrease the available thermal energy inside the exhaust aftertreatment systems. There are some other reasons for dropping an engine's exhaust gas temperature, such as

running vehicles with low engine loads which will deteriorate the aftertreatment catalyst activity. Thus, it is very important to provide higher thermal energy and temperature to increase the aftertreatment systems' temperature and hence efficiency.

Catalytic aftertreatment systems mitigate gaseous and particulate emissions from internal combustion engines to meet stringent emission regulations. These catalytic converters have light-off issues during cold-start and warm up. Some of the engine combustion strategies have given a good performance in terms of light-off time/temperature reduction, but have led to high fuel consumption and higher heat loss. Thermal management technologies, such as use of reformers, thermal energy storage systems (TES) and electrically heated catalysts (EHC) have led to significant reduction of heat and energy losses. The EHCs are an effective method to improve fuel economy and emission reductions. These EHCs could be coupled with catalytic converters in hybrid electric vehicles (HEV) for $CO_2$ and exhaust emissions' reductions [6]. To have the same thermal energy for increasing catalyst temperature, use of EHC led to 40% less fuel consumption compared to engine improvement methods [7]. Also, an electrical heater has a better transient response compared to thermal energy storage systems. The EHCs are more convenient for HEVs, where they can use energy from the battery during regenerative braking and cruising, instead of using energy generated from fuel combustion in an engine. The EHCs give a high energy-utilisation performance and low thermal energy losses to the atmosphere. They have the capability for excellent catalyst light-off time reduction and significant reduction of emissions [8]. The combination of an EHC and a DOC has been effective in achieving DPF regeneration without providing additional heat due to operating the DOC above its light-off temperature [9]. Also, addition of $H_2$ upstream of diesel oxidation catalyst has been reported as a positive promoter of CO, HC and NO oxidation [10]. Hydrogen modifies locally the catalyst

temperature as well as the exhaust gas composition by production of intermediate species to increase the oxidation reaction rate at a lower catalyst temperature.

## 1.2. Research Aim and Objectives

The overall aim of this research is to investigate synergistic effects of alternative fuels and aftertreatment systems, in order to reduce emissions and increase the effectiveness of diesel aftertreatment systems. This research includes studies into new oxygenated fuels' properties, tribological mechanisms, engine combustion and using new technique to reduce the thermal energy required for starting emissions' conversion reactions.

The primary research objectives are as follows:

- To investigate the effects of blending diesel with alternative bio-alcohols and a bio-ketone with different molecular structure on the fuel properties, lubrication and tribological mechanisms
- To study the effects of using the aforementioned fuel blends of engine combustion characteristics, gaseous emissions and PM characteristics
- To examine the passive influence of modified engine-out emissions when using alternative fuels on the performance of aftertreatment systems, i.e. to enhance catalyst activity at lower temperatures
- To investigate the active method of heating the aftertreatment system (through electrical heating) as an energy efficient heating strategy for accelerating the aftertreatment catalyst's light-off and to minimize the cold-start emissions also useful for hybrid electric vehicles
- To study the effect of the small (i.e. 500 ppm) hydrogen to the exhaust gas upstream of the diesel oxidation catalyst on its light-off temperature

## 1.3. Contributions to the New Knowledge

Bio-alcohols and bio-ketones can be produced from lignocellulosic biomass through various renewable processes which have been optimised over the years. Blends of butanol and pentanol (as heavier alcohols compared to the ethanol) with diesel have been investigated as alternative fuel candidates in diesel engines and the results showed benefits for improving the combustion performance and reducing emissions [11, 12]. They have some advantages over ethanol such as, their high blending stability, higher density, higher calorific value and higher cetane number [12]. However, their lubrication and tribological mechanism have not been studied comprehensively in the past. Detailed knowledge of these mechanisms are believed to be important for understanding the engine performance and durability as well as combustion process and emissions formation mechanisms.

In addition to the aforementioned alcohols, cyclopentanol (a cyclic alcohol) and cyclopentanone (a ketone) as new alternative fuels seem to be promising candidates for blending with conventional diesel fuel. There is no comprehensive dataset available in the literature about their physico-chemical properties, lubrication and tribological mechanisms as well as engine combustion and emissions characteristics when using their blend with diesel.

Moreover, the performance of the aftertreatment systems when using any of the aforementioned fuels have not been studied comprehensively in the past. It can be hypothesised that the higher oxygen content of these fuels as well as their higher volatility can help promote oxidation reactions within the diesel oxidation catalyst (DOC). The behaviour of the DOC would significantly affect the performance and efficiency of the other aftertreatment components such as SCR and a DPF. Additionally, in order to

compensate for the low activity of the DOC at lower exhaust temperatures, an efficient catalyst heating strategy seems very promising. This is believed to be useful for reducing the cold start emissions and emissions of the hybrid electric vehicles applications. Combination of the alternative fuels combustion and an efficient heating strategy for aftertreatment system is comprehensively investigated in this thesis for the first time.

## 1.4. Thesis Outline

Figure 1-1 shows thesis outline to study synergistic effects of fuels properties, combustion performance and aftertreatment systems into seven chapters as follows.

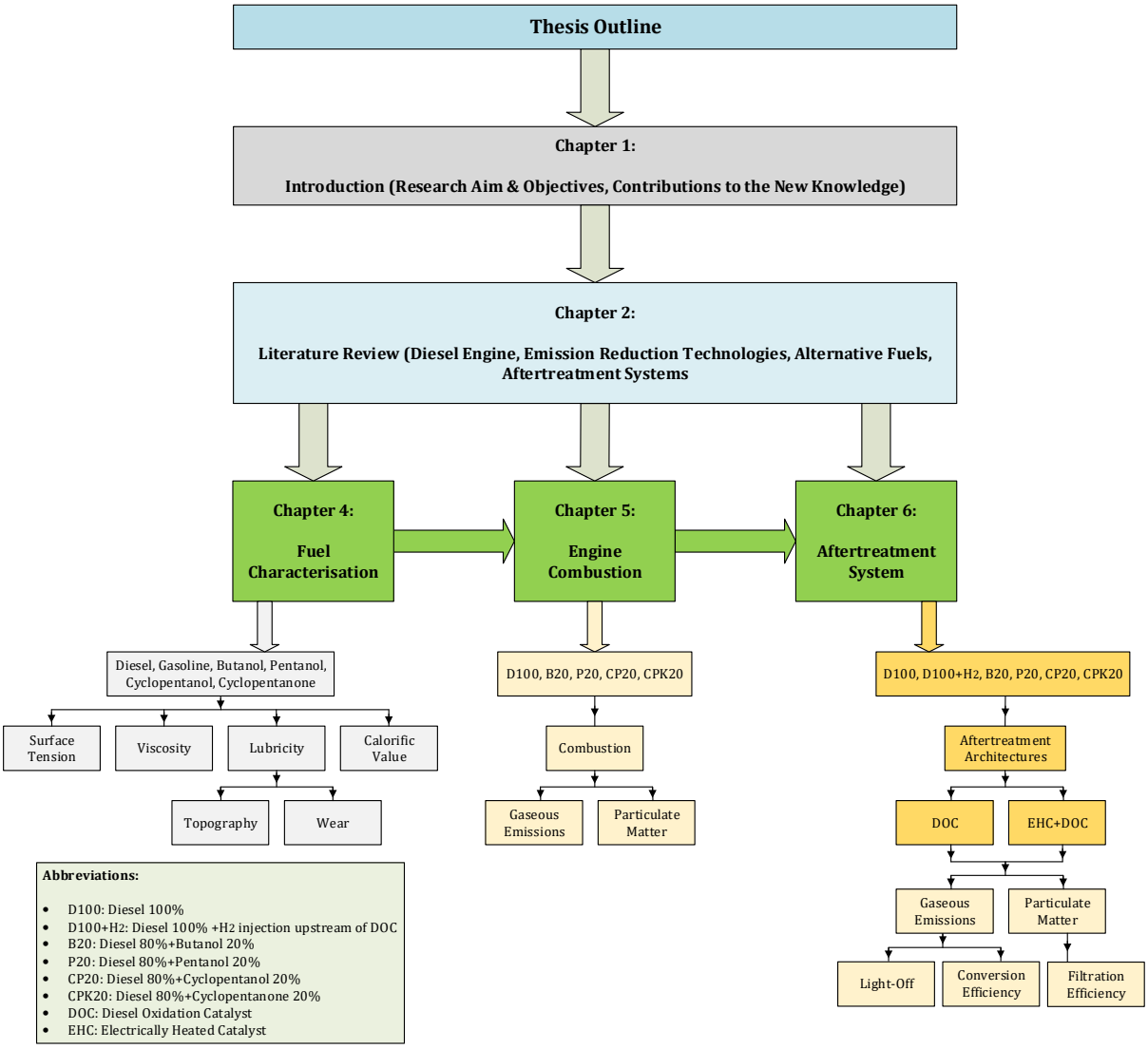



Figure 1-1: Thesis outline

**Chapter 1: Introduction**

The research's background, aims and objectives have been introduced in this chapter.

**Chapter 2: Literature Review**

This chapter is divided into three parts. The first part includes types of emissions from transportation and possible solutions. The second part provides an overview of alternative fuels and their properties. Finally, the third part reviews the literature related to diesel engines' aftertreatment technologies.

**Chapter 3: Methodology**

A detailed explanation of the experimental set-ups and methodology that were used in this research study is presented in this chapter. The experimental section introduces the tested fuels, engine and fuel characterisation test beds, their instrumentation, exhaust gas analysers, particulate analysers, catalytic aftertreatment setup and any other characterisation instruments which were used in this research.

**Chapter 4: Investigation of Lubrication Properties and Tribological Behaviour of Bio-alcohols and Bio-ketones**

Effects of physical and chemical properties of six different neat fuels: commercial ultra-low sulphur diesel (ULSD), gasoline, butanol, pentanol, cyclopentanol, cyclopentanone and their blends with diesel, on viscosity, surface tension, calorific value, lubricity, wear scar profile, microscopic topography and tribology behaviour are presented in this chapter. A lubricity analysis is carried out on a high frequency reciprocating rig (HFRR) based on the diesel lubricity standard. The worn surface analysis and microscopic topography are also presented in this chapter.

**Chapter 5: Impact of Alternative Fuels on Combustion, Gaseous and Particulate Matter Emissions Characteristics**

In this chapter, combustion characteristics (cylinder pressure, heat release rate, indicated specific fuel consumption, etc.), gaseous emissions (CO, $CO_2$, THC, $NO_2$, $NO_x$, etc.) and particulate matter characteristics (particle size distributions, total number concentration, etc.) of these blended fuels were analysed. The main outcome of this chapter can be used to understand behaviour of alternative fuels in current diesel engines.

**Chapter 6: Enhancing the Low Temperature Activity of Diesel Oxidation Catalyst by Using Electrical Heating and Alternative Fuels**

Improvement in the performance of an aftertreatment system while using the blends of the aforementioned bio-alcohols and bio-ketones is investigated in this chapter. Regulated and unregulated gaseous emissions are evaluated. The results explained in this chapter will be useful in the development of strategies for choosing the most suitable alternative fuels for aftertreatment systems, in order to gain higher conversion efficiency at lower temperature. In addition to the tested fuels, hydrogen is injected into the exhaust gas before the aftertreatment systems for enhancing the low temperature oxidation performance. Catalyst efficient heating strategies were studied to minimize the required thermal energy for achieving the optimum performance of the aftertreatment system.

**Chapter 7: Conclusions**

The main findings of this research study are presented in this chapter and it provides recommendations for future work to develop low temperature aftertreatment systems.

# CHAPTER 2. LITERATURE REVIEW

Transportation facilities are almost all powered by internal combustion engines burning liquid fuels. The demand for transport energy is increasing daily; however, the exhaust emissions are a main concern due to their harmful impact on the environment and on public health. This chapter includes literature concerning transportation emissions, diesel engines, alternative fuels and emissions' control technologies.

## 2.1. Emissions from Road Transport

The evolution of future transport energy depends on the interaction between many sectors as shown in Figure 2-1 [2]. This interaction is different in any place around the world and depends on the policies. Based on the predictions even by 2040 around 90% of transport energy will come from internal combustion engines [2-5].

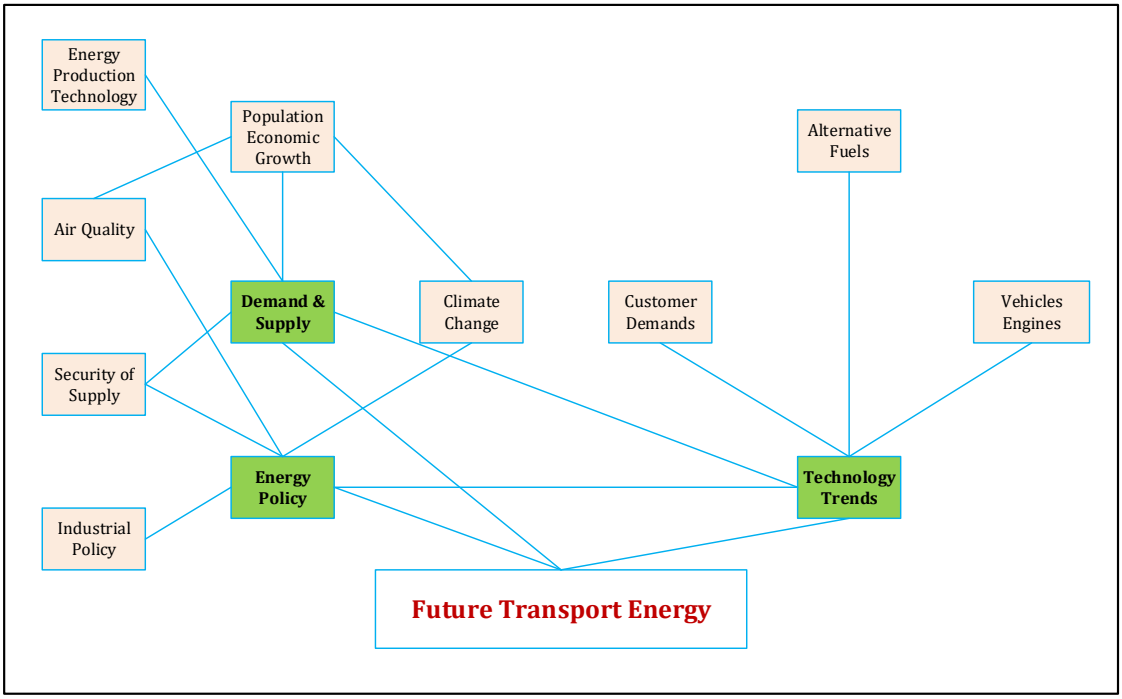



Figure 2-1: The evolution of transport energy (modified) [2]

Ideal complete combustion of fuels in engines produces heat, carbon dioxide and water. However, there are other factors that affect the by-products of the fuel combustion [13]. In addition to the $CO_2$ and $H_2O$, exhaust gas contains other harmful by-products. These products are categorized in regulated (carbon monoxide, hydrocarbons, nitrogen oxides and particulates) and nonregulated emissions (formaldehyde, acetaldehyde, toluene, etc.) [14, 15].

Incomplete fuel combustion in the combustion chamber leads to an increase of CO emissions; where HCs do not have sufficient oxygen content to oxidize and produce $CO_2$ [16]. This CO is very toxic to human health due to its ability to combine with haemoglobin in blood, which causes a reduction of the oxygen supply to biological tissue. The HC emissions consist of several organic species depending on the fuel production process, fuels' composition and molecular structures [17]. Reactive HC emissions contribute to the creation of smog as an effective greenhouse gas [18]. Nitrogen oxides' ($NO_x$) emissions mainly consist of nitric oxide (NO) and nitrogen dioxide ($NO_2$). They are mostly produced by oxidation of nitrogen in the atmosphere or nitrogen in the fuel content from different chemical reactions. Higher combustion chamber temperature and higher local oxygen access can considerably increase the $NO_x$ emission concentration in the exhaust. As with HCs, $NO_x$ contributes in the formation of low-level ozone and photochemical species. Particulate matter (PM) emissions which are seen as a black smoke in the exhaust of diesel vehicles are composed of carbonaceous soot and other absorbed solid and liquid materials. They are mainly produced from incomplete combustion of fuel hydrocarbons in rich-in-fuel in-cylinder regions. Particulate matters are measured in the atmosphere as $PM_{2.5}$ and $PM_{10}$ [19, 20]. Higher PM emissions are due to the lower charge temperature and lower local oxygen access. They have a harmful impact on the environment, such as reduction of visibility after high PM level occurrences [21]. Particulate matter can

infiltrate into the human lungs, blood, brain, and liver and have harmful impact on the respiratory system causing bronchitis, asthma and allergies [20, 22-24]. There are several other emissions in the exhaust from diesel engines such as $N_2O$, $SO_2$ and metallic oxides. They should be controlled due to their impacts on human health and the environment. All of these emissions have a harmful impact on health, such as asthma, heart attacks, and eye irritation, and need to be controlled with any emission control technologies [24].

Different emissions' legislations have restricted vehicular emissions' limits to reduce their health and environmental impact. Table 2-1 [25] indicates the European Union's emissions' standards for category M1 passenger cars.

Table 2-1: EU's emissions' standards for category M1 passenger cars

| Emissions legislation Stage | CO (g/kw.hr) | HC (g/ kw.hr) | $NO_x$ (g/ kw.hr) | PM (g/ kw.hr) | PN (#/km) |
|---|---|---|---|---|---|
| Euro 3 (2000) | 2.10 | 0.66 | 5 | 0.10 | - |
| Euro 4 (2005) | 1.50 | 0.46 | 3.50 | 0.02 | - |
| Euro 5 (2008) | 1.50 | 0.46 | 2.00 | 0.02 | $6.0 \times 10^{11}$ |
| Euro 6 (2013) | 1.50 | 0.13 | 0.40 | 0.01 | $6.0 \times 10^{11}$ |

## 2.2. Diesel Engines

In a four-stroke diesel engine, during the intake stroke only air is introduced into the cylinders, which allows engines to operate at high compression ratios. This air is compressed in the cylinders to a high temperature and pressure. When the air temperature is higher than the fuel ignition point, the fuel system injects fuel into the cylinders. The injector atomises the fuel into the droplets to mix with the compressed air. With a small delay, auto-ignition of the fuel and air mixture creates the combustion process. The fuel oxidation and its heat release continue in the expansion stroke which

produced mechanical work and then is delivered to the engine's crankshaft. Finally, combustion exhaust gases leave the engine's cylinder in the exhaust stroke [13, 17]. To describe the diesel combustion process the rate of heat release analysis can be used. The ignition delay is a period defined between the start of fuel injection (SOI) and the start of combustion (SOC). Combustion delay is defined as the duration between SOI and combustion phasing AHR-50. Combustion duration is the duration between AHR-10 and AHR-90 [17].

## 2.3. Alternative Fuels

As discussed previously, transportation vehicles mainly use internal combustion engines powered by conventional diesel and gasoline fuels, as the most cost-effective, ground-based transportation system currently [26]. In recent years the fast depletion of fossil fuels and the need to reduce the harmful impact of greenhouse gas emissions make alternative and renewable fuels much more attractive [27, 28]. The literature shows that alternative biofuels are seen to have less environmental impact. It is essential to find the most suitable alternative fuels on a potentially permanent basis with no negative effects on engine operation and maintenance. The important parameters in choosing appropriate fuels for current engines are that they must be environmentally friendly, produce fewer emissions, be economical, sustainable and able to deliver the same performance as conventional fossil fuels without any modification. Biofuels are derived from natural resources, agricultural wastes and other resources which can be considered as good alternatives to current diesel and gasoline fuels.

In Europe most automotive industries rely upon the diesel engine; thus, it is important to find the easiest solutions to be independent from fossil fuels. At the moment, fuel cells, hybrid and electric vehicles in most of the countries are not feasible in the short

term. Also, most of the biofuels would be used in hybrid vehicles rather than burning gasoline or diesel. Engines can be fuelled by a wide range of renewable fuels as a mix of fossil fuels and biofuels are compatible [29]. In developed countries, electric and hybrid powertrains will play an essential role in the future; however, it is necessary for sustainable and renewable sources of energy for these powertrains to become useable. Until, the further development of these electric vehicles, renewable fuels for internal combustion engines can be used to replace conventional fuels. Most of the alternative fuels are produced from lignocellulose biomass via gasification processes. The pathway for production of these fuels can affect the chemical properties of the products; so, based on that these fuels can be divided to alcohols, dimethyl ether, liquid ether, ketones and Fischer Tropsch hydrocarbon fuels. As a conclusion, chemical and physical methods of converting biomass to liquid fuels can produce an extensive range of fuels with different molecular structures. Furthermore, the properties of feedstock can have an effect on the type of the product too. Literature studies have indicated that the molecular structure of fuels has a significant impact on the efficiency of engines and the formation of emissions [30]. Different molecular structures are due to the different production processes of liquid fuels. The molecular structure of fuels has impressive impact on: the ignition delay of fuels; the fraction of premixed combustion; the flame temperature; the heat release rate; the emissions' concentration and the particulate matter [31].

With the growing concerns about exhaust emissions of fossil fuels combustion in engines, the instability of oil prices, greenhouse gas emissions and emission regulations, optimising the performance of energy release, while reducing emissions will be key to the success of future alternative fuels as replacements in engines [29, 32]. Also, in recent years, overall energy consumption has increased, which has led to global warming and an increase of greenhouse gas emissions. As reported by the International Energy Agency

(IEA), the energy consumption by transportation facilities will reach around 53% of total rate of global energy consumption by 2030 [24]. Automotive transportation is one of the major sources of greenhouse gas emissions, especially diesel vehicles [33, 34]. These emissions are categorised as exhaust emissions produced during the combustion process; abrasion emissions produced by the wear of vehicle components; and evaporative emissions produced from fuel evaporation [34]. Transportation is the source: of 23% of worldwide $CO_2$ emissions, of more than 50% of $NO_x$ emissions and of 10% of total energy-related particulate emissions. Recently, diesel engine vehicles produced by modern automobile manufacturers provide lower fuel consumption, a high engine performance and less gaseous emissions, but the major concern about these diesel engines is particulate matter (PM) and nitrogen oxides ($NO_x$) emissions [35, 36]. Alternative fuels as a source of renewable energy, their availability, biodegradability, non-toxicity, higher lubricity and lower emissions are all important factors when considering them as one of the short-term solutions for global warming [12]. Renewable fuels such as biogas, bio alcohols, bio ketones, vegetable or seed oils and biodiesel are environmentally friendly and available; they can fulfil the global energy demand [11, 37]. Bio-alcohols and bio-ketones fuels blended with diesel can improve diesel engine emissions. They can reduce the life cycle of greenhouse emissions, soot formation and particulate matter [38], depending on their production process [39-41]. The presence of the hydroxyl and carbonyl group in alcohol and ketones' molecular structure tends to reduce total hydrocarbon (THC), carbon monoxide (CO) and PM emissions. Due to oxygen content in the structure of these fuels, in most cases, $NO_x$ emissions increase compared to diesel but the level depends on the cetane number; so overall, molecular structure of alcohols, engine technology and operating conditions are very important [41]. There are different technologies to improve engine performance and emissions when alternative

fuels are used as a fuel. The output power of alternative fuels' combustion is lower than neat diesel combustion in a diesel engine. Also, their lower energy density increases the indicated specific fuel consumption to give the same output power.

As a conclusion, the alternative fuels can be produced from non-edible feedstocks and can be utilised in unmodified diesel engines. These fuels are categorized based on their resources and production processes to first, second, third and fourth generations. The first generation relies on food crops such as corn, soy and sugarcane. Second generations use lignocellulosic biomass, such as agricultural residue and switch grass, as a feedstock. Third and fourth generation biofuels seek to improve the feedstock by using algae or sludge as a main resources. All kinds of biofuels used as alternative fuels are of increasing interest because they offer a short-term solution for a fuel regenerating ability and reduced environmental impact. Typical biofuels contain oxygen as an additional element in their molecular chemical composition, which distinguishes them from normal hydrocarbons. Biodiesels, synthetic fuels, vegetable oils, natural gas, hydrogen, and methane are other alternative fuels which can be used as alternative fuels in current engines. Besides these, advanced combustion strategies, cylinder deactivation, variable compression ratio, the stop-start method and other engine calibration strategies are some of the solutions for reducing greenhouse gas emissions [19, 42, 43].

### 2.3.1. Alternative Fuel Properties and Behaviour in Engines

In many countries, quality and properties of fuels are strictly regulated for emissions' standards, based on the fuel and region of the application. In Europe EN228 and EN590 standards are used for properties of gasoline and diesel, respectively. In the USA these standards are ASTM D4814 and ASTM D975 [19]. In a diesel engine, a high cetane index (good auto ignition properties) is more suitable to ensure the ignition of a heterogeneous

air-fuel mixture. Fuel oxidation stability, cold-flow properties and lubricity affect performance and emissions' behaviour. The density of a fuel influences the volumetric energy content of the fuel, because the fuel injection system works based on the volumetric flow rate. High viscosity prevent fuel from flowing easily, require high energy to pass the fuel to the injector, and lead to failure in the injection system. These properties affect engine performance and emissions as shown in Figure 2-2. In this figure red and blue colours indicate disadvantage and advantage of that specific property, respectively.

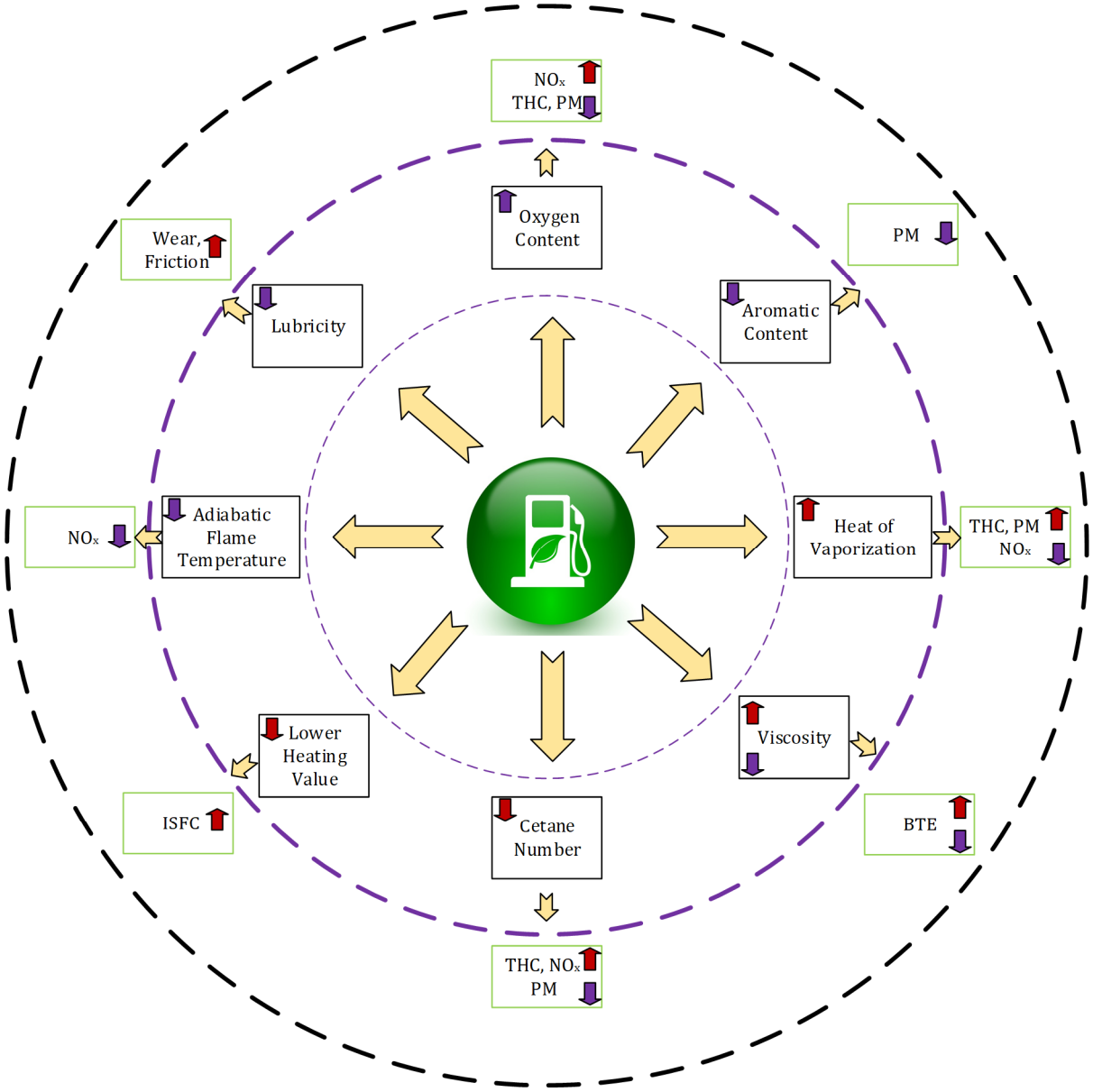



Figure 2-2: Alternative fuels performance and emissions

Exposure of the fuel on internal combustion engine systems provides lubrication of these components. Problems of insufficient lubricity of fuels on engine components were reported in different studies [44]. Figure 2-3 indicates the energy losses from vehicles' engines in different aspects; some of these losses could be controlled with different technologies and improvement. Lubrication has a direct impact of friction losses of around 33%, including engine transmission, tyres and brakes. Energy losses from friction in engine components is due to the poor lubrication behaviour of lubricants and fuels; so it would be essential to improve the lubrication properties with the available technologies. Use of alternative fuels with appropriate lubricities helps self-lubricated engine components to overcome energy losses and also helps their life durability.

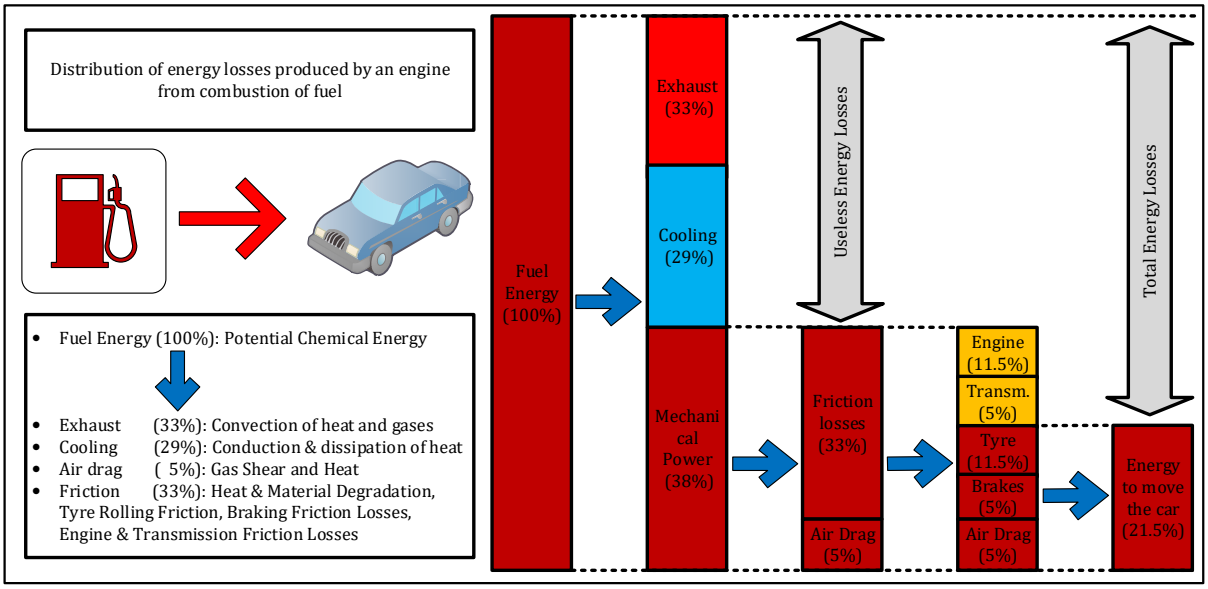



Figure 2-3: Distribution on energy losses produced from vehicles (modified) [45]

The literature indicates good lubrication from fuels is due to the formation of a protective layer on the metal surface of engine components. This protection improves with the fuels containing oxygen, so oxygenated fuels show better lubrication behaviour. The lubricity improvement additives for diesel fuels are more important due to the high-

pressure operation of a diesel fuel's pump; therefore, in diesel engines it is very important to investigate the lubricity and tribological behaviour of new alternative fuels. There are many published studies on the lubricity characterisation of diesel and bio diesel fuel, but there is lack of data on the lubricity of this research study's chosen fuels [38, 46-53].

Alternative fuels should be well-matched with current engines in the short-to-medium term to enable a quicker transition away from fossil fuels. Investigation of various molecular structure of biofuels is the focus of global fuel research; it can affect engine durability, efficiency, gaseous emissions and particulate matter. Among these fuels, oxygenated fuels are more attractive due to their lower carbon emissions. Several new technologies have been developed to improve the engines efficiency and reduce engine-out emissions. However, most of these technologies can lead to major problems in any engine parts, such as the fuel injection equipment [48, 49, 54]. The main reason behind this failure is the poor lubrication behaviour of those technologies and alternative fuels; which makes fuel lubricity one of the main properties of fuels. Due to these reasons regular legislation modifications and technology improvements push the limits of fuels' physical and chemical properties [47].

The measurement of the fuel lubricity is critical due to the introduction of ultra-low sulphur diesel fuels. The desulphurization process in the refinery brings some serious challenges in reducing the fuels' lubricities, and leads to the failure of engine components such as fuel pumps and injectors because these parts are lubricated by fuel [48, 55-57]. Further technologies have been applied to reduce other emissions, such as increasing fuel injection pressure, control of fuel injection and using alternative fuels with appropriate lubricity rather than using additives. High boiling points, high aromatics and nitrogen contents, high degree of saturation, high fatty acid and fatty esters improve the lubricity

of diesel fuels [46]. The oxygenated compounds presenting in the alternative fuels' molecular structure reduce engine-out emissions. Also, their tribological behaviour is different on comparison with commercial fuels. The lack of polar compounds and reactive species in the molecular structure of some fuels due to the process of desulphurization will cause the formation of oxide layers on the metallic surface of engine components [46]; however, this oxide film can be eliminated during the sliding process of the lubrication test and thus leads to the formation of severe wear and poor lubrication of fuels [49, 58]. Reduction of frictional losses in the engine leads in improvement of fuel economy and engine's efficiency [54, 59].

### 2.3.2. Alcohols

Alcohols can be produced from fossil fuels and lignocellulosic biomass via synthesis gas. These alcohols can be used as neat or blended in current engines. From the early years of research in the area of alternative fuels, alcohols were evaluated as a fuel alternative for diesel vehicles [60]. Methanol ($CH_3OH$), ethanol ($C_2H_5OH$), propanol ($C_3H_7OH$), butanol ($C_4H_9OH$) and pentanol ($C_5H_{11}OH$) are five alcohols which will be reviewed in this section. Cyclopentanol ($C_5H_9OH$) as a cyclic and novel alcohol will be tested in this research as well, but there is no literature regarding its application in engines. Based on its appropriate fuel properties, it was tested to compare with other alcohols. Short-chained alcohols such as ethanol, propanol and butanol have not been considered as neat fuels for CI. However, they can be used as blends with fossil diesel fuels or biodiesel [61, 62]. Generally, alcohols in CI engines reduce $CO_2$ and PM emissions with some changes in their cetane index and combustion process. They can easily be used as blends in diesel without any major changes and modifications to the engine [19].

Before using any new alternative fuels in an engine, it is fundamental to investigate their chemical and physical properties. This analysis shows how it is possible to use these new fuels without any modification or property enhancer. The advantages of alcohol application in an engine, regarding its reduction of soot formation and particle emissions, make it more attractive than other alternative fuels.

Methanol is beneficial in the reduction of $NO_x$ and particles due to its high oxygen content and also its high latent heat of evaporation. Methanol as a fuel additive has some disadvantages: low lubricity, low viscosity, low cetane number and ignitability. To solve this issue lubricity and a cetane number enhancer are needed. Cheung et al. [62] found that biodiesel had a higher fuel consumption compared with diesel fuel; while the methanol blended fuels also had a higher fuel consumption, which is due to the lower heat value of oxygenated fuels. Also, with an increase in the proportion of methanol in blended fuels, $NO_x$ emissions decreased. They concluded that the cooling effect of methanol dominated the $NO_x$ formation of blended fuels. Methanol blended fuels generate fewer particulates due to the reduction of soot formation.

In 1970 in South Africa, and in the1980s in Japan, Germany and the United States, ethanol was used as a fuel in diesel engines [61]. Ethanol combustion in diesel engine led to reductions of particulate matter emissions. Ethanol has low ignitibility, low lubricity, limited miscibility and low heating value, which make its blending proportions limited. The best solution to use ethanol as an additive is to blend it with biodiesel to improve stability, cetane number and lubricity of blends [48, 61]. Lapuerta et al. [61] reported that biodiesel fuel acts as a stabilizing component in ethanol-diesel bends. The higher ethanol content in blends increases the total hydrocarbon emissions, decreases smoke emissions and could present a nuclei mode because the high THC emissions leads to the nucleation

of hydrocarbons. They concluded that the effect of oxygen content in these blends on the particle size depends upon its functional group. Ethanol has low energy density and high hygroscopicity in comparison to gasoline. Propanol as a possible alternative fuel can be produced from biomass through various kinds of processes. It has a higher energy density and cetane number compared to ethanol and methanol [12]. Low carbon chain length alcohols like methanol and ethanol have been used extensively in SI engines because of their good anti knock properties and lower gaseous emissions such as CO and THC [63-65]. Short-chain alcohols with a low cetane number in diesel engines result in a significant increase of duration in ignition delay [29]. The addition of ethanol or butanol has been observed to have a longer ignition delay and a significant reduction in PM formation [66]; because an increase in fuel ignition delay allows more time for fuel and air mixing before the start of combustion and leads to fewer fuel rich-zones and a decrease in PM emissions [29]. These fuels are not of good compatibility with diesel fuels due to their poor blending stability, poor cetane number and lower heating value. Butanol is a promising fuel with several advantages over ethanol, such as higher energy content, is less corrosive, has better miscibility with current fuels and lower water absorption [41, 67]. The same production process for ethanol can be adapted to produce butanol from different feedstocks. There are other technologies such as fermentation and transesterification [68] with lower required energy, which lead to the production of desirable alcohols such as butanol [12]. The THC emissions from ethanol blended with diesel are higher than butanol blended with diesel, due to the higher heat of vaporization of ethanol [41]. Longer chain alcohols are more suitable for blending with diesel fuel. They have proper lubricity, high calorific value, lower volatility, a high flash point, high viscosity and cetane number compared to lighter alcohols [12, 38]. Pentanol, butanol and other higher alcohols, have a low affinity for water and a higher energy density and fit well into current

transportation vehicles without any needed modification [69]. The literature has shown that pentanol has good physical properties as an alternative fuel [69]. Pentanol is also an excellent alternative fuel because it can be produced from biological processes such as microbial fermentation using micro-organisms and bio-synthesis from glucose [12]. Pentanol as a long-chain alcohol requires even less production energy than butanol and compared to other alcohols [70]. Heavier alcohols are more advantageous than lighter alcohols due to their better blending stability, hydrophobic properties, higher cetane numbers, heating value and their low carbon counterparts [71-73]. Butanol as a blend with diesel fuel has been extensively studied in diesel engines [36, 74-77]. It was concluded that the alcohol content in a diesel engine increased ignition delay due to its low cetane number. In-cylinder pressure and heat release rate increased due to an enhanced premixed combustion phase. The presence of oxygen improved the combustion process and reduced soot formation. Pentanol's similar properties to diesel, and also the fewer emissions produced together with a good engine performance, make it advantageous as a short-term replacement in diesel engines [70, 78]. It has shown more advantaged than butanol and other light alcohols [70, 78]. The use of pentanol as an alternative fuel in a diesel engine is not as well-known as butanol, so it needs more investigation due to its properties being similar to diesel fuel. Generally, the low cetane number of alcohols increases ignition delay and so leads to a higher combustion temperature and then higher $NO_x$ emissions [67]. However, the higher heat of vaporization in alcohols reduces the cylinder flame temperature and so reduces $NO_x$ emissions [79]. It can be concluded from the different emissions' analyses in the literature that engine operating conditions and injection strategies could have an effect on the emission characteristics. A lower carbon to hydrogen ratio and the presence of oxygen in

alternative oxygenated fuels leads to decreasing soot emissions from internal combustion engines.

As a conclusion, butanol and pentanol are two long carbon chain length alcohols that could be categorized as the second or third generation of biofuels with potential for use as alternative fuels in internal combustion engines. The literature has reported that their closely similar properties to conventional fuels make them more attractive as a short-term solution for emission reduction. They could be used with up to 45% as a blend with diesel without any modifications. Their low viscosity and low density compared to diesel, improves their spray characteristics and presents a higher brake thermal efficiency compared to neat diesel combustion [11]. The THC and CO emissions of pentanol depend on the engine operating conditions. Atmanli reported improvements in engine performance and emission characteristics of heavier alcohols [80]. Butanol and pentanol improved the cloud point (CP) and cold filter plugging point (CFPP); however, they led to a slight reduction in density, viscosity, cetane number, flash point and calorific value [80]. Also, an increase of CO emissions and a reduction in HC emissions were reported. The HC and CO emissions were due to a reduction in post-oxidation, which could be solved by an aftertreatment system. Lower $NO_x$ emissions, lower smoke, higher indicated thermal efficiency, lower ISFC were reported by Li Li et al. for the combustion of pentanol as injection timing was rerated [72].

Eveleigh et al. [81] studied the effects of the molecular structure of fuels on the formation of particulate matter. Their method was based on the $^{13}C$ stable isotope to trace the conversion of carbon atom to particulates. When –C-OH functional group is incorporated from pentanol into cyclopentanol, the conversion rate of carbon atom increases. So carbon atom in molecules contribute differently in PM formation based on

their position in the molecular structure; such as the presence of oxygen containing functional groups significantly reducing the contribution of carbon atom in PM formation [81]. In another study, results showed that, carbon atom in the double bonds were converted to PM at the same rate as average carbon atom in the molecular structure of tested oleic acid in diesel engine combustion [82].

### 2.3.3. Ketones

Cyclopentanone ($C_5H_8O$) can be produced from the conversion of agricultural wastes to biofuels. It is a colourless liquid with low toxicity and very similar properties to gasoline and ethanol, which makes it a very attractive fuel, especially to use in spark ignition engines [83]. It has a higher volumetric density, higher heat of vaporization, lower stoichiometric air/fuel ratio, higher auto ignition temperature and high oxygen contents compared to an SI engine's gasoline fuel. This means that cyclopentanone is an attractive biofuel not only due to it bio-derived production process but also because of its engine efficiency and beneficial properties leading to a reduction in greenhouse gas emissions. The addition of the carbonyl group to an alkane creates a ketone hydrocarbon group. In its molecular structure hydrogen abstraction becomes more difficult due to reducing the number of hydrogen for H-abstraction by one. Also the C-H bond close to the carbonyl group changes and then the ability of the fuel peroxy radical to undergo isomerization is reduced [84]. This increases ignition delay in combustion in the engine. Cyclopentanone (CPK) is a ketone which can be bio-derived due to its chemical class which is formed when fungi are converted to cellulose as a major component of biomass. There are some limited studies in the use of cyclopentanone, but they agree that it has very attractive fuel properties to use in SI engines in terms of auto ignition, high efficiency and reduction of greenhouse gas emissions [39, 83, 85, 86]. There is no literature on the

use of these fuel as an alternative fuel in CI engines but it is thought that its properties would lead to a reduction in soot formation.

## 2.4. The Way Forward to Sustainable Transport

As a conclusion, ethanol and methanol show a reduction of emissions and also act as a good replacement for fossil fuels. Other heavier alcohols such as butanol and pentanol could also become sustainable alternatives as they could be produced from renewable raw materials, biomass and wastes. Ethanol and methanol formation via fermentation and biomass gasification is used to convert these simple alcohols to butanol and pentanol and other fuels via the Guerbet reaction [38]. The poor lubrication properties of commercial gasoline fuels, due to their low viscosity and non-polar composition, cause some problems for engine components which are lubricated by fuels. Much research has been done on the use of lubricity additives, but the presence of these additives has some disadvantages regarding emission formation. Finding alternative fuels with appropriate tribological behaviour would be the best solution [53]. Thus, it is necessary to find the appropriate alternative fuels with good lubrication and tribology behaviour. Use of alcohols blended with biodiesel was suggested due to a lack of aromatic, higher solubility and better lubrication performance. However, among the alcohols, choosing those alcohols with a higher cetane number would be more advantageous; therefore, it is essential to choose the bio-alcohols and bio-ketones with higher solubility and appropriate compatibility with diesel fuel [38, 40, 48, 87-90]. Use of these fuels also gives some advantages with engine exhaust emissions and particulate matter. Alcohol-diesel blends increase hydrocarbon emissions, but they decrease particles; they behave differently with about carbon monoxide and nitrogen oxides in different aftertreatment architectures [36, 40, 61, 74, 87, 91].

Gasoline compression ignition (GCI) has shown great potential for future internal combustion engines [92]. Use of gasoline in CI engines has been demonstrated to have high efficiency and lower fuel consumption compared with running on gasoline in SI engines [92]. At higher loads, $NO_x$ and soot can be controlled in GCI compared with a diesel engine. As lower cetane number fuels such as cyclopentanone are blended with diesel to use in CI engines, gasoline as a baseline case study was considered on its validity as a replacement fuel in diesel engines.

## 2.5. Diesel Exhaust Gas Aftertreatment Technologies

Engine fuel injection strategies (such as injection pressure and timing and combustion calibration), exhaust gas recirculation and exhaust aftertreatment systems are some of the engine-based strategies for controlling diesel engine emissions to comply with emission standards' legislation, as presented in Table 2-1. Aftertreatment systems in CI engines' exhaust are used to oxidize CO and HC emissions, reduce $NO_x$ emissions, oxidize PM emissions and filter soot. In aftertreatment systems, a catalyst decreases the activation energy of the emissions' conversion reactions. To increase the catalyst's contact surface area, several axial channels have been coated with catalysts. In automotive aftertreatment applications, catalysts' substrates are made of ceramic materials and metallic substrates [93]. Furthermore, different active catalytic components are used based on their activity and selectivity for particular applications. Platinum, palladium, vanadium, copper, iron and their oxides as precious metals are the most commons materials in automotive catalytic aftertreatment systems. To facilitate the adsorption and desorption of the exhaust species in the presence of catalytic reactions, aluminium oxide ($Al_2O_3$) and titanium oxide ($TiO_2$) are used in the washcoat due to their high porosity for increasing the surface area.

In the diesel exhaust gas aftertreatment systems, normally a diesel oxidation catalyst (DOC) is the first component. The DOC oxidizes CO, NO and HCs emissions based on the following reactions:

$$CO + \frac{1}{2}O_2 \rightarrow CO_2 \quad \text{Equation 2-1}$$

$$C_nH_m + \left(n + \frac{m}{4}\right)O_2 \rightarrow nCO_2 + \frac{m}{2}H_2O \quad \text{Equation 2-2}$$

$$NO + \frac{1}{2}O_2 \rightarrow NO_2 \quad \text{Equation 2-3}$$

The DOC increases the exhaust gas temperature downstream of the aftertreatment system after emissions' light-off (T50). This is due to the above exothermic reactions through the catalyst. The DOC does not reduce $NO_x$ emissions but based on the above reactions, it converts NO to $NO_2$. Also, based on the above reactions, the DOC can oxidize the particulate matter and NO in the exhaust which leads to an increase of the $NO_2$ concentration [94]. The $NO_2$ can improve soot oxidation at lower temperatures in diesel particulate filters (DPFs) and also improve the $NO_x$ conversion reactions rate in selective catalytic reduction (SCR) aftertreatment systems [19, 95]. The optimal addition of $NH_3$ and $H_2$ for high de-NOx activity can be used to limit any $NO_2$ slippage downstream the catalysts which could be harmful for the environment [96]. To fulfil the emissions' regulations, aftertreatment systems as emissions' control technologies have been developed. It is an essential role to improve emissions' conversion reactions at the required lower temperatures. In particular during engine cold-start conditions, to provide more thermal energy to improve catalytic converter performance, various heating strategies are used. Engine based strategies increase exhaust temperature and decrease $NO_x$ emissions; however, they lead to increased fuel consumption and $CO_2$ emissions.

The addition of $H_2$ upstream of the catalyst has been reported to have a positive effect on CO and hydrocarbon oxidation, and also on $NO_2$ formation for enhancing the high oxidation performance over the DOC at low temperatures [10, 97]. This is due to an increase in the rate of CO desorption from the catalytic active sites, which has led to an increase in the catalyst active surface sites to oxidising the species. The presence of hydrogen increased the formation of species for increasing the CO oxidation [98]. For real application, exhaust gas reforming or electrolysis can be used to produce the required amount of hydrogen to promote DOC activity [10].

Apart from the DOC's physical and chemical properties, the operating conditions are essential for its emissions' conversion performance. These could be exhaust gas properties, temperature, exhaust flow rate and exhaust gas species concentrations. The DOC's inlet temperature is the most important parameter affecting its efficiency. To activate DOC at required lower temperatures, the use of alternative fuels, efficient heating strategies, catalysts' insulation strategies, a thermal energy storage (TES) system strategy combined with phase change materials (PCM) for advanced thermal management of aftertreatment systems have been studied [16, 99, 100]. This TES system integrated into the exhaust gas aftertreatment system works as storage of the excessive thermal energy during high load engine conditions, and supplies this thermal energy to the catalysts when their temperature is low in cold-start conditions, to prevent the catalyst from experiencing light-out [99, 101]. This TES with PCMs has the capability to reduce up to 84% of HCs and 91% of CO emissions in cold-start conditions [102].

Electrically heated catalysts (EHC) as efficient heating strategies in aftertreatment systems deliver thermal energy directly. The vehicle's battery or an on-board electricity generator is used as an electrical energy source [103-105]. This system is very compatible

with hybrid vehicles, which prevents the high level of energy coming from engine's fuel as the main energy source. Also, it is an effective method for emission and fuel consumption reduction. Its compatibility with HEVs indicates the potential for $CO_2$ mitigation [6]. Pace et al. [7] presented an improvement in fuel economy with the use of EHCs as a thermal energy source, to increase the catalysts' temperatures. The presence of an EHC reduced light-off times by at least three minutes, compared to the fuel enrichment method [106].

## 2.6. Summary

In this chapter, emissions from transport are briefly presented and then potential emissions mitigation technologies and strategies are discussed. Use of alternative fuels, and their physical and chemical properties, as renewable biofuels are also introduced. Different diesel engine aftertreatment technologies such as the DOC, SCR and DPF were explained too. The need for the thermal management of the aftertreatment systems for high conversion efficiency in cold-start and low-load engine conditions is highlighted in this chapter. The advantages of the alternative fuels and efficient heating strategies were described as a short-term solution to control vehicles' emissions.

Overall, this chapter introduces the main literature and motivation related to this thesis which is to examine the tribological behaviour of alternative fuels, combustion, emissions and particulate matter characteristics and aftertreatment performance interacting with this fuel combustion.

Based on the previous studies in the literature, there are some areas needing further research to discover the alternative fuels' characterisation and the impact of their molecular structure on aftertreatment performance, in order to reduce gaseous

emissions and particulates. Differences in the molecular structure of fuels affect their physical and chemical properties, such as lubrication and tribological behaviour. Furthermore, they affect the physical and chemical processes that occur during atomisation, vaporisation and combustion of the fuel inside the combustion chamber. These in turn affect the fuel energy release rate, the combustion behaviour and pollutant formation from various fuels' molecules.

Trends in this research area show the scope for investigation of alternative fuels to reduce gaseous emissions and particulate matter from diesel engines while maintaining the engine condition. Furthermore, use of an exhaust catalytic aftertreatment system seems to be a good option to comply with emissions' standards' legislation. It is obvious that the type of fuel, engine behaviour and aftertreatment system's efficiency are worthy of study in the scope of this research. The concentration and composition of the exhaust gas produced from different alternative fuel's combustion could affect the catalytic activity at different temperatures. The development of alternative fuels' combustion, interacting with a thermally managed efficient diesel aftertreatment system, requires further experimental research to fulfil emission legislation standards.

# CHAPTER 3. METHODOLOGY

This chapter describes the experimental facilities that have been used for this research. This includes all tested fuels, fuel characterisation instruments, the specification of the diesel engine and the emission analysers' instrumentation.

## 3.1. Fuel Characterisation

In total, six different fuels: n-butanol, n-pentanol, cyclopentanol, cyclopentanone, gasoline and the reference diesel fuel were tested to study the influence of molecular structure features on fuel properties, combustion behaviour, emissions' production and aftertreatment efficiencies. A fossil-derived fuel was tested as a reference fuel at the start and end of every day of the experimentation to monitor the experimental variations. In addition to the repeat testing of the reference diesel fuel, the test conditions were repeated at least twice to provide indications of any experimental errors. The repeatability of the results was explained for each instrument. Gasoline-diesel blended fuels as a baseline mixture for gasoline-type fuels were studied based on their great potential, as discussed in Chapter 2 [92].

The diesel and gasoline used for this study were supplied by Shell Global Solutions UK. The diesel was neat, normal, European ultra-low sulphur diesel (specification EN 590) and the gasoline was normal, European gasoline (specification EN 228). The butanol, pentanol, cyclopentanol and cyclopentanone were purchased from Sigma Aldrich UK. The molecular structure of these tested fuels is listed in Figure 3-1. The main physical and chemical properties of neat alcohols, ketones, diesel and gasoline fuels are shown in Table 4-1.

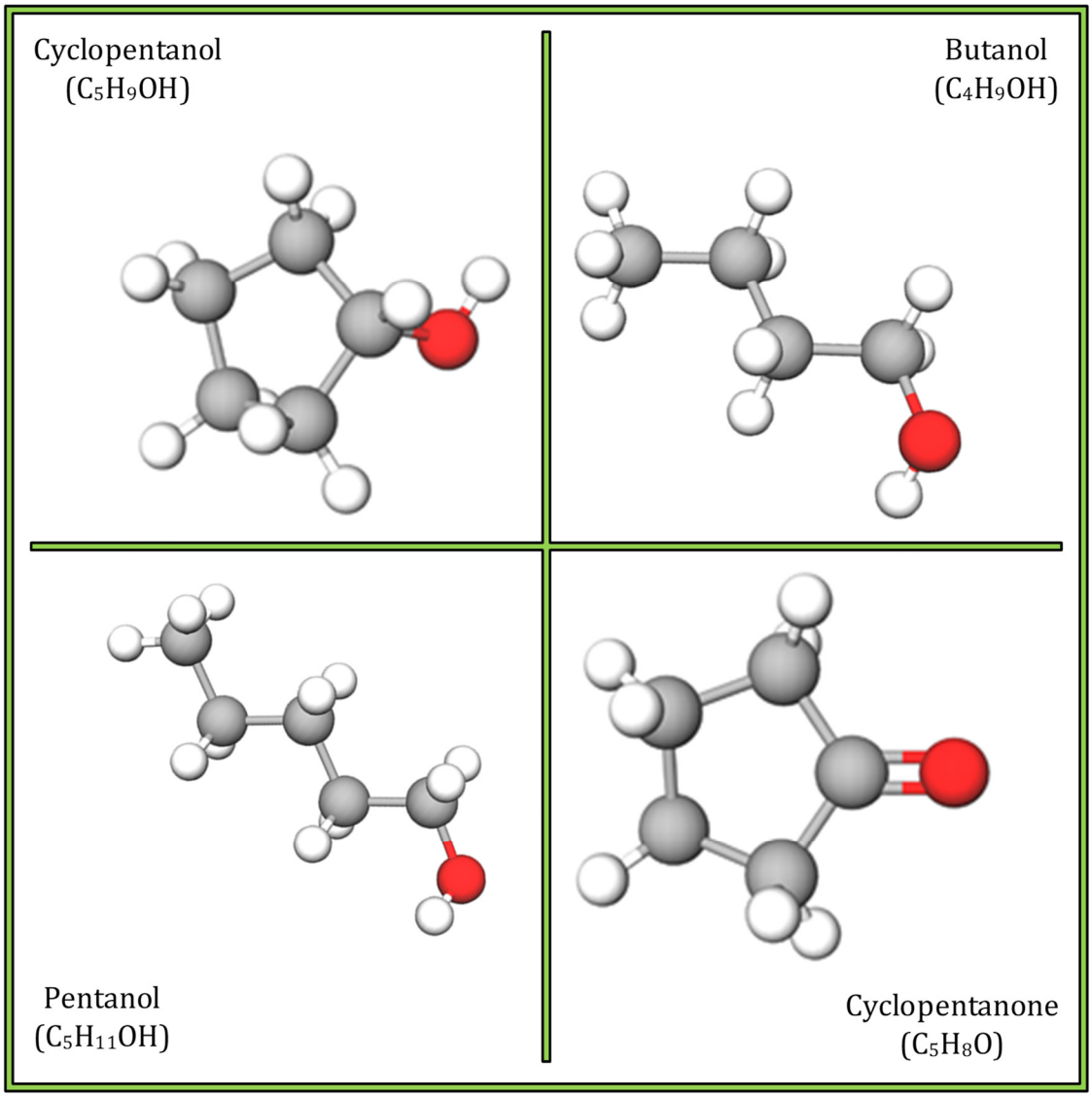



Figure 3-1: Molecular structure of the neat tested fuels

For this thesis, for the lubrication and fuel properties' studies the concentrations of the blends are 20%, 40%, 60% and 80%, including the blend of the gasoline-diesel samples. Also, based on the research findings from Chapter 4, for combustion in the CI engine, only 20% (v/v) of the alternative fuels were blended with 80% (v/v) of the diesel fuel.

The blending stability of these alternative fuels was investigated based on the literature. Alcohols with three or more carbons indicate better blending stability than short-chain alcohols; this is due to their lower polarity. The stability of propanol, butanol and pentanol is very similar, and the difference in their stability appears at high concentrations of around more than a 60% ratio; their unstable blends are due to the appearance of a gel phase. The stability of ethanol and methanol is more sensitive to temperature and the appearance of a liquid phase separation. In addition, the low stability of ethanol and methanol blends make it very difficult to investigate their properties [38, 40]. Filter plugging problems are one of the main concerns for new alternative fuels which should be investigated. Bio-alcohols as a sustainable alternative for diesel engines have the potential to improve the cold-flow properties. Heavier alcohols with more carbon numbers show an advantage in the cold filter plugging point, pour point, cloud point and freezing point. An equation was proposed by Lapuerta et al. [38, 40] to estimate the cold filter plugging point of the alcohols which indicated that CFPP values are higher for long carbon chain alcohols. This equation was also extended for cyclopentanone and shows the same trend. This method is confirmed with experimental results which were presented in the literature. They indicated that in alcohol groups only some ethanol blends could have some filter plugging problems in cold conditions [40]. The CFPP modelled results indicate that a high alcohol concentration would be good for cold weather, but due to the low cetane number of higher concentrations it is not suggested to use high concentrations and neat alcohols in current diesel engines. Following on, the density, viscosity, surface tension and lubricity of the fuels were studied.

### 3.1.1. Kinematic Viscosity

The viscosity of the fuel samples has been analysed with an ultra-shear viscometer (USV) provided by PCS Instruments, UK [107]; and then based on the Grunberg-Nissan equation [108] for binary blends, the absolute viscosity was calculated and compared with measured values, and they were in good agreement. The USV can carry out fully automated viscosity measurements over a shear rate range from $10^6$ $s^{-1}$ to $10^7$ $s^{-1}$ and temperatures between 40 °C and 150 °C. The meter is fitted with a DC servo motor capable of speeds of over 20,000 rpm and an electromagnetic clutch which engages the rotor for only a very short time of around 100 ms. This brief shearing interval minimizes the shear heating in the lubricant. The motor and clutch are controlled by the built-in micro-processor which also logs torque data from a piezo force transducer coupled to the stator. The results were analysed to adhere to the ASTM D6751-15a and ISO 3150 standard specifications; where they are required to be between 1.90 $mm^2s^{-1}$ and 6.00 $mm^2s^{-1}$ [39, 107]. The USV temperature control system checks the test sample temperature within 0.1 °C of the target temperature. All the tested results are the average of three measurements to guarantee reliability of results. The accuracy of the results shows an achievement of only a 2% error in the repeatability of the viscosity value. For high shear rates at high temperature, the repeatability was as good as 0.03 mPa.

Based on the EN 590 standard, diesel fuel viscosity should be more than 2 cSt [38]; so all the cyclopentanol, cyclopentanone, pentanol and butanol blended with diesel fuel with different concentrations are suitable for use in diesel engines based on the legislated limits.

### 3.1.2. Surface Tension

A Sita Proline T15 tension meter system was used to obtain the dynamic surface tension measurements as it complies with the ASTM D971 standards. The tested fuel samples for surface tension measurements were kept constant at 25 °C. For this test, a maximum bubble pressure method was used with a Sita Proline T15 Tension meter [39, 109]. This method makes use of the bubble pressure which is higher than the surrounding water environment. The gas which is pumped into the fluid creates some bubbles as shown in Figure 3-2 [39, 109]. The meter adjusts the bubble lifetime in a 15 ms to 15000 ms range and is capable of measurements within 10 $mNm^{-1}$ to 100 $mNm^{-1}$. To monitor the repeatability of the results, tests were repeated three times in different periods of the year during the engine tests' duration; the final results are an average of these findings.

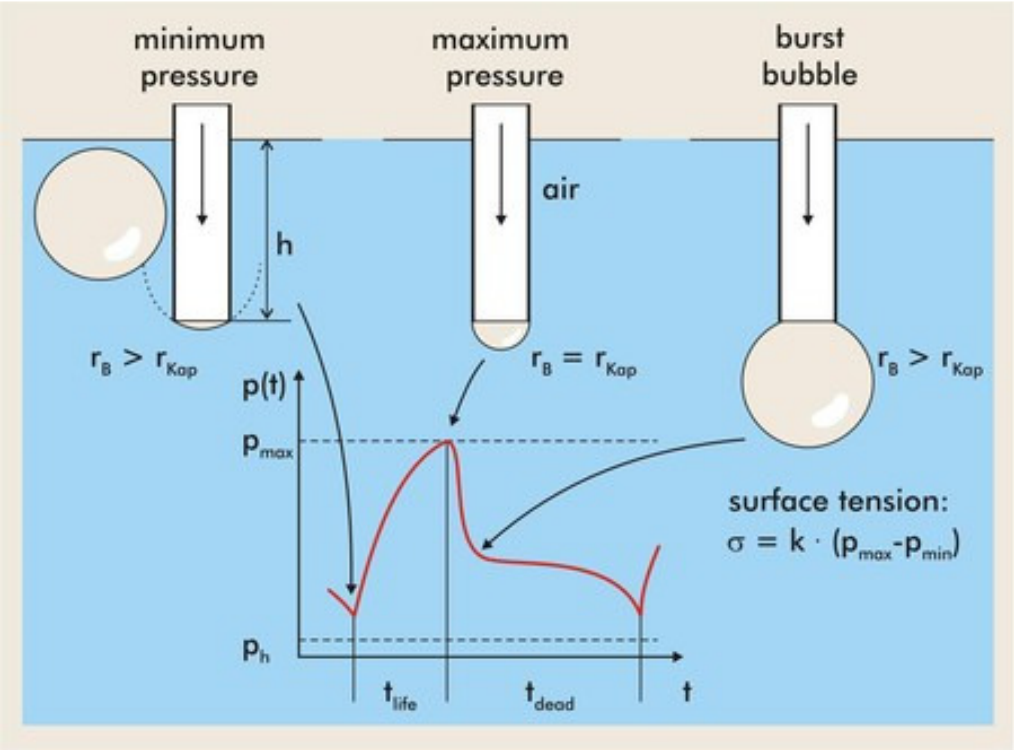



Figure 3-2: The Sita T15 surface tension meter method [109]

### 3.1.3. Calorific Value

The lower heating value measurements were carried out in an IKA C200 calorimeter with the oxygen bomb method under the following specific conditions and assumptions: a temperature of 25 °C for the fuel and its combustion products; and the decomposition vessel to be filled with 99.5% pure oxygen at a pressure of 30 bar to optimize the combustion process. The heat of combustion is computed from temperature observations before, during and after combustion, with the proper allowance for thermochemical and heat transfer corrections. Tests were also repeated three times in different periods of the year to monitor the repeatability of the findings.

The tests were done to adhere to the EN 14213 standard with a minimum value of 35 MJ $kg^{-1}$. The higher (gross) heating value (HHV) was measured and then the lower (net) heating value (LHV) was calculated based on the following equation, taking into account the hydrogen presence in the fuel [39, 110].

$$Q_n = Q_g - 0.2122 \times H \qquad \text{Equation 3-1}$$

where:

$Q_n$= Net heat of combustion (LHV), $MJ.kg^{-1}$

$Q_g$= Gross heat of combustion (HHV), computed from instrument, $MJ.kg^{-1}$

$H$= mass % of hydrogen in the sample

## 3.2. Analysis of Lubrication Mechanisms

Various experimental methods exist to investigate the lubricity and tribology behaviour of liquid fuels and oils. In this study, a high frequency reciprocating rig (HFRR) is used in accordance to European standards for the measurement of lubricity. The HFRR

was supplied by PCS Instruments, UK [111] as shown in Figure 3-3 schematically. The HFRR is a microprocessor-controlled reciprocating friction and wear test system which provides a fast and repeatable assessment of the performance of fuels and lubricants. It has become the industry standard test for diesel fuel lubricity and confirms ASTM D6079, ISO 12156 and EN 590. The technical data for the HFRR is summarized in Table 3-1 [111].

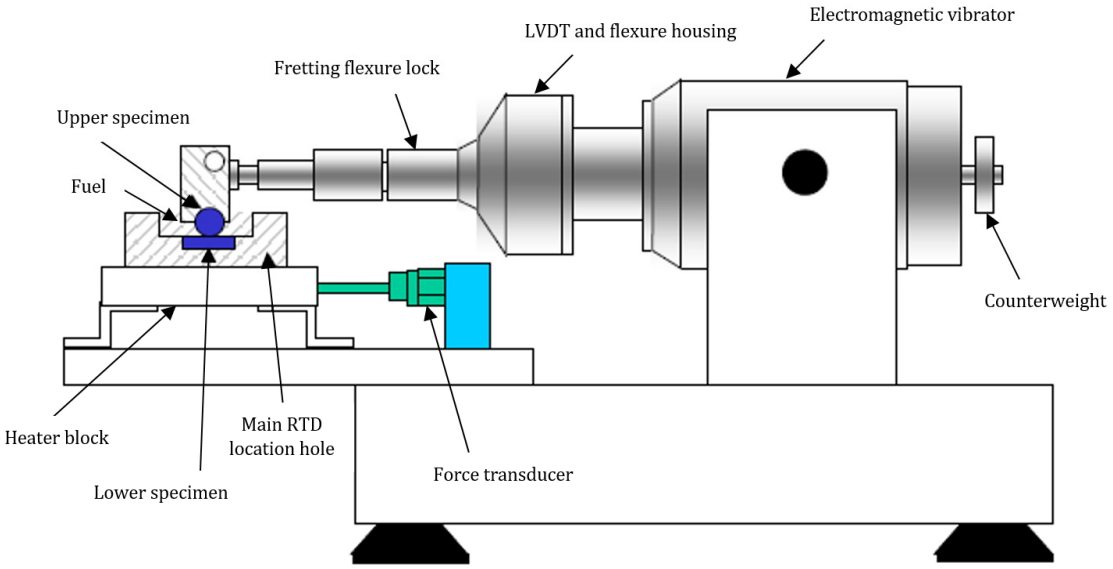



Figure 3-3: The HFRR experimental set-up

Table 3-1: The HFRR technical data

| Operating conditions | |
|---|---|
| Frequency | 10 to 200 Hz |
| Stroke length | 20 µ to 2.0 mm |
| Load | 0.1 to 1.0 kg |
| Maximum friction force | Max 10.0 N |
| Temperature | Ambient to 150 °C |
| Standard upper specimen | 6.0 mm diameter ball |
| Standard lower specimen | 10.0 mm diameter × 3.0 mm thick disc |

The system has the mechanical and the control units linked to a computer to allow data logging, graphical representation of test parameters and results file storage. The unit also has the capability to control humidity with the provided probe option, where output is automatically logged at the beginning and end of the test in accordance with the test method.

The control software has the capability for a user-defined profile with different temperatures and frequencies in addition to the HFRR standard for the diesel fuel lubricity test process. The HFRR results such as the friction force between the upper and lower specimens, the contact resistance (film) value, and the test fluid temperature are always displayed and saved in a graphical format throughout the test, and in text format after the test, respectively.

For safer and more repeatable lubricity testing of volatile fuels such as gasoline, the gasoline conversion kit has been developed. This reduces the toxicity of the volatile samples too. The high volatility of gasoline-type fuels means that even at room temperature a significant fraction of the samples will evaporate from an open specimen holder, changing the blend concentration in the remainder and posing an explosion hazard. The gasoline lower test specimen holder has been designed to hold up to 15ml of test fuel. The most innovative part of the design of the gasoline kit is the use of a two-piece PTFE sliding seal. The larger outer ring clips securely around outside of the volatile fuel sample. The upper specimen holder is inserted through the hole in the smaller inner part of the seal which forms the upper part of the sliding seal. This kit prevent any evaporation of volatile fuels and leads to more repeatable results.

The HFRR humidity-controlled cabinet is designed as an additional accessory for the HFRR test bed for running tests at a constant temperature and relative humidity. The

cabinet temperature can be controlled from ambient up to 50 °C with a stability of ±1 °C. The relative humidity within the cabinet can also be adjusted between 0% and 100% using appropriate non-toxic salt solutions. The ambient temperature and humidity are recorded using the HFRR integrated humidity probe.

The atmospheric condition before, during and after the test has a significant influence on the result of the lubricity experiment and final wear scar. The acceptable ranges of atmospheric conditions and relative humidity are shown in Figure 3-4:

1) Unacceptable range of condition (too moist),

2) Acceptable range of condition,

3) Unacceptable range of conditions (too dry) [111].

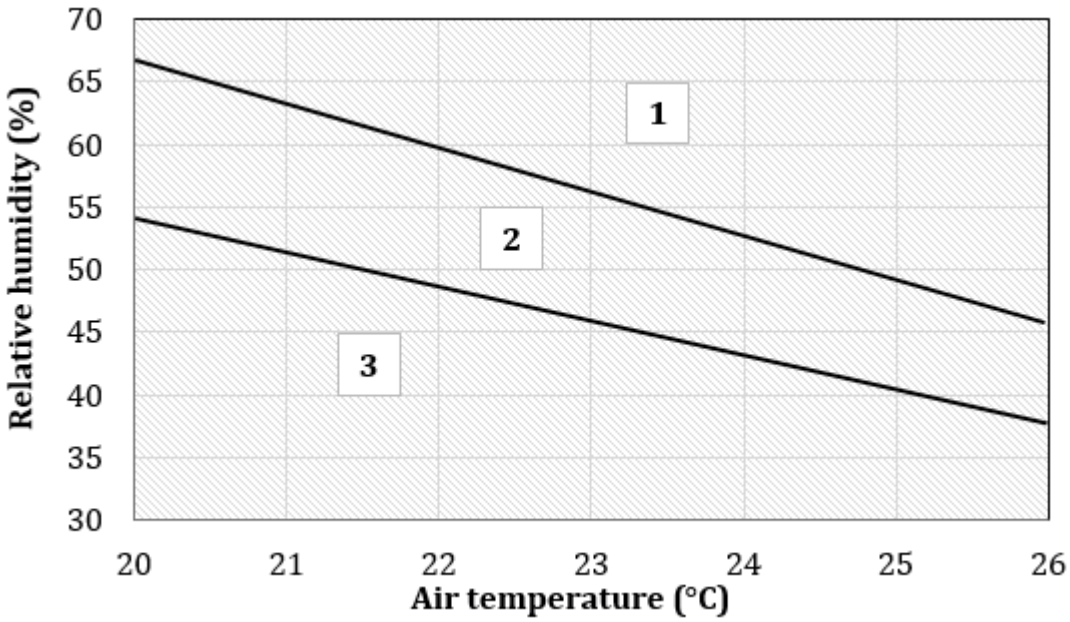



Figure 3-4: The HFRR acceptable test condition (ISO 12156 -1) [111]

Before the beginning of the experiments, the HFRR must be calibrated to confirm accurate operation of the test rig. To check the repeatability and error of the experiments,

after each 6 experiments the device was calibrated. The test specimens consisted of a 6 mm diameter steel ball and steel disc. The HFRR has the capability of carrying out tests based on different standards. For this study, all tests were conducted according to EN ISO 12156-1:2016 standard as listed in Table 3-2 [111, 112]. This included the fuel temperature maintained at 60°C and the volume of the fuel sample used set at 15 ml.

Table 3-2: HFRR ISO 12156-1 test condition

| Parameter | Value |
|---|---|
| Fluid volume | 15±0.2 ml |
| Stroke length | 1±0.02 mm |
| Frequency | 50±1 Hz |
| Fluid temperature | 60±1°C |
| Test load mass | 200 g |
| Test duration | 75±0.1 minutes |

The humidity control cabinet increases the repeatability and consistency of the tests. During the tests, the disc was fully submerged in the tested sample fuels at a reciprocating frequency of 50 Hz for 75 minutes. The HFRR reported the friction coefficient and lubrication film concentration. At the end of each test, all components were cleaned using acetone. To attain the best performance for the rig, the wear scar for the reference diesel fuel was measured after each 12 experiments (at the end of each day).

A, Meiji Techno, Somerset, UK, microscope with a 100× magnification lens camera was used for measuring the length of the wear scar on the tested ball in the X and Y directions. This was connected to a computer that allows the user to capture a calibrated image of a wear scar of the upper specimen and measure the wear scar on the controller's computer screen. The wear scar image and measurements were saved and compiled with the test data file. The appearance of the wear scar on the upper specimen (ball) was

different for each tested fuel, so the photographic images needed to be analysed by a camera. As shown in Figure 3-5, the wear scar with an indistinct boundary needed to be analysed: where, (1) is the test ball, (2) is the unworn area, (3) is a less distinct worn area and (4) is a worn area.

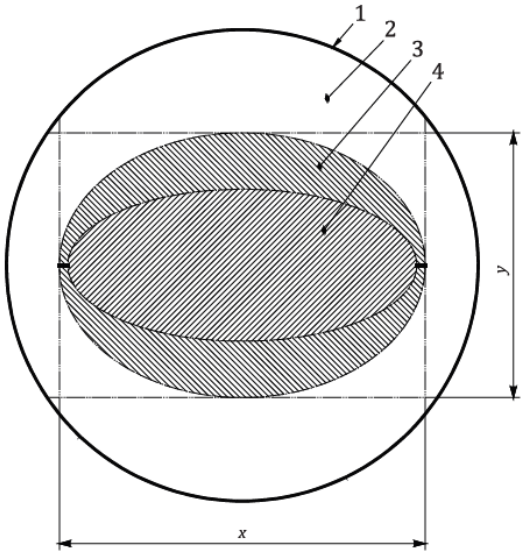



Figure 3-5: The example of a wear scar (ISO 12156-1)

From the above image the average wear scar diameter was calculated based on the following equation:

$$WSD = \frac{x+y}{2} \qquad \text{Equation 3-2}$$

where $x$ is the wear scar dimension perpendicular to the oscillation direction, expressed in micrometres (μm) and $y$ is the wear scar dimension parallel to the oscillation direction, expressed in micrometres (μm), as both shown in Figure 3-5.

To consider the ambient temperature and the presence of the humidity which significantly affects the fuel lubricity during the test, acceptable test conditions from

Figure 3-4 the European standard of diesel fuel lubricity [111] required approximately 25% to 65% humidity at an ambient temperature of 25 °C.

It should be mentioned that all of the experimental data for the fuel lubricity studies in this research are the average of multiple measurements. All the HFRR lubricity experiments were repeated at least twice and repeatability was demonstrated to be less than 20 μm.

Also, in order to analyse the wear scar on the disk as well as measure the wear scar depth, measurements of the worn surface were made using JCM-6000 plus NeoScope-SEM/EDS Benchtop JEOL UK Ltd. This is equipped with high sensitivity semiconductor detectors found in high-end instruments, making it easy to acquire composition contrast information about the specimen and enabling efficient analysis with a wide magnification range from the lowest 10x for a wide area of view up to 60,000x. It has a high sensitivity solid-state backscatter detector, which provides both composition and topographic information. Finally, the surface of the lower disc test sample was analysed using a 10× magnification lens on a G5 Infinite Focus optical 3D microscope Alicona UK Ltd, Kent, UK. This instrument allows for complete 3D surface analysis. Measurements were used for the analysis of surface roughness and wear scar depth size. The way that wear scar dimeter and depth were measure are presented in Figure 3-6. For surface analysis based on the instrument standards ISO 4287, three main profiles which are called as primary profile (structure parameter), roughness profile (roughness parameter) and waviness profile (waviness parameter) could be analysed. But for the purpose of this research roughness profile is measured based by taking average of at least five profile measurement from surface of worn area.

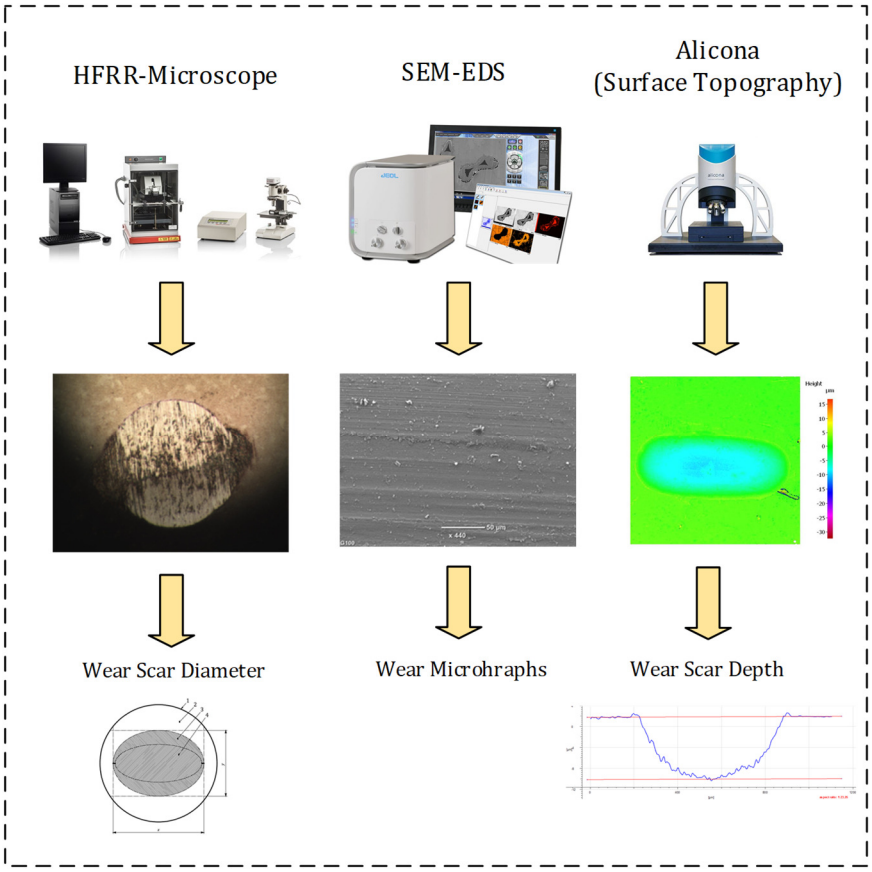



Figure 3-6: Methodology for Lubrication and tribology experiments

## 3.3. Engine Test Bed and Instrumentation

This section describes details of engine experimental and analytical systems used for the current research work. This includes a description of the laboratory, the engine test bed, the emission and particulate analysers, as well as the measurement and analysis of the engine performance and emission characteristics.

### 3.3.1. Engine Laboratory

All engine experiments presented in this thesis were done in the ‘‘Future Fuel and Engine Lab’’ in the Vehicle Research Technology Centre within the Department of Mechanical Engineering at the University of Birmingham. The laboratory as shown in

Figure 3-7 was specially designed and equipped for engine test bed experimentation and consisted of two rooms: an engine test cell and an engine control room. In the engine control room, all the engine control, data acquisition systems and emission analysers' computers were located. Control of the engine was conducted in the control room, with an armoured glass window between the control room and the test cell for safety reasons and to allow clear observation of the experiments. The engine test cell has single and two-phase electrical power, along with cooling water, compressed air, gaseous fuels' pipelines, and heating and exhaust gas extraction.

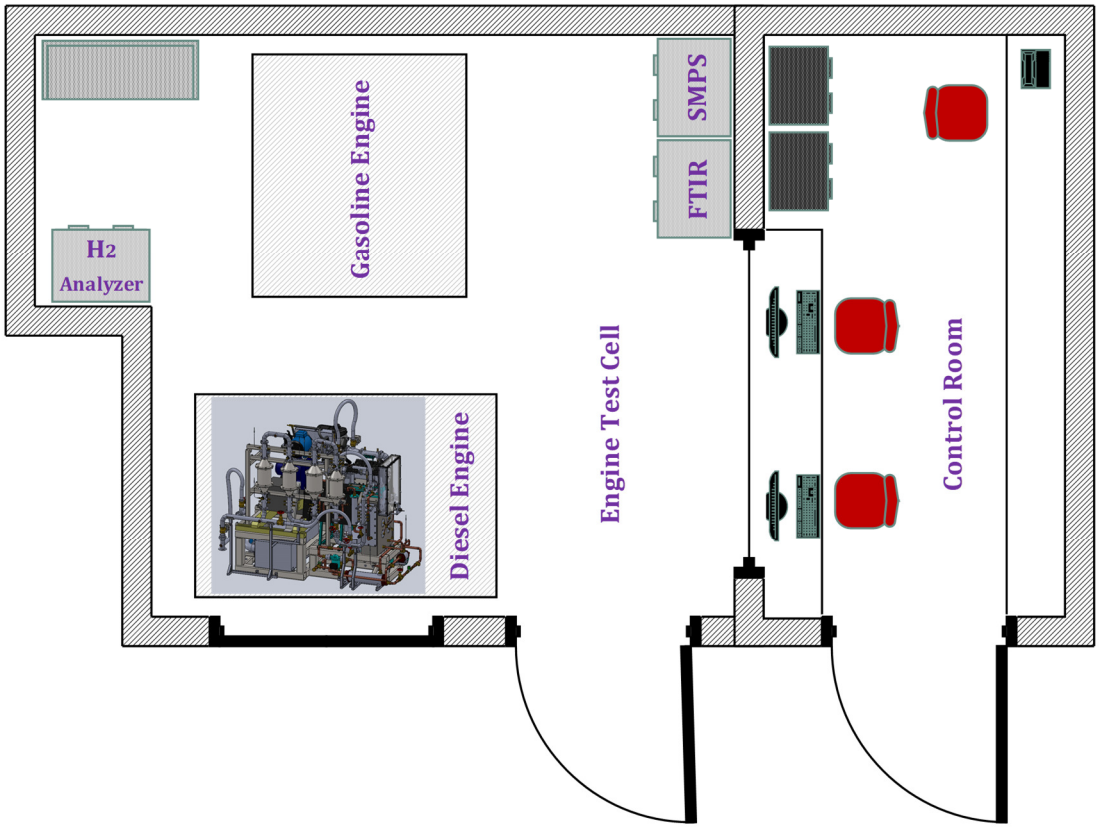



Figure 3-7: The engine laboratory

### 3.3.2. Single Cylinder Research Diesel Engine

For the engine combustion experimental set-up, a single cylinder research diesel engine was used as shown in Figure 3-8. Figure 3-9 indicates the schematic experimental set-up which has been used for this work. The engine technical data and specifications are summarized in Table 3-3. The four-stroke diesel engine is naturally aspirated, water cooled, EGR equipped and utilises a common rail direct fuel injection. An alternating current (AC) electric dynamometer was used to motor and load the engine. The engine was fuelled with diesel fuel supplied by Shell Global Solutions UK, as a reference fuel and four other fuels blended with diesel as explained in previous sections. The engine has an exhaust gas recirculation (EGR) system, but for the purpose of this research, it wasn't considered in the test conditions.

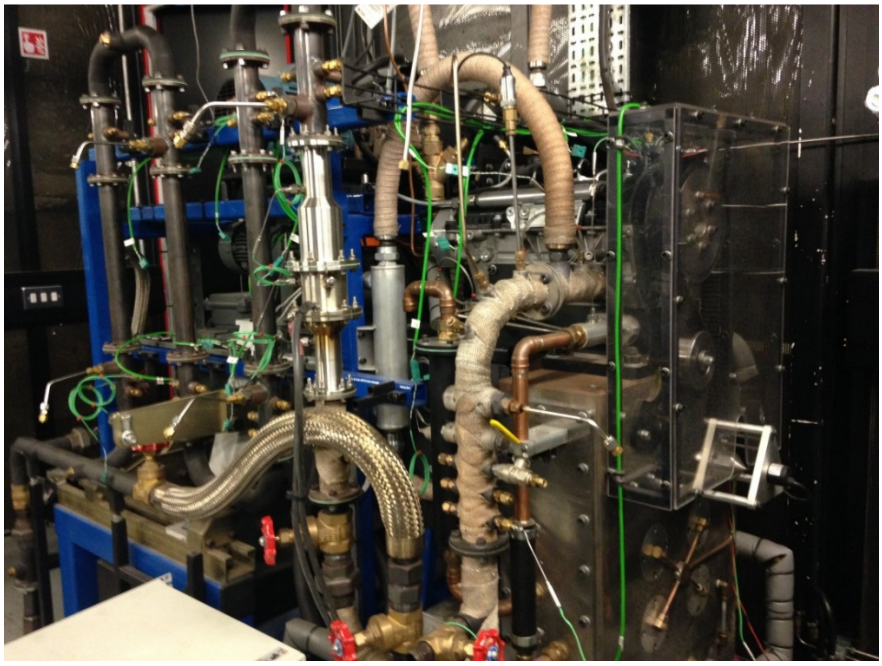


Figure 3-8: Single cylinder research diesel engine test bed

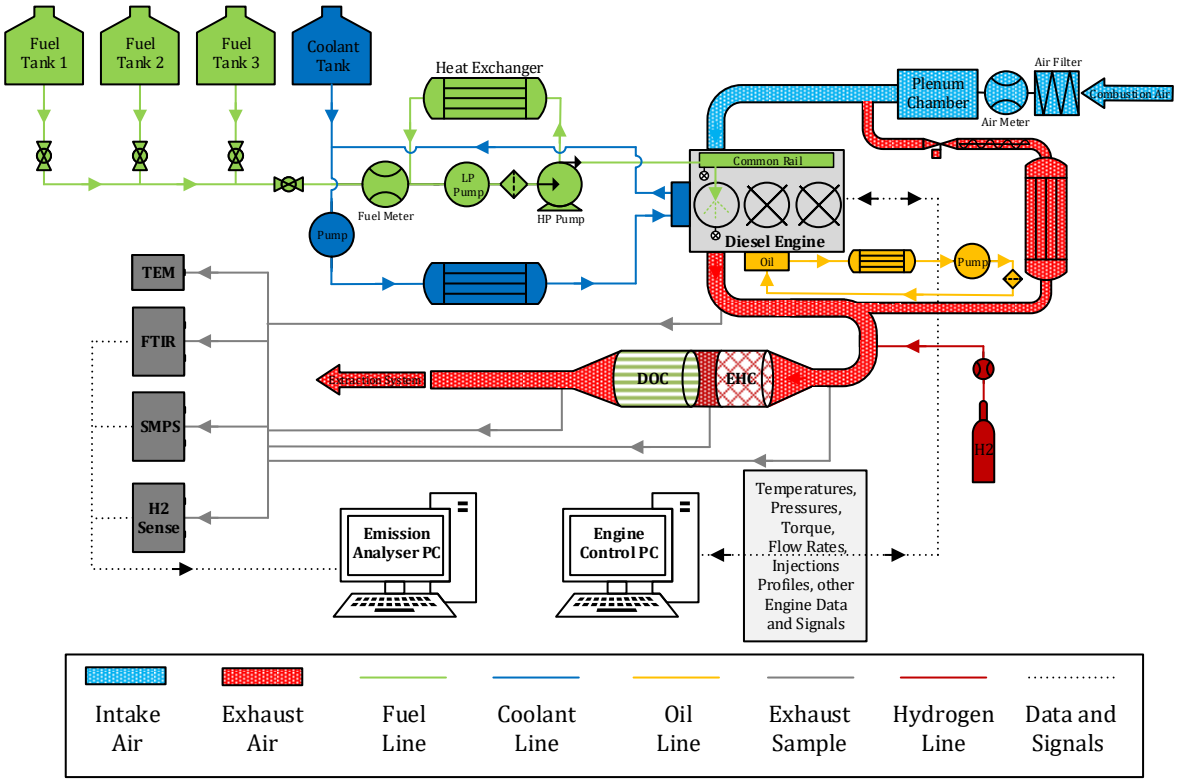



Figure 3-9: Experimental set-up diagram

Table 3-3: Test engine specifications

| Engine specification | Data |
|---|---|
| Number of Cylinders | 1 |
| Bore | 84 mm |
| Stroke | 90 mm |
| Connecting Rod Length | 160 mm |
| Displacement Volume | 499 $cm^3$ |
| Compression Ratio | 16.1:1 |
| Maximum Injection Pressure | 1500 bar |
| Emissions' Standard | Designed for Euro 5 |

An AVL GH13P pressure transducer mounted in the cylinder head was used to record in-cylinder pressure and its signal was amplified by an AVL FlexiFEM 2P2 amplifier. Also, a digital shaft encoder producing 360 pulses per revolution measured the crank shaft

position. The pressure and crank shaft position data was combined to create an in-cylinder pressure trace. The temperatures at different points, such as on the exhaust manifold, before the electrical heater, before the DOC, after the DOC and at other engine set-up parts were recorded by using k-type thermocouples and a Pico Technology TC-08 thermocouple data logger. To monitor the air/fuel ratio in all tested conditions, an airflow meter was used to measure the engine intake air flow. Then λ as a ratio of actual air/fuel ratio to stoichiometric air/fuel ratio was calculated and checked for all tested conditions.

An in-house developed LabVIEW programme connected to a National Instruments PCI-6023E data acquisition device was used to monitor and control the engine operating conditions, such as injection pressure, timing and duration. To confirm combustion stability and minimize cyclic variability, the coefficient of variation (COV) of the IMEP for 200 cycles was monitored and kept below 4% during the testing procedure. The LabVIEW programme analyses the engine's indicated mean effective pressure (IMEP) for each cycle by considering the equation below:

$$IMEP = \frac{Indicated\ Work\ per\ Cycle}{Displaced\ Volume} = \frac{\oint pdV}{V_d} \qquad \text{Equation 3-3}$$

In-cylinder pressure data was pegged to have the same in-cylinder pressure at the bottom dead centre of the intake stroke and intake manifold [113]. With logged average data of the in-cylinder pressure in 200 engine operating cycles, the heat release rate was obtained based on the equation below:

$$\frac{dQ}{d\theta} = \frac{\gamma}{\gamma-1} P \frac{dV}{d\theta} + \frac{1}{\gamma-1} V \frac{dP}{d\theta} \qquad \text{Equation 3-4}$$

where $Q$ is heat release; $\theta$ is crank angle degree; $\gamma$ as the heat capacity ratio ($\frac{Cp}{Cv}$) is the ratio of specific heats; $P$ is in-cylinder pressure in Pa; and $V$ is in-cylinder volume in

$m^3$. In addition to these, combustion phasing (AHR-50), combustion duration and ignition delay were monitored, as well.

Under steady-state condition, the engine's fuel consumption was recorded and its corresponding indicated specific fuel consumption (ISFC) was calculated by the equation below:

$$ISFC\ (\frac{g}{kWh}) = \frac{\dot{m}_{Fuel}}{Indicated\ Power} \quad \text{Equation 3-5}$$

Also, the indicated thermal efficiency (ITE) of the tested conditions was calculated based on the following equation to monitor the same efficiency of the tested fuels.

$$ITE = 100 \times \frac{Indicated\ Power}{\dot{m}_{Fuel} \times Q_{HV}} \quad \text{Equation 3-6}$$

where $\dot{m}_{Fuel}$ is the fuel consumption rate ($kg.s^{-1}$); and $Q_{HV}$ is the fuel's higher heating value ($J.kg^{-1}$).

Also, in the gaseous emissions' analysis, FTIR measures the gaseous species in ppm (v/v) format, which was converted into the brake specific format (g/kWh).

To ensure consistency, the engine was warmed up for approximately one hour prior to testing. The engine's oil, coolant and fuel temperature, and the test cell's atmospheric conditions were monitored. The engine operating conditions are summarized in Table 3-4; 1500 rpm with 2 bar and 4 bar IMEP were selected as the engine rotational speed and load respectively, to reproduce low-load driving conditions. The common rail fuel injection pressure was set at 550 bar and 650 bar based on the condition. The pilot fuel injection was set to start at 15 °bTDC with the duration of 0.150 ms; whereas the main injection started at 3 °bTDC with the variable duration of around 0.443 ms to have constant IMEP. In the studied cases there is not any post fuel injection.

Table 3-4: Engine test conditions abbreviations and colour codes

| Test abbreviation | | Fuel blends with diesel (%v/v) | Engine speed (rpm) | Fuel injection pressure (bar) | IMEP (bar) | Injection timing BTDC-(CAD) | |
|---|---|---|---|---|---|---|---|
| | | | | | | Pre | Main |
| D100L | | Diesel 100% | 1500 | 550 | 2 | 15 | 3 |
| B20L | | Butanol 20% | 1500 | 550 | 2 | 15 | 3 |
| P20L | | Pentanol 20% | 1500 | 550 | 2 | 15 | 3 |
| CP20L | | Cyclopentanol 20% | 1500 | 550 | 2 | 15 | 3 |
| CPK20L | | Cyclopentanone 20% | 1500 | 550 | 2 | 15 | 3 |
| D100M | | Diesel 100% | 1500 | 650 | 4 | 15 | 3 |
| B20M | | Butanol 20% | 1500 | 650 | 4 | 15 | 3 |
| P20M | | Pentanol 20% | 1500 | 650 | 4 | 15 | 3 |
| CP20M | | Cyclopentanol 20% | 1500 | 650 | 4 | 15 | 3 |
| CPK20M | | Cyclopentanone 20% | 1500 | 650 | 4 | 15 | 3 |

### 3.3.3. Aftertreatment System and Instrumentation

The advanced thermal aftertreatment system was designed and built by a previous PhD student, Dr Mohammadreza Hamedi. Its detailed design description and modelling studies can be found in his PhD thesis [16]. The engine exhaust aftertreatment system consists of an efficient heater system (electrically uncoated heated catalyst-EHC) and a diesel oxidation catalyst (DOC). The size of the aftertreatment reactor was selected to keep comparable gas hourly space velocity (GHSV) to commercial multi-cylinder diesel engines' exhaust aftertreatment systems. The GHSV is a measure of the volumetric flow rate of the exhaust reactant feed divided by the volume of the catalytic monolith, based on the following equation:

$$GHSV\ \left(\frac{1}{h}\right) = \frac{Reactant\ feed\ flow\ rate\ \left(\frac{m^3}{h}\right)}{Catalyst\ bed\ volume\ (m^3)} \qquad \text{Equation 3-7}$$

The tested DOC in this study was purchased from Johnson Matthey PLC with the dimensions of 101 mm in length and 58 mm in diameter. The ceramic catalyst substrate was made of cordierite with at cell density of 600 cpsi and wall thickness of 3 mil. The

catalyst was coated with a platinum group metals' (PGM) loading of 100 g/ft$^3$ and formulation ratio of 2:1:0 for platinum, palladium and rhodium respectively. Zeolite was also incorporated into the catalyst coating for improved low-temperature hydrocarbon adsorption and oxidation. At Johnson Matthey PLC, the DOC was hydro-thermally aged at 700 °C for 16 hours prior to testing. Prior to any experiment conditions, the catalyst was thermally conditioned in a furnace at 550 °C for 6 hours. It was also thermally conditioned in the aftertreatment system by turning on the electrical heater at 350 °C to 550 °C for 30 minutes before the catalyst light-off experiments, to limit any possible physisorption or chemisorption effects. Light-off experiments were repeated three times to check the constancy and repeatability of results. Light-off results which are presented as T50, is a DOC inlet temperature where conversion efficiency of that specific emissions reach to 50%.

The S shape electrical heater was supplied from Continental Emitec GmbH with the dimensions of 60 mm in length and 63 mm in diameter. It is made of a metallic substrate with 130 cpsi cell density and wall thickness of 2 Mil. The heating element has a resistance of 0.08 Ω with a maximum operating voltage of 12 V. In this study, the heater was not coated and it was essentially used as an exhaust gas heater to investigate the efficient heating strategy effects individually. However, for commercial uses it can be coated for packaging purposes when used on a vehicle. The heater was powered using a TDK-Lambda GEN12.5-120 power supply which can deliver variable voltage up to 12.5 V and variable current up to 120 A. The aftertreatment reactor was packaged in an in-house designed stainless-steel canning as shown in Figure 3-10 [16].



Figure 3-10: Aftertreatment reactor set-up

As schematically illustrated in Figure 3-9, the exhaust gas travels from the exhaust manifold and passes through 164 cm of pipework to reach the main aftertreatment reactor. This configuration helps to cool down the exhaust gas considerably and provides a more challenging environment for the emissions' reduction in the aftertreatment system. Three thermocouples were integrated into the reactor to measure the temperature before the electrical heater, after the heater (before the DOC) and after the DOC. Heated exhaust gas sampling lines were used to direct the exhaust gas to the emissions' analysers from the exhaust manifolds, before the reactor, before the DOC and after the DOC. Also, the sampling lines' temperature was kept at 179 °C to avoid hydrocarbon condensation and nucleation.

Instead of using a furnace for light-off investigation, the on-board electrical heater (its application and advantages have been previously explained), was used for the catalyst light-off investigations. In addition to the emissions' concentration, the conversion efficiency of

these emissions was plotted versus the diesel oxidation catalyst inlet temperature, to analyse the catalyst's activity at a given temperature.

### 3.3.4. Emission Analysers

In this study, legislated regulated European emissions are analysed. This includes HCs, CO, $NO_x$ and PM emissions. The study of gaseous emissions and particulate matter emissions is the main aim in this research work.

For the analysis of the engine's exhaust gaseous emissions a MKS MultiGas 2030 Fourier Transform Infrared (FTIR) spectroscopy analyser was used. The FTIR spectroscopy technique distinguishes different gaseous species based on their light absorption characteristics (molecular infrared absorption). The real-time concentrations of the emissions were recorded with the frequency of one hertz and the data was averaged in steady-state conditions. The FTIR spectrum is unique for each gaseous species which make it a highly effective technique for gaseous sample analysis. The following species concentration were analysed: carbon dioxide ($CO_2$), carbon monoxide (CO), nitrogen oxides (NO and $NO_2$), total hydrocarbons (THC), diesel (heavy hydrocarbons), methane ($CH_4$), ethane ($C_2H_6$), ethylene ($C_2H_4$), acetylene ($C_2H_2$), propane ($C_3H_8$), propylene ($C_3H_6$), formaldehyde ($CH_2O$) and water ($H_2O$).

The V&F HSense, as a hydrogen analyser was used to measure online hydrogen concentration in the sampling points. Its method is based on the electron impact ionization mass spectrometry principle. It uses the electron ion source. The gas sample ions are energized and distinguished further on in a magnetic field in order to detect hydrogen concentration [114]. The HSense is currently the only instrument on the market that is capable of monitoring the exhaust's hydrogen levels in real time with a

range of below 1 ppm up to 100%. It has the capability of avoiding cross-interferences that could be caused by $H_2O$ in the exhaust [114].

A TSI Scanning Mobility Particle Sizer (SMPS) was employed for analysis of the PM emissions. This has a 3080 electrostatic classifier, a 3081 differential mobility analyser and a 3775 condensation particle counter. The SMPS measures the size and number distribution of the particles in the exhaust sampling points. It is based on the motion of a charged particle in an electric field. The particles enter in the electrostatic classifier where they are neutralized through a small radioactive source. Then, the particles are categorized in accordance with their mobility in DMA units, resulting in a narrow particles' range of mobility, successfully existing the output slit. The mono-disperse distribution then passes to a CPC unit which can determine the number of particles for the specific sizes.

To use a SMPS it is necessary to use a diluter to achieve the dilution of the sample and avoid nucleation and condensation of moisture or hydrocarbons. The samples were diluted with compressed air at 2 bar; a high-efficiency particle arrestance (HEPA) filter was fitted to precondition the air system. The dilution ratio (DR) based on $CO_2$ or NO concentration before and after the diluter, was measured and controlled based on the equation below to have the same condition for all the testing matrix.

$$Dilution\ Ratio \cong \frac{Before\ Diluter\ CO_2\%\ concentartion}{After\ Diluter\ CO_2\%\ concentartion} \approx \frac{Before\ Diluter\ NO\%\ concentartion}{After\ Diluter\ NO\%\ concentartion}$$

Equation 3-8

### 3.4. Experimental Errors and Repeatablity

In this study, to minimize the experimental variability, uncertainties and error, special care has been taken. Before and after each testing session, the emissions analysers and sampling lines were cleaned with nitrogen gas to remove condensed residuals such as water and impurities. Also, the baseline (zero level) of the emissions analysers (FTIR, HSense and SMPS) was performed, measuring the ambient air through the sampling heated lines as background data, before and after each tested condition. Before testing new fuels in the engine, fuel tanks were cleaned with acetone and left for 24 hours to make sure there was no fuel remaining from previous studies. Prior to testing, the fuel lines and pump were cleaned with the new tested fuels to make sure that there was only the studied fuel in the combustion system. A reference engine operating condition running with diesel was defined and tested before each measurement session, to ensure the repeatability of the experiments.

Furthermore, all the measurements were repeated at least three times and the averaged results are presented. These measurements were additionally repeated when uncertain results were achieved. The repeatability of the results was monitored by the calculation of the standard deviation of the measurements. This repeatability is very important especially in the case of light-off tests, to monitor experimental variability and uncertainty. In most of the presented results' graphs, error bars are shown, too.

Table 3-5 lists some random results of the experiments. Each FTIR measurement is the average of sampling for at least 20 minutes. These measurements were repeated randomly in different periods of the year. Each SMPS result is the average of at least three measurements in a day, which were repeated also in different periods of the year. This is due to reduction in variability of particulate size measurement which is so sensitive to

testing conditions, particularly temperature. The HSense measurements are also the average of at least 20 minutes of sampling on the same day as the other measurements. The standard deviation of all measurements was monitored during this research as one random error experiment result and is presented in Table 3-5.

Table 3-5: Random error experiment to monitor repeatability

| Parameter | CO | $CO_2$ | $NO_x$ | THC | CO | $CO_2$ | $NO_x$ | THC | Total particle concentration |
|---|---|---|---|---|---|---|---|---|---|
| Unit | ppm | | | | g/kWh | | | | $\#/cm^3$ |
| Average | 222.06 | 33633 | 239.52 | 250.2 | 3.0692 | 730.4 | 8.984 | 20.536 | $6.98\times10^6$ |
| Standard deviation | 7.19 | 461 | 8.65 | 8.96 | 0.1 | 10.23 | 0.21 | 0.25 | $2.55\times10^3$ |

### 3.5. Summary

This chapter highlights the experimental setup facilities used in this research: including the tested fuels; the fuel characterisation instruments such as the HFRR and calorimeter; the engine set-up, which is a single cylinder research diesel engine equipped with an efficient heating strategy diesel oxidation catalyst; and emissions' analysers, such as the FTIR, HSense and SMPS.

# CHAPTER 4. INVESTIGATION OF LUBRICATION PROPERTIES AND TRIBOLOGICAL BEHAVIOUR OF BIO-ALCOHOLS AND BIO-KETONES

## 4.1. Introduction

The properties of five different fuels blended with ultra-low sulphur diesel (ULSD) were investigated in this chapter. The detailed experimental set-up and detailed measurement methods were explained in Chapter 3. Surface tension, viscosity and the calorific value of fuels were analysed. Lubrication and tribological mechanisms of these oxygenated fuels were studied by use of various instruments. The main physical and chemical properties of neat alcohols, ketones, gasoline and diesel fuels are shown in Table 4-1. These results are a summary of the literature and also findings of this research. The tested fuels are alcohols and ketones (butanol, pentanol, cyclopentanol and cyclopentanone) blended with diesel at 20% and 40% ratios (volume basis-%v/v). The ratios for the gasoline-diesel blends are 20%, 40%, 60% and 80%. Gasoline-diesel blends were tested as a baseline case due to the great potential of gasoline types fuels in diesel engines [92]. Due to the low cetane number of the alcohols and ketones, low alternative fuel contents were selected. No other additives were used in any of the blends (such as lubricity enhancers). The blends and the diesel properties are also listed in Table 4-2, Table 4-3 and Table 4-4; these were also taken from the literature and from the outcome of the studies described in this chapter.

As mentioned in Chapter 3, all of the experimental data for fuel characterisation and lubricity studies are an average of multiple measurements. The standard deviation of the measurements was calculated and monitored to ensure the high quality of the data.

## 4.2. Fuel Properties

Following on from the viscosity, surface tension, lower heating value and lubricity of fuels which were studied in this chapter, blending stability and other properties of the tested alternative fuels are gathered from the literature. As discussed in detail in Chapter 2, alcohols with three or more carbons indicate better blending stability than short-chain alcohols; this is due to their lower polarity. Heavier alcohols with more carbon numbers show advantages with the cold filter plugging point, pour point, cloud point and freezing point [38, 40]. As explained in Chapter 3, based on the Grunberg-Nissan equation [108] for binary blends, the absolute viscosity could be calculated and compared with measured values, which were in good agreement. As viscosity and surface tension of fuels affect the injection timing, injection pressure and atomization quality during the combustion process, the results indicated that based on the EN 590 standard (diesel fuel viscosity should be more than 2 cSt), all the cyclopentanol, cyclopentanone, pentanol and butanol blended with diesel fuel with different concentrations are useable for diesel engines in contrast with ethanol and propanol [38].

Table 4-1: Physical and chemical properties of neat tested fuels

| Property | Method | Diesel | Gasoline | Butanol | Pentanol | Cyclopentanol | Cyclopentanone |
|---|---|---|---|---|---|---|---|
| Molecular formula | | ~$C_{12}H_{22}$ | $C_{5.88}H_{11.06}$ | $C_4H_9OH$ | $C_5H_{11}OH$ | $C_5H_9OH$ | $C_5H_8O$ |
| Molecular weight (kg.kmol$^{-1}$) | | 166.3 | 81.78 | 74.112 | 88.15 | 86.1323 | 84.12 |
| Purity (%, v/v) | | - | - | 99 | 99 | 99 | 99 |
| Density at 15 °C (kg.m$^{-3}$)[a] | EN ISO 3675 | 834.8 | 746.6 | 811.5 | 814.8 | 949 | 948.7 |
| Kinematic viscosity at 40 °C (cSt)[b] | EN ISO 3104 | 2.627 | 0.8 | 2.17 | 2.74 | 2.84 | 1.3 |
| Lower heating value (MJ.kg$^{-1}$)[c] | ASTM D240-02 | 45.97 | 41.66 | 33.81 | 34.65 | 35.96 | 36.43 |
| Heat of evaporation (kJ.kg$^{-1}$)[d] | | 270-350 | 373 | 581.4 | 308.05 | - | 433 |
| Lubricity at 60°C (µm)[e] | EN ISO 12156-1 | 462.5 | 676 | 628 | 579 | 452 | 521 |
| Surface Tension at 25°C(mN.m$^{-1}$)[f] | ASTM D971 | 26.07 | 18.92 | 23.05 | 24.02 | 31.35 | 30.45 |
| Cetane number[g] | ASTM D6890 | 53 | - | 15.92 | 18.2 | 9.8 | 9 |
| Carbon (wt%) | | 86.44 | 83.12 | 64.86 | 68.13 | 69.82 | 70.28 |
| Hydrogen (wt%) | | 13.56 | 13.4 | 13.51 | 13.72 | 11.61 | 10.7 |
| Oxygen (wt%) | | 0 | 3 | 21.62 | 18.15 | 18.57 | 19.02 |
| H/C ratio | | 1.83 | 1.88 | 2.5 | 2.4 | 2 | 1.8 |
| Stoichiometric air/fuel ratio | | 14.48 | 14.6 | 11.14 | 11.71 | 11.18 | 10.63 |
| Water content (mg.kg$^{-1}$)[h] | EN ISO 12937 | 41.7 | - | 11.46 | 29.7 | - | - |
| Boiling point (°C)[i] | | 180-360 | 35-200 | 117.4 | 137.9 | 140.4 | 131 |
| Freezing point (°C)[i] | | - | - | -89.8 | -78.9 | - | - |
| CFPP (°C)[j] | EN 116 | -20 | - | -41.7 | -47.02 | -47.09 | -46.47 |
| Cloud point (°C)[j] | EN 23015 | -4.1 | - | -115.5 | - | - | - |
| Pour point (°C)[j] | ASTM D97 | -21 | - | <-120.7 | - | - | - |
| Flash point (°C)[j] | | 68 | -40 | 35 | 49 | 51 | - |

[a]Measured and provided by fuel suppliers (Shell and Sigma Aldrich)
[b,c]Measured and compared with literature [11, 12, 40]
[e]Measured and analysed (no corrected values-humidity effect ignored)
[f]Measured
[g]Provided by fuel suppliers, taken from literature [60, 115, 116]
[d,h,I,j]Taken from literature [12, 39, 40, 86, 87, 117, 118]

Table 4-2: Properties of 20%vol blending of fuels

| Property | Method | B20D80 | P20D80 | CP20D80 | CPK20D80 |
|---|---|---|---|---|---|
| Density at 15 °C (kg.m$^{-3}$)[a] | EN ISO 3675 | 830.14 | 830.8 | 857.64 | 857.84 |
| Kinematic viscosity at 40 °C (cSt)[b] | EN ISO 3104 | 2.27 | 2.6 | 2.75 | 2.35 |
| Lower heating value (MJ.kg$^{-1}$)[c] | ASTM D240-02 | 43.54 | 43.99 | 43.97 | 43.86 |
| Lubricity (µm)[e] | EN ISO 12156-1 | 570 | 562 | 480 | 425 |
| Surface Tension at 25 °C(mN.m$^{-1}$)[f] | | 25.48 | 24.78 | 26.3 | 26.3 |
| Carbon (wt%) | | 82.39 | 83.03 | 82.92 | 83.28 |
| Hydrogen (wt%) | | 13.39 | 13.41 | 12.97 | 12.51 |
| Oxygen (wt%) | | 4.22 | 3.56 | 4.11 | 4.21 |
| Stoichiometric air/fuel ratio | | 13.83 | 13.94 | 13.75 | 13.63 |
| CFPP (°C)[j] | EN 116 | -19.99 | -20.06 | -20.07 | -20.03 |

Table 4-3: Properties of 40%vol blending of fuels

| Property | Method | B40D60 | P40D60 | CP40D60 | CPK40D60 |
|---|---|---|---|---|---|
| Density at 15 °C (kg.m$^{-3}$)[a] | EN ISO 3675 | 825.48 | 826.8 | 880.48 | 880.88 |
| Kinematic viscosity at 40 °C (cSt)[b] | EN ISO 3104 | 2.16 | 2.65 | 2.78 | 2.11 |
| Lower heating value (MJ.kg$^{-1}$)[c] | ASTM D240-02 | 41.11 | 42.01 | 41.97 | 41.76 |
| Lubricity (µm)[e] | EN ISO 12156-1 | 592 | 576 | 465 | 441.5 |
| Surface Tension at 25 °C(mN.m$^{-1}$)[f] | | 24.48 | 24.51 | 26.85 | 26.55 |
| Carbon (wt%) | | 77.93 | 79.25 | 79.89 | 80.56 |
| Hydrogen (wt%) | | 13.44 | 13.49 | 12.68 | 11.84 |
| Oxygen (wt%) | | 8.63 | 7.26 | 7.43 | 7.6 |
| Stoichiometric air/fuel ratio | | 13.14 | 13.37 | 13.16 | 12.94 |
| CFPP (°C)[j] | EN 116 | -20.01 | -20.86 | -20.92 | -20.56 |

Table 4-4: Properties of gasoline-diesel blends

| Property | Method | G20D80 | G40D60 | G60D40 | G80D20 |
|---|---|---|---|---|---|
| Density at 15 °C (kg.m$^{-3}$)[a] | EN ISO 3675 | 817.16 | 799.52 | 781.88 | 764.24 |
| Kinematic viscosity at 40 °C (cSt)[b] | EN ISO 3104 | 2.15 | 2.1 | 2 | 1.8 |
| Lower heating value (MJ.kg$^{-1}$)[c] | ASTM D240-02 | 45.11 | 44.25 | 43.38 | 42.52 |
| Lubricity (µm)[e] | EN ISO 12156-1 | 469.5 | 474 | 484 | 497 |
| Surface Tension at 25 °C(mN.m$^{-1}$)[f] | | 24.9 | 24 | 22 | 20.5 |

[a]Measured and provided by fuel suppliers (Shell and Sigma Aldrich)
[b,c]Measured and compared with literature [11, 12, 40]
[e]Measured and analysed (no corrected values-humidity effect ignored)
[f]Measured
[g]Provided by fuel suppliers, taken from literature [60, 115, 116]
[d,h,I,j]Taken from literature [12, 39, 40, 86, 87, 117, 118]

Summaries of all the results tested, calculated and taken from the literature are listed in Table 4-1 to Table 4-4 and Figure 4-1 to Figure 4-3. Density, lower heating value, viscosity and surface tension indicated a linear relationship between blending concentration and the final results. Some of these properties, such as surface tension and viscosity, have an impact on the lubrication and tribological behaviour of the tested fuels. The high density of cyclopentanone and cyclopentanol can affect the engine output power due to the change in fuel injected mass; as in the fuel injection system, fuel is measured by volume [119]. Based on the presented results in Figure 4-2, surface tension increases together with viscosity and density for straight chain hydrocarbons such as butanol and pentanol, in contrast to cyclopentanol and cyclopentanone due to their cyclic structure.

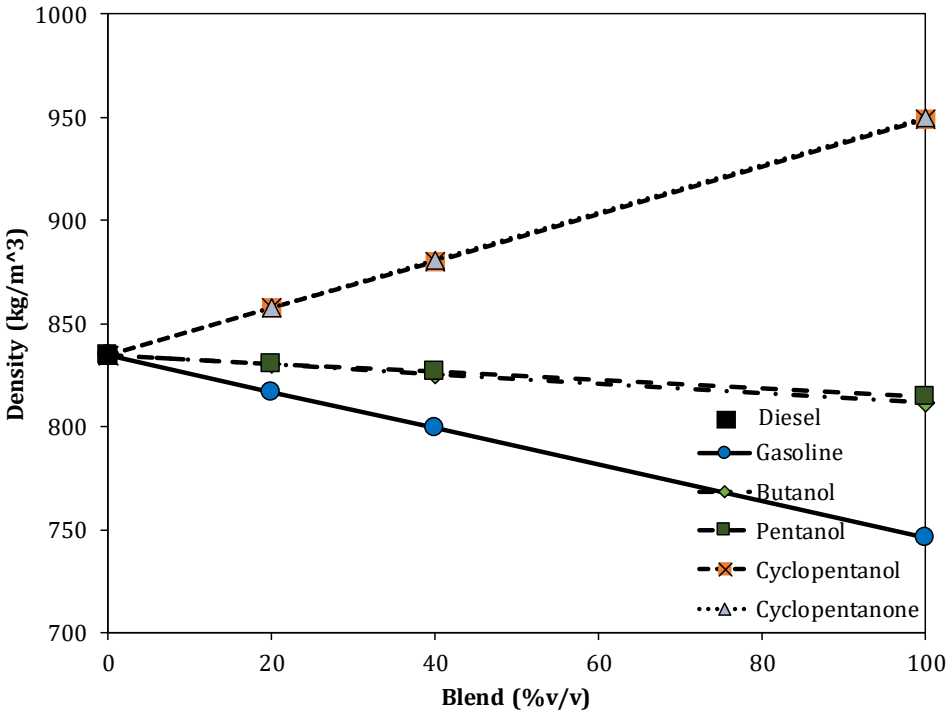



Figure 4-1: Density of fuels

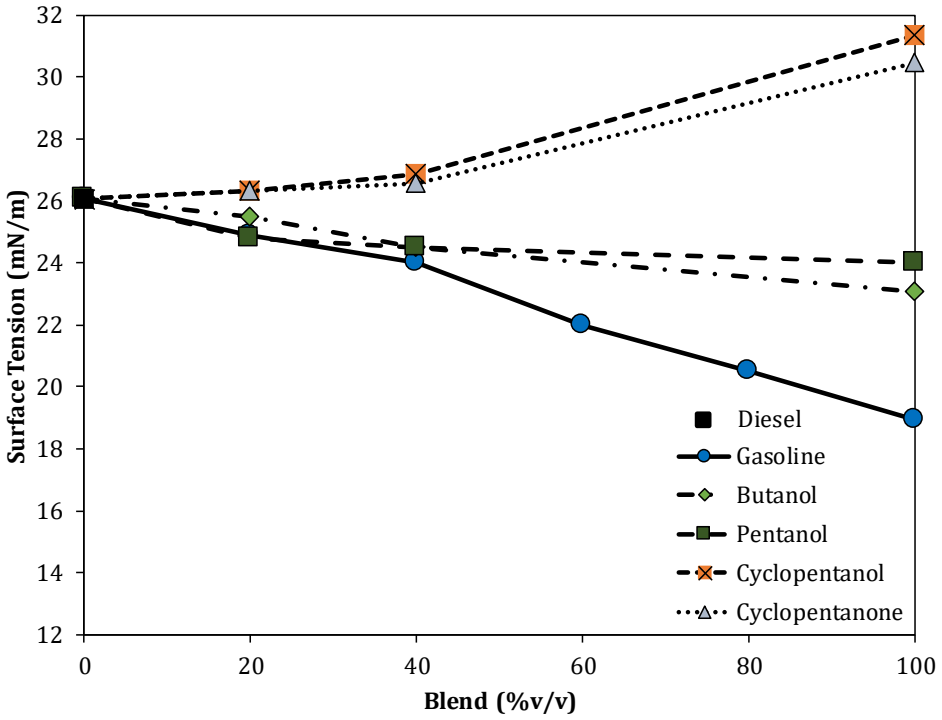



Figure 4-2: Surface tension of fuels

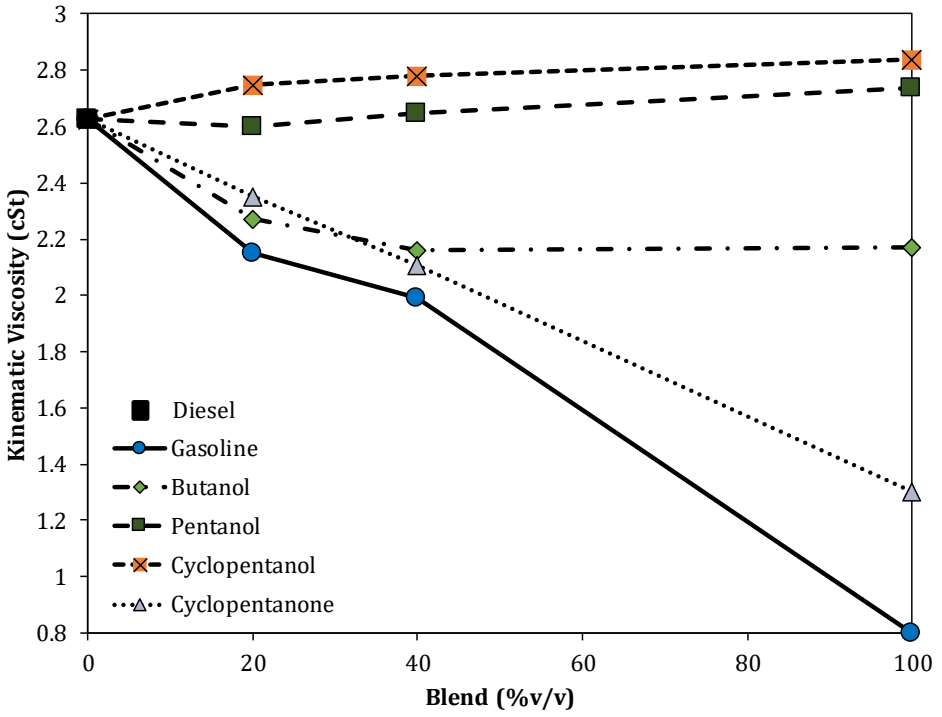



Figure 4-3: Viscosity of fuels

The viscosities of the tested fuels are within the legislated standards; as a high kinematic viscosity in most biodiesels leads to poor atomisation during spraying of fuel and causes deposits and wear in the fuel injection systems [120]. The results of the heating value are presented in the aforementioned tables and Figure 4-4. These results indicated that calorific values of blended fuels with diesel have a linear relationship with blending ratios.

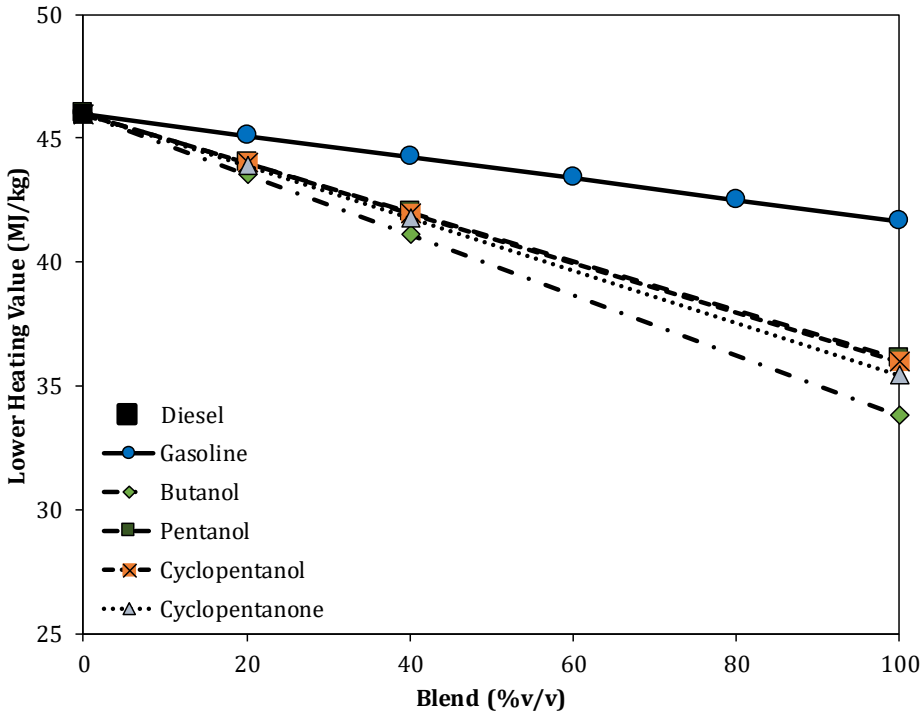



Figure 4-4: Lower heating value of fuels

Based on the presented results in Figure 4-1 to Figure 4-4, the blendings of the 20% oxygenated alternative fuels with diesel proved their validity as appropriate diesel replacements. For a more detailed investigation, tribological mechanisms were carried out as in the following sections.

## 4.3. Lubricating Properties of Alternative Fuels

Figure 4-5 shows that the average friction coefficient of neat diesel is lower than all other tested sample fuels. Gasoline has the highest value due to its poor lubrication behaviour. The presence of polar impurities (oxygen, nitrogen and sulphur-containing molecules) in diesel improve its lubrication properties compared to gasoline [47, 121]. The poor lubrication behaviour of gasoline with a high friction coefficient will be further discussed later in this chapter by presenting the surface topography results. It can be clearly observed that, cyclopentanone as a ketone shows a low friction coefficient and good lubrication performance. The presence of diesel in all the samples decreased the average friction coefficient. These tested neat fuels have friction coefficients of 0.197, 0.283, 0.272, 0.252, 0.238 and 0.2955 for diesel, butanol, pentanol, cyclopentanol, cyclopentanone and gasoline, respectively. Gasoline has an almost 50% higher friction coefficient than diesel; however, cyclopentanone has only a 20% higher friction coefficient than diesel. By comparing the results with the neat diesel friction coefficient, it is clear that the friction coefficient of butanol-diesel blends increased by 7% from 33.5% (0.263) to 41.12% (0.278) with increasing the concentration of butanol from 20% to 40%. This difference in pentanol is lower: it increased from 31.97% (0.260) to 37% (0.270); and in cyclopentanol is much lower: from 26.64% (0.2495) to 27.91% (0.252). This is due to the effect of polarity in the molecular structure of these alcohols. Heavier alcohols such as pentanol have similar properties to diesel fuel. Also, cyclic alcohols such as cyclopentanol have a strong molecular structure and high polarity, which is very difficult to break and evaporate; thus, it has good compatibility with diesel and also a lower friction coefficient and better lubrication performance. Cyclopentanone as a bio-ketone shows a very good lubrication performance, and increasing the concentration of

it from 20% to 40% did not have any significant effect on the friction coefficient, which stayed the same at around 0.202 for both concentrations. Finally, gasoline-diesel blends with different concentrations show that increasing the concentration of the gasoline did not show a significant drop or increase in the friction coefficient. Gasoline concentrations of 20%, 40%, 60% and 80% show an increase of the friction coefficient of only 0.2095 (6.34%), 0.221 (12.18%), 0.223 (13.19%) and 0.225 (14.21%), respectively. Cyclopentanone and gasoline show the best performance in the friction coefficient when they were blended with diesel. These could be due to the high volatility of cyclopentanone and gasoline at high temperatures, which causes a reduction in concentration of these fuels during the rubbing process. As explained in Chapter 3, a gasoline conversion kit was used to prevent evaporation of the fuels, but further studies were carried out to find the tribological mechanisms of fuels.

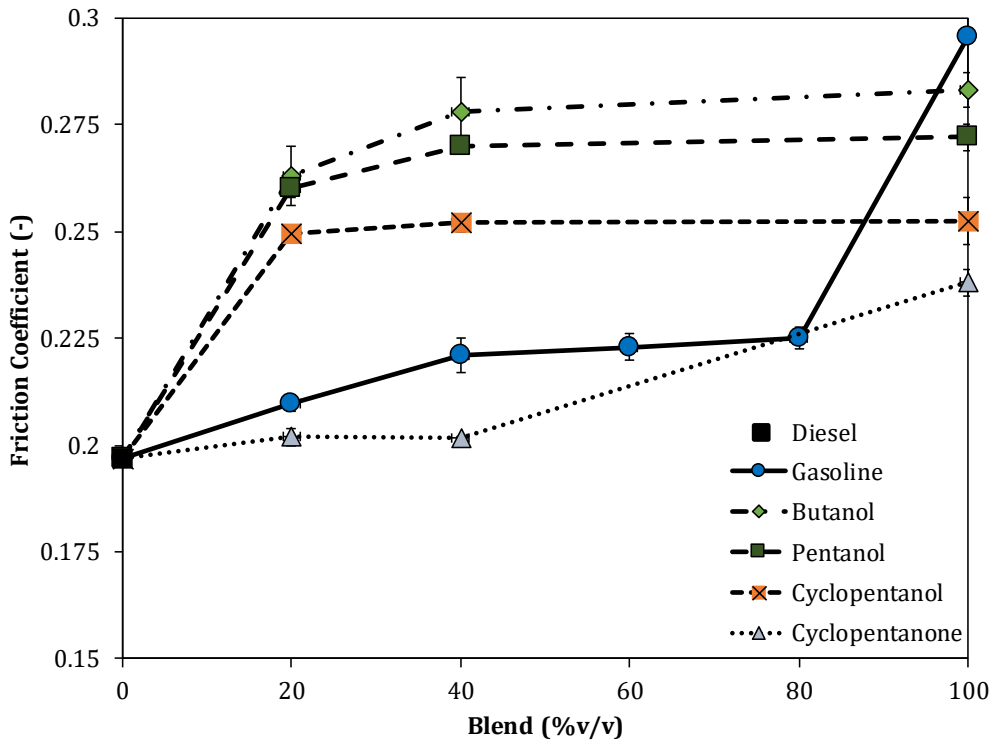



Figure 4-5: Friction coefficient of tested fuels and their blends with diesel

### 4.3.1. Wear Resistance of Alternative Fuels

The variation in wear scar diameter of alternative fuels with different molecular structures and their blends with diesel can be seen in Figure 4-6. It can be observed that neat cyclopentanol shows a good lubrication performance compared to other fuels: by a reduction of around 4% in wear scar diameter in comparison to neat diesel. Its blends with diesel also show a good lubrication performance. For other tested fuels, by the addition of 20%vol in diesel blends the wear scar diameter increases by 23% in butanol-diesel, 21% in the pentanol-diesel blend, and 3% in the cyclopentanol-diesel blend. Cyclopentanol in neat and blending format shows good lubrication behaviour and it does not have a large impact on wear scar diameter. This is also due to its appropriate viscosity [122]. The cyclopentanone blend with diesel shows better lubrication behaviour than neat diesel and neat cyclopentanone. It can be hypothesised that this is due to the cyclic molecular structure and also the double bond oxygen in its structure, which make a lubrication film around the sliding section and improve the formation of the oxide layer around it. The wear scar diameter showed a reduction of 8% and 4.5% by adding 20%vol and 40%vol of cyclopentanone to diesel, respectively. This opposite behaviour of the cyclopentanone blends needed a more in-depth investigation, which is included in the topography section. Finally, the gasoline-diesel blend's performance in its lubrication properties shows that the addition of 20%vol gasoline to diesel increased the wear scar diameter by 1.5%. This is increased to 2.5%, 4.7% and 7.5% with the addition of 40%, 60% and 80% of gasoline to diesel, respectively.

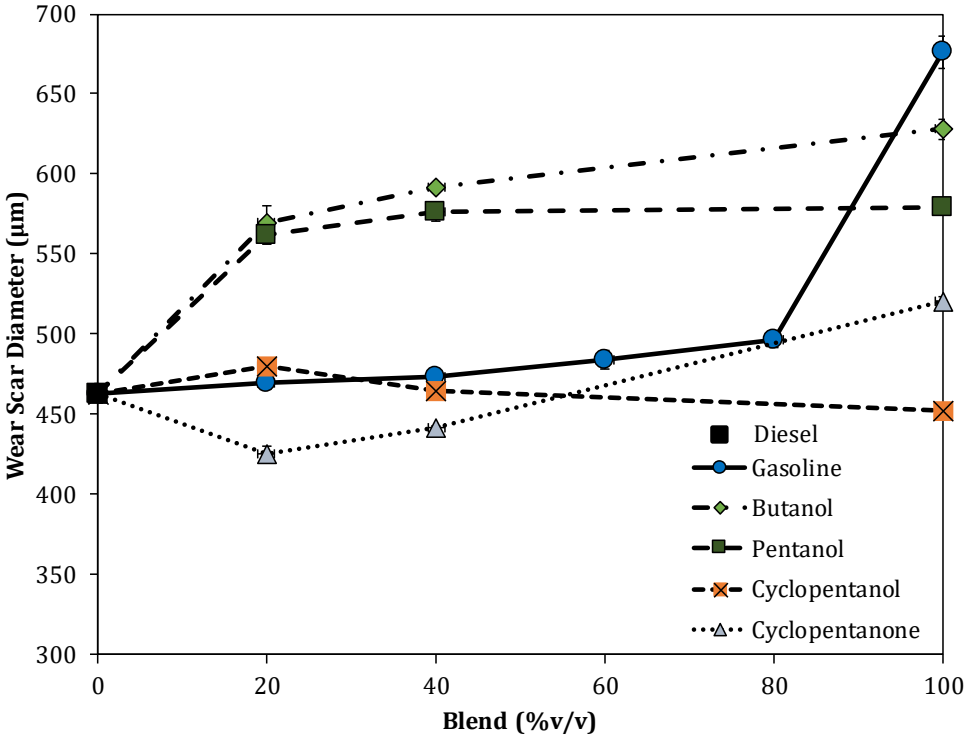



Figure 4-6: Wear scar diameter of tested fuels and their blends with diesel

The presented results indicated that cyclic alcohols/ketone-diesel blends have proper lubrication properties within the standards, which lead to less impact on the fuel injection system and improvement of the overall engine efficiency. This overall conclusion may suggest that cyclic alcohol and ketone blends with diesel would be more appropriate for high injection pressure application in engines [47]. Furthermore, based on the results in Figure 4-6, the neat alcohols possess high wear scar values and these values highlight the effects of hydrocarbon chain length and unsaturation on lubricity which have also been discussed in previous studies [56, 59]. An increase of the chain length and the presence of the unsaturated compounds improve the lubricity. The presence of double bond oxygen or OH in the end of the cyclic structure of the

hydrocarbons in cyclopentanone and cyclopentanol is especially effective in enhancing lubricity; C=O in the molecular structure of cyclopentanone, as a ketone, is an observation of lubricity enhancement, which has also been stated by other authors [56]. In blends with diesel, reduction of the OH moieties will lead to the improvement of the lubrication properties [56]. Oxygen moiety and carbon chain length, which increase the viscosity of the tested fuels, could have a sufficient effect on the lubricity improvement. The polar-imparting O atom of most of the molecular structures can lower the friction and wear scar diameter. In some of the cases, increasing the blended fuels' (butanol, pentanol, etc.) concentrations does not have a linear relationship with the wear scar diameter, which is due to different tribological behaviour, blending stability, volatility of samples, etc. Reduction of the viscosity of fuels causes reduction of increasing of the wear scar.

The tested oxygenated fuels indicated a high affinity to the metallic surfaces forming a thin, protective, metal to metal contact layer. This layer is a lubricant film which is formed by the adsorption of the polar species of fuels on the negatively charged metal surfaces [48]. The OH groups in the alcohols' group make the tested samples more effective as wear protectors [48, 56]. In most of the studies, biodiesel is added to the diesel fuel as a lubricity enhancer [48]. The addition of smaller carbon chain length alcohols such as ethanol, caused a reduction of lubrication quality (increase of wear scar diameter), which is a consequence of the lower lubricity of ethanol [48]. The lubricity of alcohols and most of the hydrocarbons is very sensitive to their molecular weight; thus, by increasing the molecular weight of the straight chain alcohols lubricity improves. This means large molecules have better lubricities than light molecules [38, 46]. The lubrication mechanism of the heavy alcohols and ketones could be attributed to the polar groups and oxygenated compounds making the adsorption of the samples on the surface of the sliding specimens, and to the creation of frictional chemical reactions that generate

a lubrication boundary. In addition, this oxygen content could quicken the corrosion wear on the disc surface.

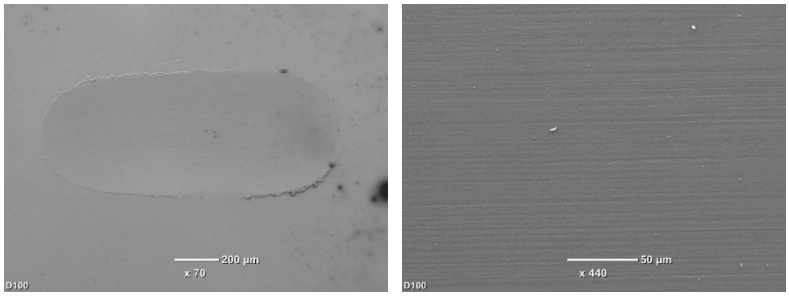
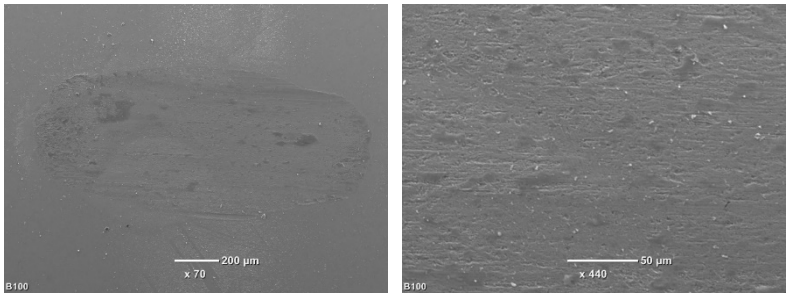
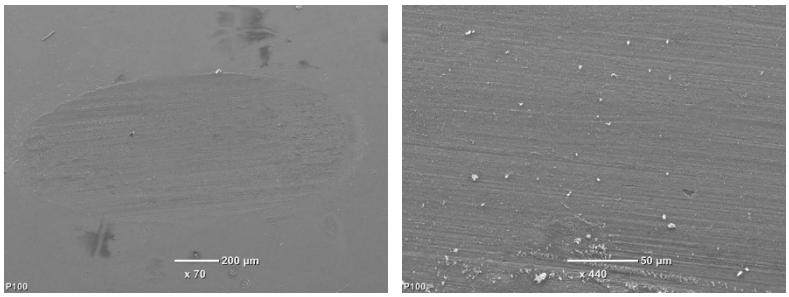
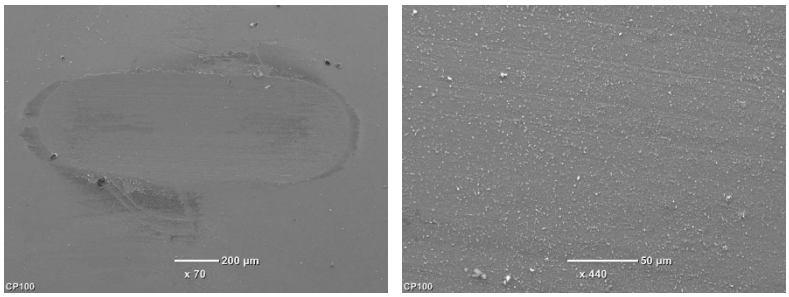
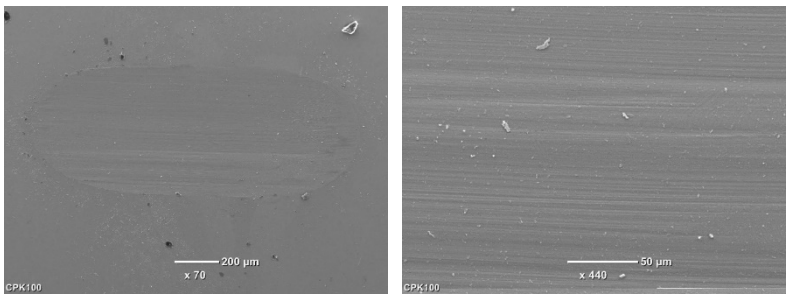
As a conclusion, the trends for friction coefficient and wear scar diameter show little correlation except for cyclopentanol and cyclopentanone. This could be due to their molecular structure that shows different behaviour when it is added to the diesel fuel. These improvements can be explained by the polar nature of cyclopentanol and cyclopentanone. These polar molecules are able to bind to the disc and ball material surface which causes the formation of a thin film that acts as lubrication to reduce the wear scar diameter. The fuels with better lubrication behaviour such as cyclopentanol and cyclopentanone would lead to increased longevity and reliability of components within the fuel delivery systems.

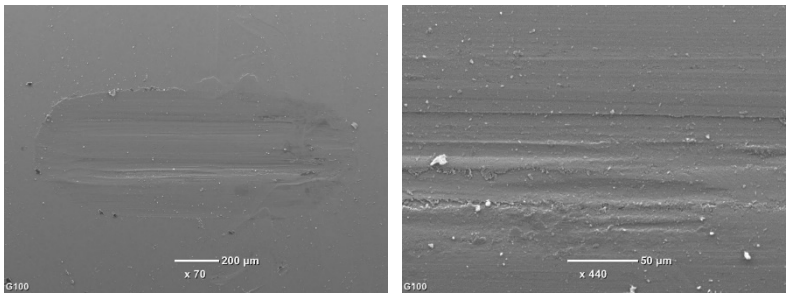
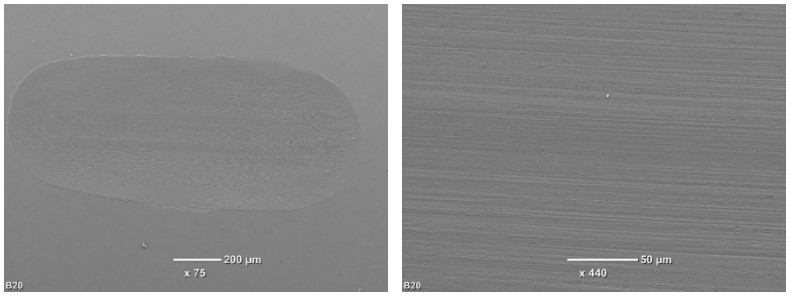
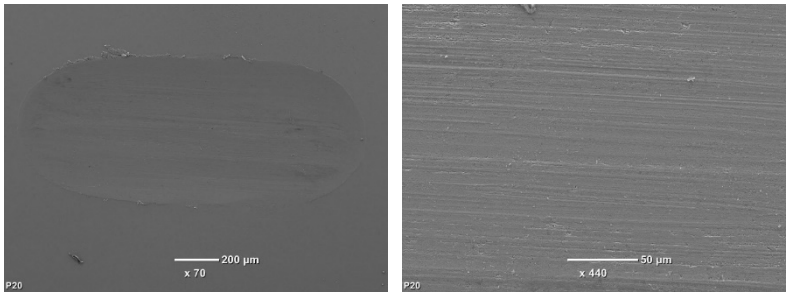
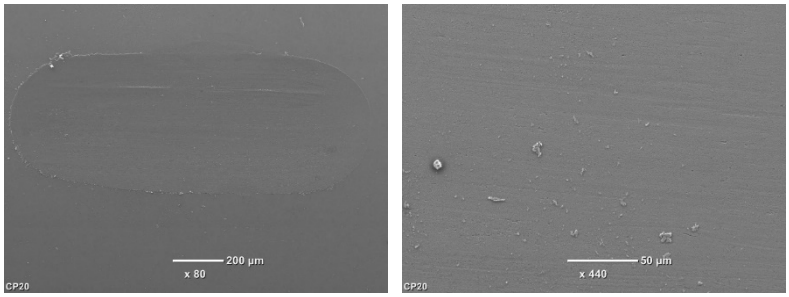
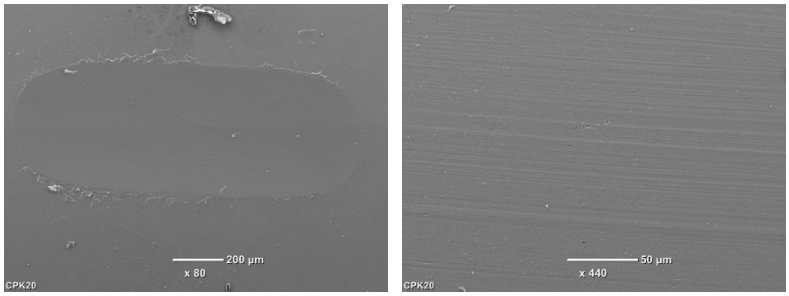
Following on from the above discussion and based on the presented results, the sequence of oxygenated moieties enhancing the lubricities as a neat format at the tested standard are: cyclopentanol > cyclopentanone > pentanol > butanol. This behaviour is different with respect to blending with diesel. It is due to the fact that alcohols have higher polarity because of their hydrogen bonding capabilities and the presence of oxygen atom rather than ketones with a double oxygen bond in in their molecular structure. This can be seen from their higher boiling point as well; high polarity leads to a high boiling point of the hydrocarbons [123]. Heavy alcohols are more polar than light alcohols. In contrast, cyclopentanone has a large dipole moment due to its carbonyl structure. The existence of the electronegative oxygen atom, makes it less polar than heavy alcohols due to the incapability of the intermolecular hydrogen bond. Cyclopentanone-diesel blends show the best lubrication performance, which can be due to the change of its behaviour after

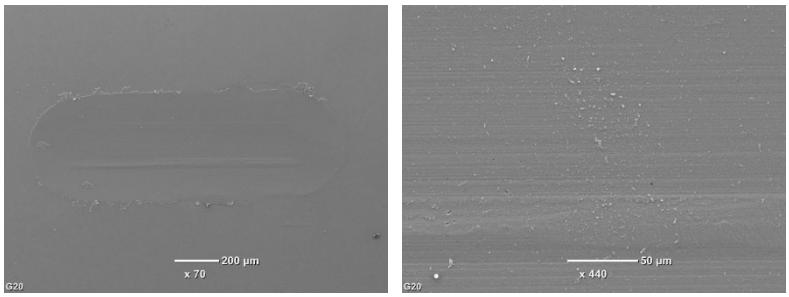
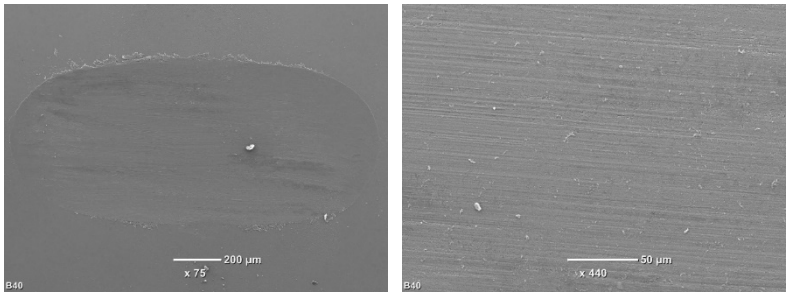
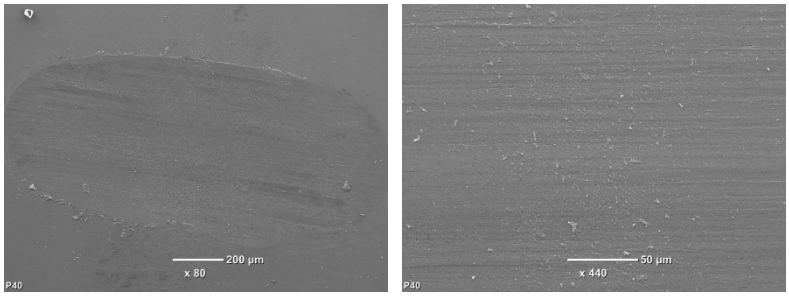
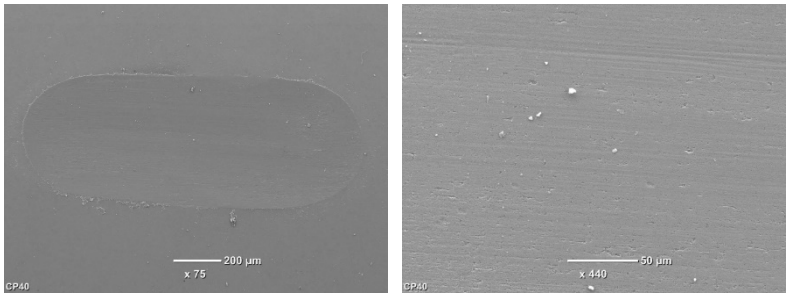
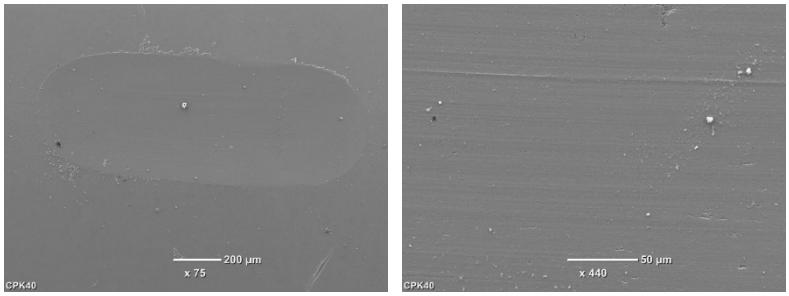
mixing with diesel; but other alcohols show the same trends whether neat or blended which follows their polarity ranking.

### 4.3.2. Wear and Lubrication Mechanisms

The wear scars on the lower specimen disc were also investigated using SEM and EDS and results are shown in Figure 4-7. The specimen tested with the neat gasoline had a large wear scar with lots of abrasive grooves due to the poor lubricity and higher friction coefficient of gasoline. The wear scar of the cyclic compounds is smaller than that of the straight chain, which indicates that this cyclic molecular structure and oxygen can adsorb on to metal surfaces and then create tribo-films to lubricate the surface, leading to a lower wear scar diameter. This is not true in some blending ratios, as this film can be destroyed during tests of a long duration. Having a stronger molecular structure means a higher bonding strength, such as the double bond oxygen in cyclopentanone and the cyclic structure in cyclopentanol; which will provide a more robust lubrication regime and protect the surface of the disc from wear. The weak bonding strength between butanol and diesel failed to protect the metal surface by generating a tribo-film, causing a higher wear scar diameter. In some of the images in Figure 4-7 there was a partial corrosion field at the junction of the wear and non-wear surfaces. This happened in the samples where their molecules adsorbed on the wear surface to act as lubrication. This could be also due to the electric media during the sliding and friction process leading to the formation of a lubrication boundary. The close observation of the worn surfaces shows that samples with lower wear scar diameter and depth have a quite smooth surface with some small grooves. Gasoline with poor lubricity causes both grooves and material losses in the wear section; all of the presented SEM images for the upper and lower specimens are in good agreement with the lubricity wear scar diameter results.

| Fuel | Wear Scar Micrographs |
|---|---|
| D100 |   |
| B100 |   |
| P100 |   |
| CP100 |   |
| CPK100 |   |

| | |
|---|---|
| G100 |  |
| B20 |  |
| P20 |  |
| CP20 |  |
| CPK20 |  |

| | |
|---|---|
| G20 |   |
| B40 |   |
| P40 |   |
| CP40 |   |
| CPK40 |   |

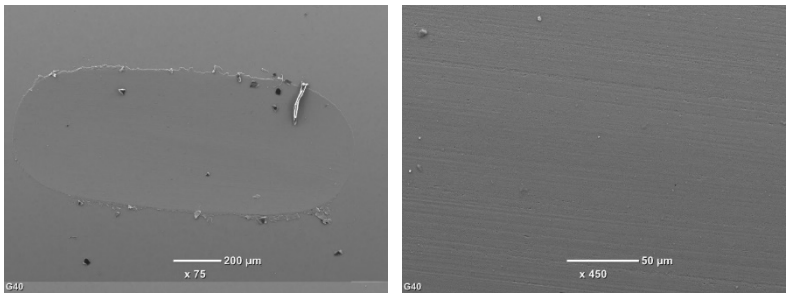
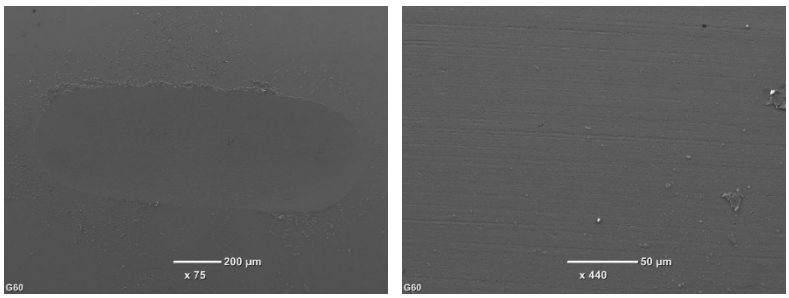
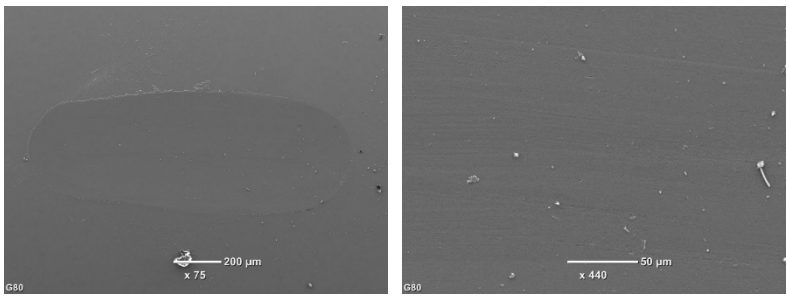
| | |
|---|---|
| G40 |  |
| G60 |  |
| G80 |  |

Figure 4-7: SEM and topography micrographs of disc tested in different fuels

Some fine and dense furrows and a few pits can be seen in some of the SEM images for the lower specimen. Fuel pits are like small dots which can be seen in the images and parallel furrows are presented clearly as lines. Slight furrows appeared for the good lubrication behaviour of fuels such as cyclopentanol. Creation of the lubrication film, composed of adsorbed and tribo-reacted organics on worn surfaces during the lubricity test have minimized the wear damage and created small furrows [124]. This smooth worn surface from the SEM and Alicona images are due to the strong polarity of the compounds. Stronger polarity leads to the creation of a robust lubrication regime and

protect the metal surface from wear. The presence of the large amount of ferrite around the carbide particles is due to the detachment of the carbide particles from the surface, which is shown in the poor lubricity samples such as gasoline, butanol and pentanol. These micrographs show surface damage that is in good agreement with other measured tribological behaviours.

The element contents of the worn surface analysis with EDS confirms all lubrication investigations and showed that similar elements such as Fe, C, O and Cr exist due to the material of the ball and disc. The carbon formation is due to the adsorption and chemical reaction of hydrocarbons as a result of friction during sliding of the ball over the disc in the HFRR. In the SEM image of the surfaces that show severe damage and grooves, such as the tested gasoline fuel, the carbon content significantly increased and the Fe content decreased. The increase of carbon is expressed as organic deposits, including the layer of oxides on the worn surfaces. The existence of the oxygen in the molecular structure of the tested fuels accelerated the generation of oxides, which play an important role in the formation of the lubrication film on the disc surface. This caused a reduction of the Fe content in the sampling area, and also confirms the result of the friction coefficient and lubricity from the HFRR. This reduction could be due to the corrosion effect of the tested fuels on the surface of the specimen too [125]. On the edge of the wear scar surface the carbon content is more than in the middle of the surface; which is due to adsorption from the chemical reactions of the fuels during sliding [58]. This is obviously seen from SEM the images too.

The oxidation process happened in most of the biofuels such as the tested fuels, due to the presence of oxygen associated with the generation of inorganic oxides such as $Fe_3O_4$ and $Fe_2O_3$. This is detected in most of the literature studies such as [52, 54, 126],

which help in the creation of lubrication film and reduction of worn surface dimensions. Light alcohols have the biggest wear scar due to their low viscosity; which means the generation of a very thin boundary of lubrication and elastohydrodynamic films and an increasing wear scar [46]. Cyclopentanone shows very good lubrication behaviour due to the lack of the hydroxyl group. This hydroxyl group makes the adsorption of the lubrication film on the metal surfaces weaker than ketones. Another point which must be considered is the low boiling point of the light alcohols, which causes their evaporation during tests and a change of testing conditions; but the use of a gasoline conversion kit in the HFRR reduces this error effectively.

### 4.3.3. Surface Topography

Data collected from analysis of the lower disc sample wear scars created during lubricity testing can be seen in Figure 4-8. This figure shows the average wear scar depth of the disc when at least three profile measurements were taken, perpendicular to the sliding direction. The profile of the wear scar depth follows the same pattern for the wear scar diameter for some the tested samples. For the neat fuels, the wear scar diameters are higher for butanol > pentanol > gasoline > cyclopentanone > cyclopentanol. The wear scar depths are higher for butanol > pentanol > cyclopentanone > gasoline > cyclopentanol. The depth of the wear scar for diesel is around 10.2281 μm and it decreased around 38% for cyclopentanol and 22% for cyclopentanone. This increased by 13% for butanol and 5% for pentanol. The addition 20%vol of pentanol, butanol and cyclopentanone to the diesel, show the same trend for depth and diameter. This reduced by 9% for the addition 20%vol of cyclopentanone to diesel. Gasoline and cyclopentanol had a small difference. In contrast, with the addition of 40%vol of fuels to the diesel only the cyclopentanol patterns for depth and diameter are the same. This difference in some

of the cases is due to deformation of the upper specimen ball during lubricity testing, as the steel material is removed and did not have the same behaviour, especially in the less lubricated fuels.

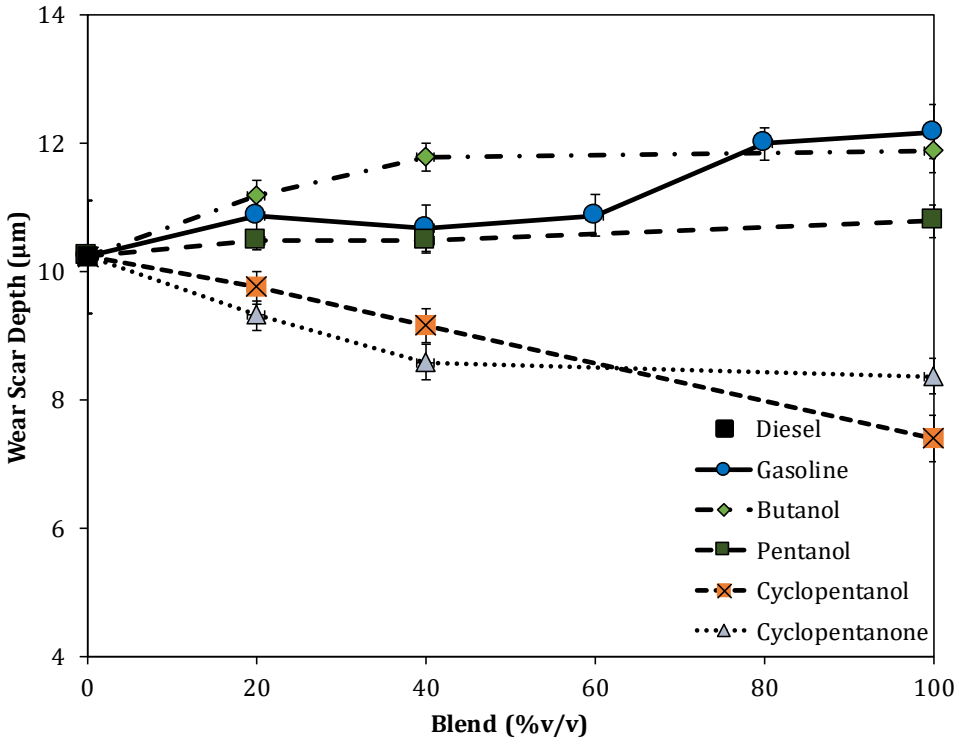



Figure 4-8: Wear scar depth of tested fuels and their blends with diesel

The surface roughness summaries for all the tested samples are listed in Figure 4-9. All of these results confirm the SEM images as well. Increasing the oxide thickness and metallic oxide wear particles, increases the wear scar diameter, depth and surface roughness [46]. The surface roughnesses of the tested samples are almost all less than for diesel, except for neat gasoline and its blends and also 20% butanol. This lower surface roughness could be due to the oxide layer which was discussed in previous sections. Diesel's wear scar diameter and depth are less than for other fuels in most of the cases,

but its surface roughness is not good enough which could be due to impurities in its structure.

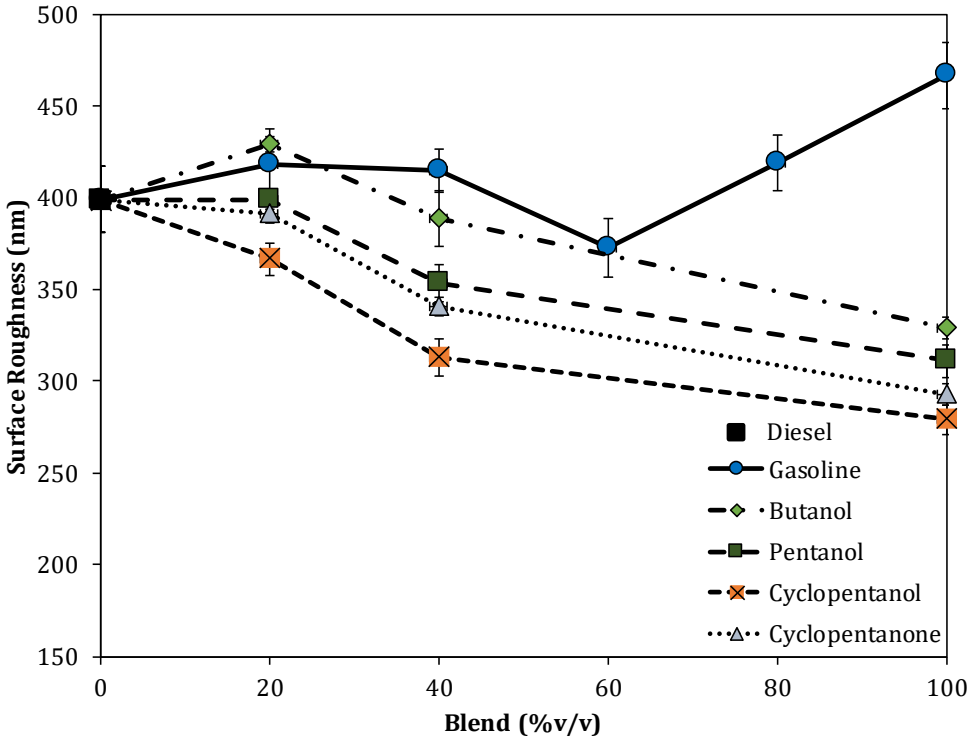



Figure 4-9: Surface roughness of tested fuels and their blends with diesel

As a conclusion, worn surface analysis by SEM, EDS and Alicona confirm the hypothesis from the HFRR results in order to choose the best lubricated fuels for current engines. In general, cyclopentanol and cyclopentanone in terms of wear scar diameter, wear scar depth and worn surface roughness show the best behaviour. Pentanol indicates better lubrication performance than butanol. By all of these comparisons the optimum fuel in terms of minimising wear is the 20% fuel blend, as it has appropriate wear scar diameter and depth, good roughness and a less corroded area which would be suitable for an engine's fuelling system.

## 4.4. Summary

The physicochemical properties, lubrication and tribological mechanisms of butanol, pentanol, cyclopentanol, cyclopentanone and gasoline fuels and their blends with diesel have been comprehensively investigated.

It was found that viscosity decreases by the addition of alcohols and ketones to diesel, and this reduction is larger for lighter alcohols and ketones due to their lower viscosity. Density, surface tension and lower heating values have the same trend as the blending ratio. It means that these properties are proportional to the blending ratios. Fuels with cyclic structures have better lubricating characteristics compared to diesel and other alternative fuels, due to the significant effect of the polarity of the functional group on the creation of a lubrication film around the sliding area. In terms of wear scar diameter, cyclopentanone and cyclopentanol showed better lubrication performance than the others. The presence of oxygen and the cyclic structure lead to the formation of a lubrication film and consequently, reduction of wear scar dimensions. Pentanol with a longer carbon chain length shows better lubricity than butanol. The influence of molecular structure on enhancing lubricity compared to diesel can be ranked as cyclic hydroxyl > hydroxyl > ketone. This has a direct link with the polarity of the molecules as high polarity of molecules due to hydrogen bonding capabilities, cyclic structure and the presence of oxygen atom in cyclopentanol make the results higher in lubricity. The CPK20 shows the best lubrication performance. It is hypothesised that this is due to the strong lubrication film formation on the worn surface. The large dipole moment due to the carbonyl group in the ketones having electronegative oxygen could be a reason. For the corrected wear scar diameter, the humidity correction factor was considered, based on the different fuels characterisation, and it showed an insignificant effect.

Surface roughness when using different blends of fuels has the same trend as the wear scar sizes for the neat fuels. These alternative fuels in the neat form shows lower roughness than neat diesel which is hypothesised to be due to the creation of lubrication film. All of the characterisation methods confirm that heavier alcohols have better lubrication performance and better behaviour in terms of tribological mechanisms compared to gasoline and diesel.

In general, manipulating the molecular structure of the fuel affects the lubrication and tribological mechanics. These changes have a significant impact on the combustion profile, exhaust gas emissions and particulate characteristics.

# CHAPTER 5. IMPACT OF ALTERNATIVE FUELS ON COMBUSTION, GASEOUS AND PARTICULATE MATTER EMISSIONS' CHARACTERISTICS

## 5.1. Introduction

All of the combustion experiments explained in this chapter were conducted on a single cylinder research diesel engine with defined engine speed, IMEP, injection pressure, timing, duration and ratio, which were explained in detail in Chapter 3. In order to minimise variations of combustion, gaseous and particulate matter emissions characteristics when investigating the impact of the physico-chemical properties of bio-alcohols and bio-ketones EGR was eliminated. Butanol, pentanol, cyclopentanol and cyclopentanone blended with diesel, and also neat diesel as the baseline fuel were tested to study the influence of various alternative fuels with different molecular structures. The baseline diesel fuel was tested every day to monitor experimental data repetition. The alternative fuels were tested only at 20%v/v ratio with diesel fuel as a result of the findings in Chapter 4. Each of the fuels was tested at the two engine operating conditions of 2 bar IMEP and 4 bar IMEP. As explained in detail in Chapter 3, injection timing (start of injection) was kept constant but injection duration was adjusted for different fuels to keep the IMEP value equal for all fuel blends. This was due to the difference in the energy densities of the studied fuels. Gaseous and particulate matter emissions' results presented in this chapter are from samples taken at the engine-out location in the exhaust pipe. A summary of the engine operating test conditions is listed in Table 3-3.

## 5.2. Results and Discussion

### 5.2.1. Combustion Analysis

Table 5-1 shows the indicated specific fuel consumption (ISFC), indicated thermal efficiency (ITE) and the actual air/fuel ratio over stoichiometric air/fuel ratio (λ). The λ was found to be almost similar for the tested fuels and this helped to identify the direct effects of fuel composition and molecular structure on the differences in combustion, emissions and particulate matter.

Table 5-1: Summarised combustion analysis for test conditions

| Test abbreviation | ISFC ($kg.kwh^{-1}$) | ITE (%) | λ | Exhaust temperature (°C) |
|---|---|---|---|---|
| D100L | 0.2936 | 26.67 | 3.28 | 226 |
| B20L | 0.3262 | 25.35 | 3.03 | 231 |
| P20L | 0.3321 | 24.64 | 3.01 | 227 |
| CP20L | 0.3477 | 23.55 | 2.91 | 237 |
| CPK20L | 0.3317 | 24.75 | 3.08 | 225 |
| D100M | 0.2603 | 30.08 | 1.84 | 342 |
| B20M | 0.2643 | 31.28 | 1.91 | 331 |
| P20M | 0.2718 | 30.11 | 1.81 | 338 |
| CP20M | 0.2678 | 30.58 | 1.86 | 337 |
| CPK20M | 0.2704 | 30.28 | 1.84 | 336 |

The in-cylinder pressure and heat release rate versus crank angle degree for the five different tested fuels at two engine loads of 2 bar and 4 bar IMEP are shown in Figure 5-1 (a) and (b), respectively. It has to be noted that the fuel properties affected the combustion process in the diesel engine. The physical properties of fuel such as density, surface tension and the volatility profile control the atomization quality, vaporization quality and mixing [127]. The auto ignition property of the fuel (linked with the cetane number) can effectively change the ignition delay and therefore fuel-air mixing time [128].

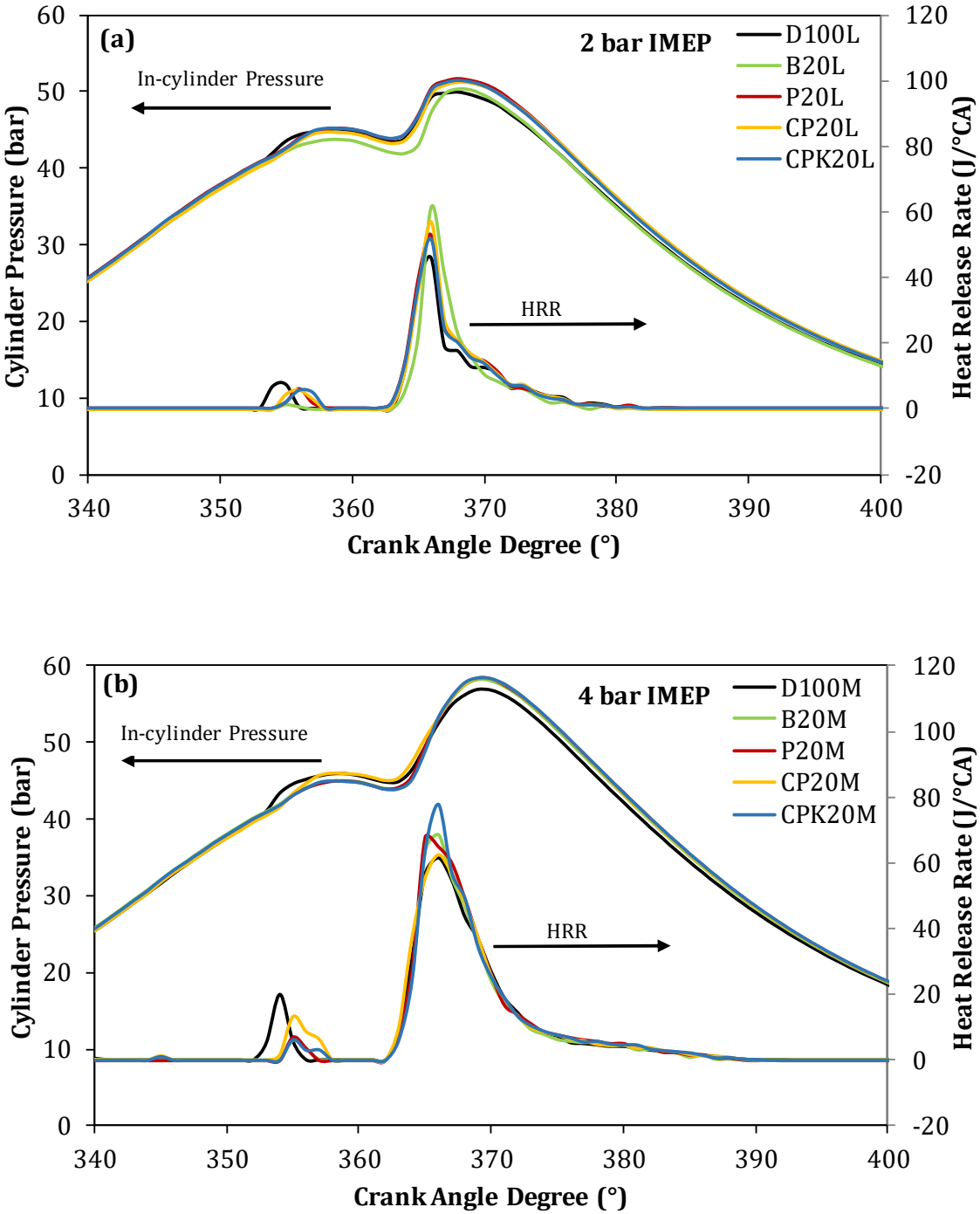



Figure 5-1: In-cylinder pressure and heat release rate

Using alternative fuel blends, generally the ISFC was higher than the baseline due to the lower heating value. This increase is from 11% to 18% compared to the baseline diesel. It can be observed from Table 5-1 that the ITE at higher loads improved very little with the use of alternative fuels due to the faster burning rate and hypothetically, less heat loss to the cylinder walls. The change of the exhaust temperature can be due to the change in the duration of combustion, based on net cumulative heat release analysis (duration between AHR-10 to AHR90, which showed CP20 has the longest and CPK20 has the shortest duration). More useful work drawn from the combusting mixture during the expansion stroke can lead to lower exhaust temperatures. Moreover, the amount of oxygen content in fuels which increases oxygen-rich regions in the combustion chamber, can lead to higher peak in-cylinder temperatures and exhaust gas temperature. The same reasons were reported in previous studies [62, 80, 129].

Among the tested alternative fuels, pentanol has the highest cetane number and cyclopentanone has the lowest (Chapter 4, Table 4-1). Looking at the heat release rate results for the first peak of combustion associated with the pre-injection (Figure 5-1), diesel had the shortest ignition delay at both loads. One possible reason for a longer ignition delay can be due to high electronegativity of an oxygen atom in the molecule of oxygenated fuels; this was also discussed as a reason for lubrication and tribological behaviour of the fuels in Chapter 4. A longer ignition delay can help the fuel-air mixing process and therefore reduce particulate matter emissions, as discussed later in this chapter. An increase of the engine load leads to a higher amount of injected fuel and therefore combustion duration [130].

The addition of butanol to diesel led to a slightly longer combustion delay compared to other fuels, probably due to its low cetane number and high heat of vaporization (the

cooling effect) [74]. This resulted in a lower maximum cylinder pressure at 2 bar IMEP. An increase of oxygen content in the blends led to a higher peak of the HRR. From Figure 5-1 it can be concluded that the increase of the carbon chain length attached to the OH in the alcohols can decrease the ignition delay [131]. In cyclic structures, especially cyclopentanol, this reduction in ignition delay is a bit more than with pentanol.

### 5.2.2. Gaseous Emissions

Engine-out gaseous emissions for five different fuels at two different engine conditions are shown in Figure 5-2 to Figure 5-6. Carbon monoxide (CO), nitrogen oxides ($NO_x$), total hydrocarbons (THC), heavy hydrocarbons (Heavy HCs) and light hydrocarbons (acetylene, formaldehyde, propylene, ethylene, ethane and methane) are presented in these figures. As explained in Chapter 3, the experimental results are the average of multiple measurements and the uncertainty is shown in these figures.

#### 5.2.2.1. THC Emissions

It can be observed from Figure 5-2 and Figure 5-3, that HC emissions were lower at high load compared to low load. Lower HC emissions were also obtained for the alternative fuel blends compared to those emitted by the diesel fuel combustion, due to more complete combustion. A general decrease of HC emissions has been also reported previously when using oxygenated biodiesels [74, 75, 132-134]. The presence of oxygen in the blended fuels can lead to more complete combustion and lower HC emissions [90, 135]. An increase of the carbon chain length in straight chain alcohols led to higher THC due to the reduction of the total oxygen content of the blend. This can also be a consequence of the higher viscosity of blended fuels [41]. Based on the presented results in Chapter 4 (Table 4-1), cyclopentanone has the lowest viscosity and cyclopentanol has the highest viscosity among these fuels, this trend is the same in THC emissions as well.

An increase of fuel viscosity and density make combustion more incomplete due to worse vaporisation and atomisation of fuel [41, 80]. This trend is true at lower loads since the low in-cylinder temperature and pressure led to less complete combustion. For example, CP20 shows higher total hydrocarbons at a low load; however, it shows better behaviour at a higher load, among the alcohol fuels. The CPK20 shows the best reduction in heavy and total hydrocarbons due to the molecular structure of cyclopentanone and the oxygen content and low viscosity of the blend; this leads to more complete combustion compared to other tested fuels.

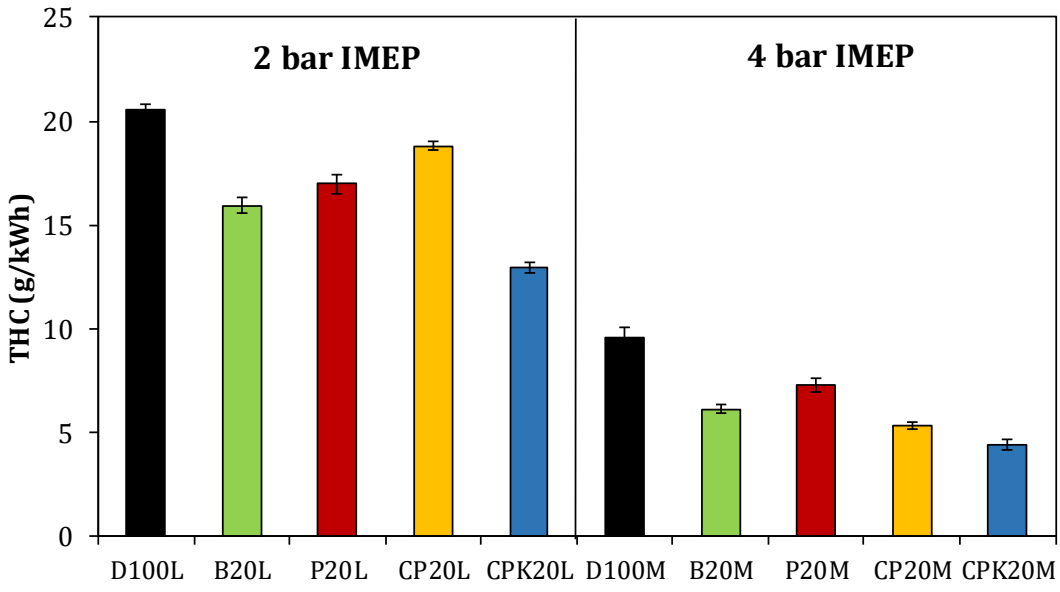



Figure 5-2: Total hydrocarbon emissions at 2 bar IMEP and 4 bar IMEP

Hydrocarbon species are presented in Figure 5-3. The characterised light HCs' emissions from combustion of the blends were in the same range as those of the baseline diesel – the differences were a few ppms. A higher ratio of light hydrocarbons can be seen from CPK20 compared with other fuels. Total hydrocarbon emissions are very dependent

on the engine operating conditions, engine performance and the use of aftertreatment systems; thus, it is beneficial to combine some emission reduction technologies to overcome these hydrocarbon emissions [87], this is discussed in Chapter 6.

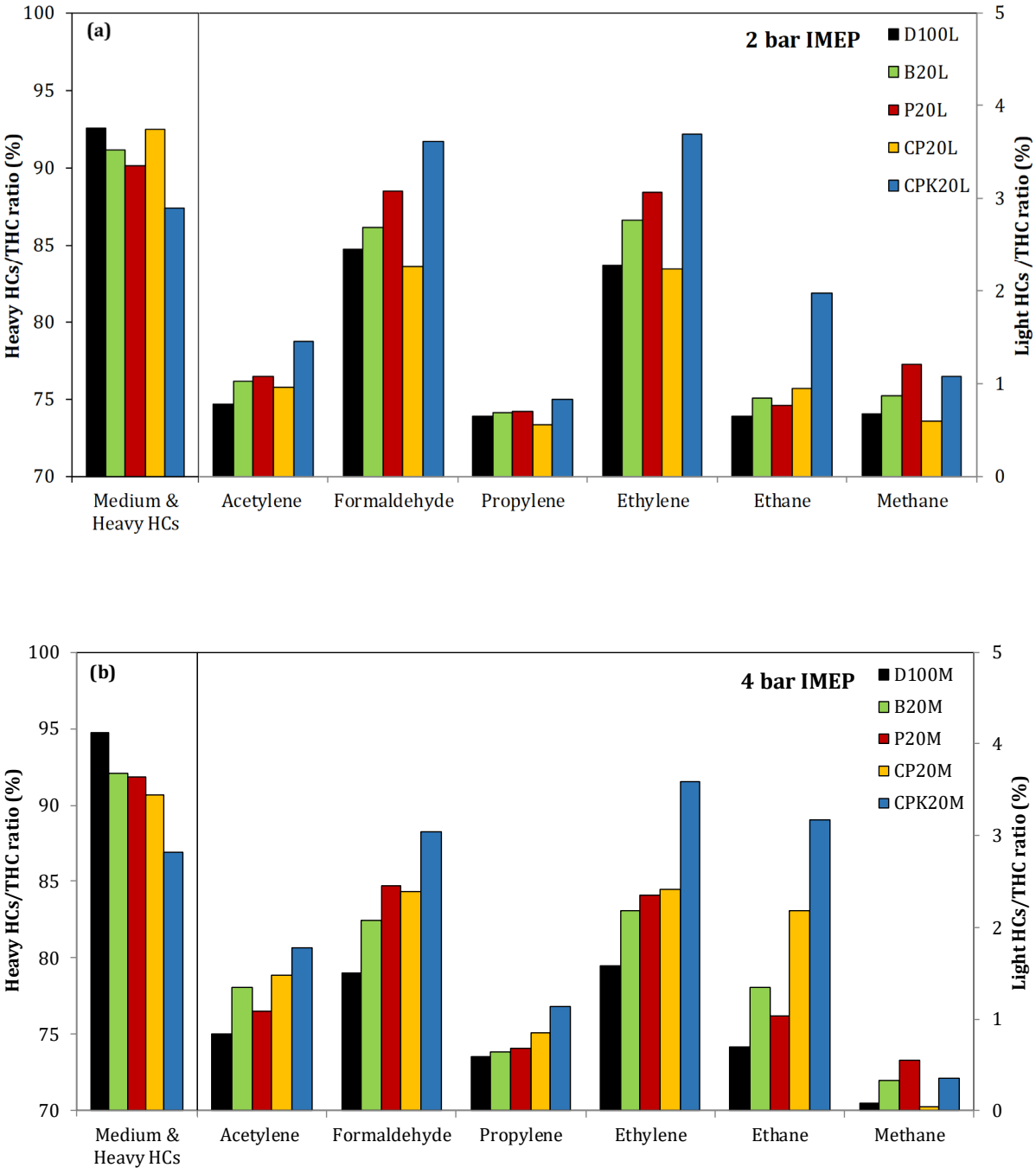



Figure 5-3: Hydrocarbon emissions' speciation

#### 5.2.2.2. CO and $CO_2$ Emissions

From Figure 5-4 and Figure 5-5, it can clearly be observed that due to the more complete combustion at the higher IMEP, indicated specific CO and $CO_2$ emissions were lower. Carbon monoxide is produced by incomplete combustion of fuels containing carbon in fuel-air under-mixed and over-mixed regions within the combustion chamber [72]. Combustion of the blends of oxygenated fuels with diesel led to a slight increase of CO emissions at both loads with respect to the baseline diesel [118, 136]. The higher concentration of CO emissions in the exhaust of the blended fuels can be due to two major factors: the higher heat of evaporation of these fuels and their lower cetane number which can lead to more fuel-air premixing and consequently a higher number of locally lean fuel-air mixture packets [74, 80, 136, 137]. Both of the aforementioned factors can lead to a higher CO formation rate and can prevent its oxidation to $CO_2$. Based on the results, lower HC emissions for the case of CPK20 is probably due to breakdown of the fuel which led to relatively higher CO emissions (Figure 5-4). From the results it can be concluded that for straight-chain alcohols such as butanol and pentanol, an increase in the carbon chain length leads to a very slight increase in CO emissions due to a decrease of oxygen content. This increase is more for cyclic structures; which can be a result of a higher unsaturation degree.

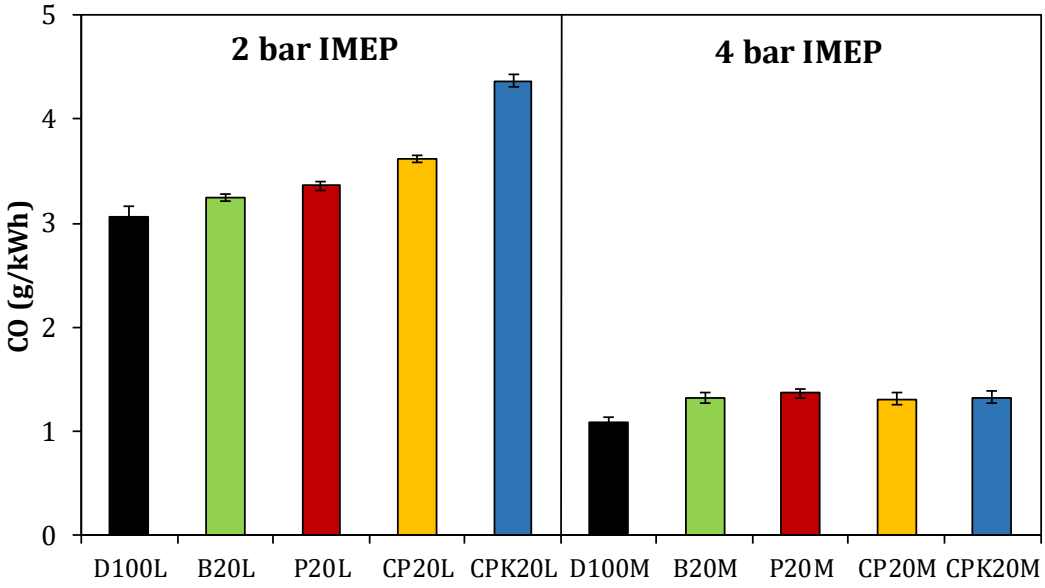



Figure 5-4: Carbon monoxide emissions at 2 bar IMEP and 4 bar IMEP

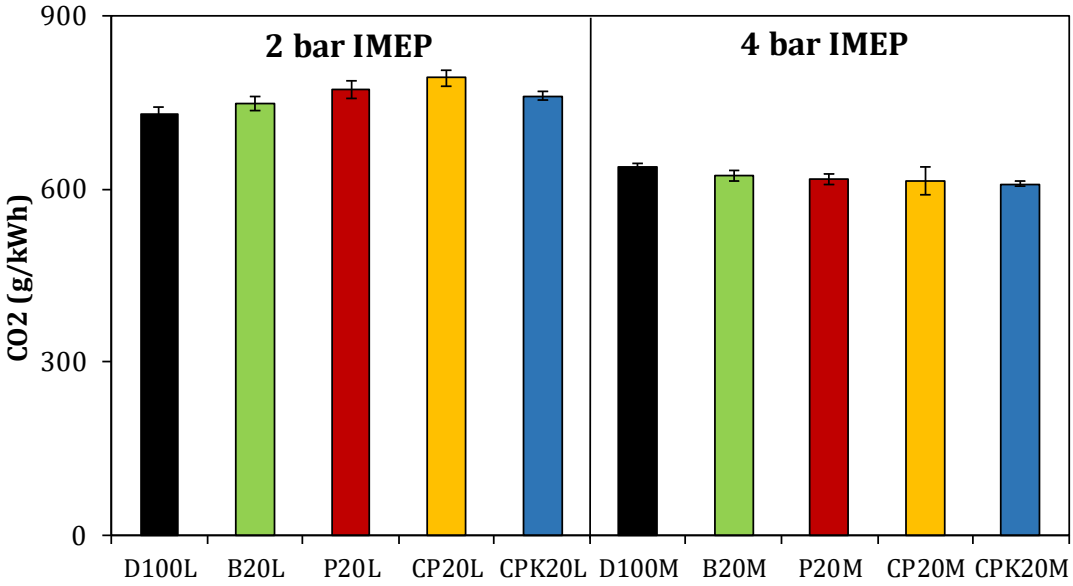



Figure 5-5: Carbon dioxide emissions at 2 bar IMEP and 4 bar IMEP

#### 5.2.2.3. $NO_x$ Emissions

$NO_x$ formation depends on the cylinder temperature, oxygen concentration and reaction residence time, which are functions of equivalence ratio (λ), fuel density, cetane number and fuel composition [138]. Thermal $NO_x$ is formed mainly due to the oxidation of nitrogen present in the intake air during combustion. A more pronounced premixed phase of the combustion as a result of a longer ignition delay can result in higher $NO_x$ emissions, due to higher in-cylinder peak temperature [139]. A higher peak of the HRR for the fuel blends was shown in Figure 5-1. Engine-out $NO_x$ emissions are shown in Figure 5-6. It can be concluded that the high oxygen content of the blended fuels, high combustion pressure and temperature can promote formation of $NO_x$ emissions. This has also been reported in previous studies on the oxygenated fuels [74, 140].

As presented, the tested oxygenated fuels have higher $NO_2$ due to the oxygen content of the fuels. Formation of $NO_2$ increases by use of these oxygenated fuels. This is very beneficial due to the ability of $NO_2$ to oxidize soot at lower temperatures compared to oxygen (useful in regeneration of soot filters in diesel vehicles). There is a very slight difference between P20L and B20L in terms of $NO_x$ emissions. Kumar et al. [73], reported that at low loads, the amount of $NO_x$ emissions from pentanol-diesel combustion is more than neat diesel combustion, but the increase of the load has an opposite effect. They found that the amount of soot formation for this blend is less compared to diesel, due to the presence of oxygen atom in the hydroxyl group.

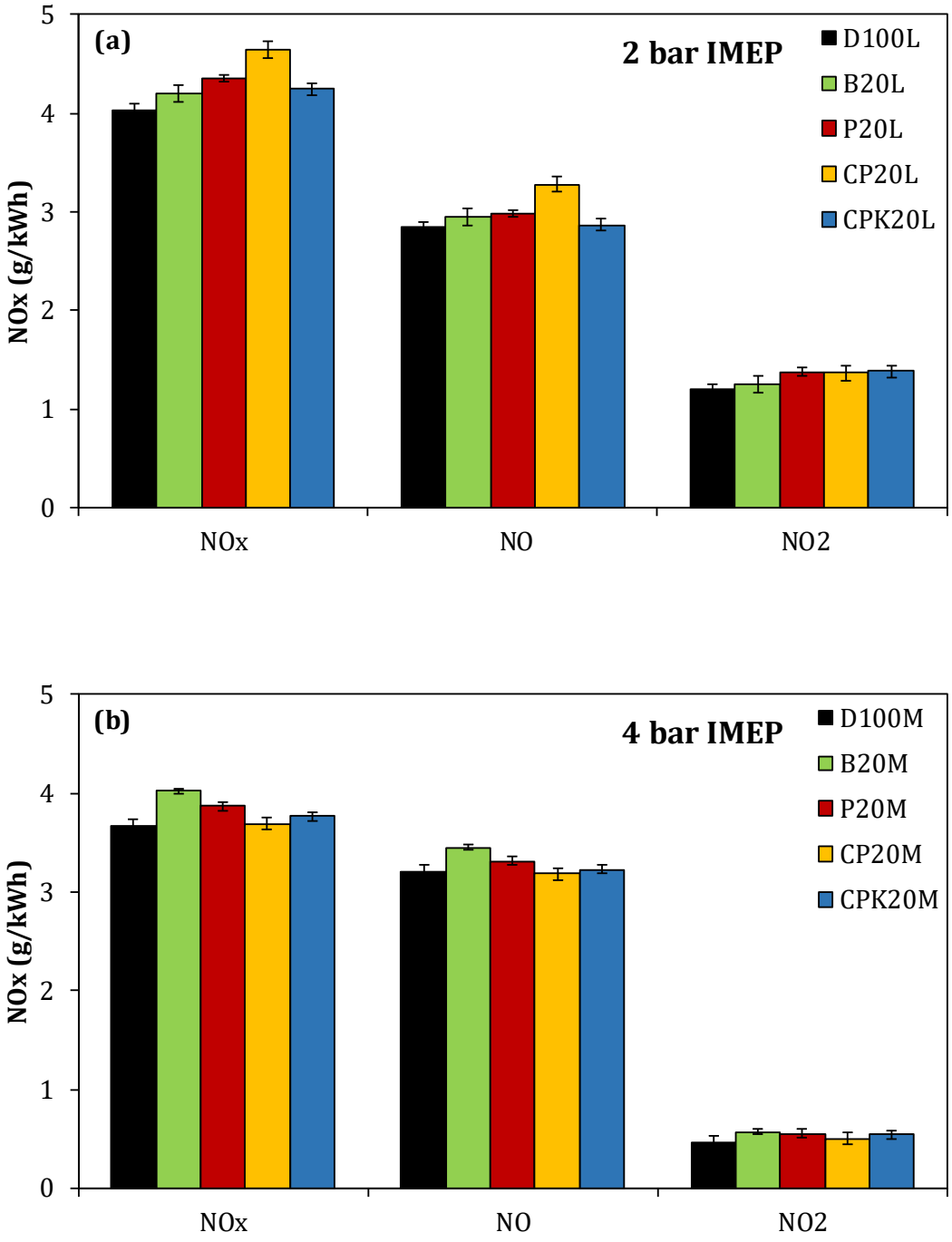


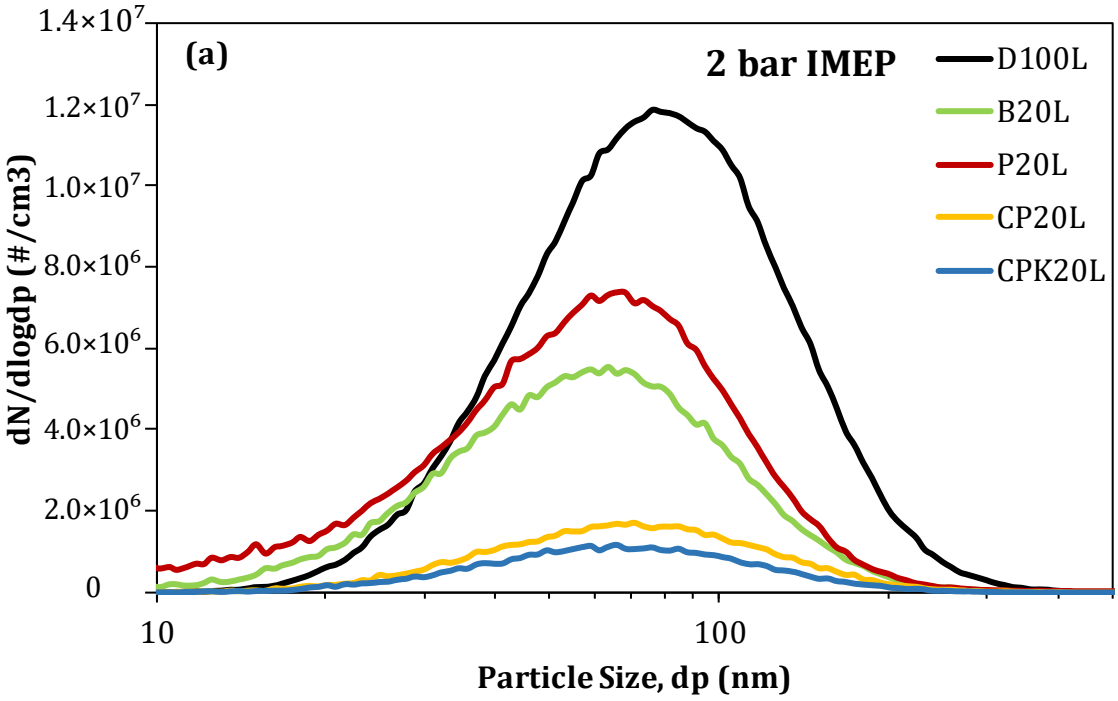

Figure 5-6: Nitrogen oxides' emissions at 2 bar IMEP and 4 bar IMEP

### 5.2.3. Particulate Matter

The number concentration of particulate matter emissions from combustion of the alternative fuels was significantly lower than those emitted from diesel combustion. These particles have a smaller mean diameter as shown in Table 5-2 and Figure 5-7. Lower particle emissions compared to the diesel baseline can be due to less formation of particles as a result of better premixing and the higher fuel oxygen content; and the absence of aromatic and/or improved soot particle oxidation due to the higher fuel oxygen content. A lower carbon to hydrogen ratio of straight-chain alcohol fuels can inhibit formation of particles too. In straight-chain alcohols, as the oxygen content in the molecular structure decreases, the number of particles increases [141]. Viscosity and, the boiling point and melting point of fuels affecting spray properties/fuel and air mixing via fuel droplet size, affects soot formation [67, 128].

Table 5-2: Particle size distribution for tested fuels

| Test abbreviation | Total number concentration (#/cm$^3$) | Maximum number concentration (#/cm$^3$) | Median diameter (nm) |
|---|---|---|---|
| D100L | $6.98\times10^6$ | $1.19\times10^7$ | 76.88 |
| B20L | $3.37\times10^6$ | $5.56\times10^6$ | 58.76 |
| P20L | $4.47\times10^6$ | $7.39\times10^6$ | 59.32 |
| CP20L | $1.03\times10^6$ | $1.72\times10^6$ | 68.25 |
| CP20L | $6.48\times10^5$ | $1.17\times10^6$ | 65.67 |
| D100M | $4.76\times10^6$ | $7.51\times10^6$ | 67.78 |
| B20M | $1.01\times10^6$ | $1.72\times10^6$ | 63.01 |
| P20M | $1.67\times10^6$ | $2.67\times10^6$ | 58.56 |
| CP20M | $6.41\times10^5$ | $1.08\times10^6$ | 69.25 |
| CPK20M | $4.15\times10^5$ | $6.73\times10^5$ | 69.39 |



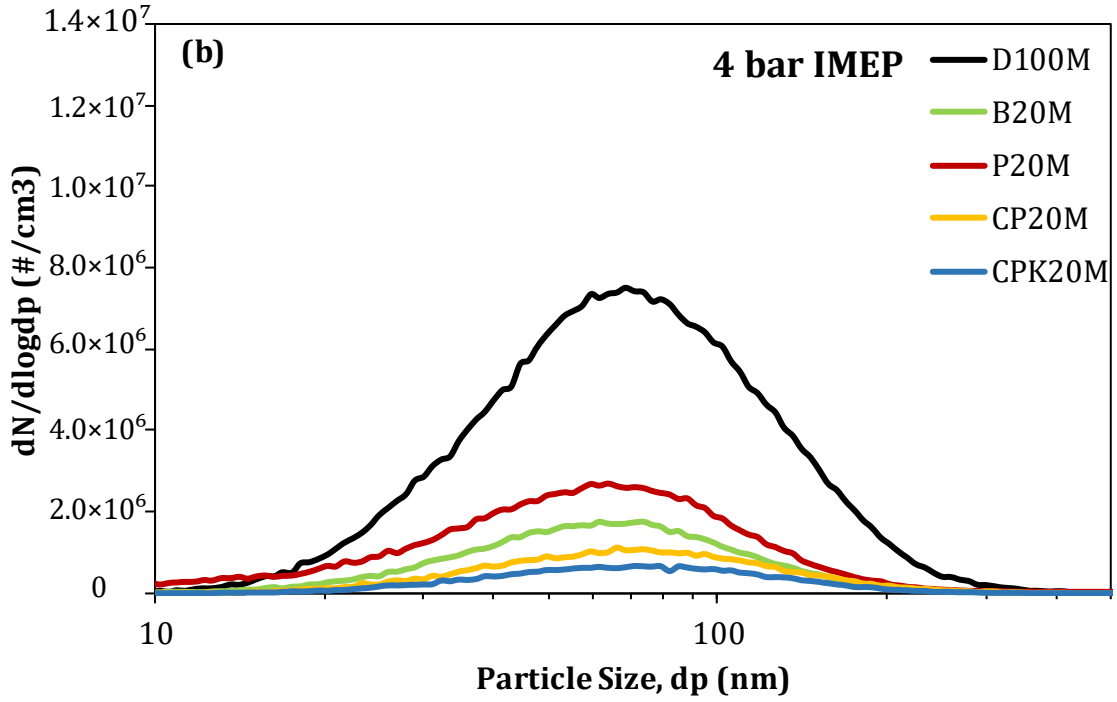




Figure 5-7: Particle size distribution at (a) 2 bar IMEP; (b) 4 bar IMEP

It is shown in Figure 5-7 and Table 5-2 that using the blended fuels reduces total particle number concentration compared to neat diesel combustion. At 2 bar IMEP, compared to D100, the total particle number for P20 decreased by 35%; for B20 by 51%; for CP20 by 85%; and for CPK20 by 90%. These reductions at a higher load of 4 bar IMEP were larger; P20 decreased by 65%; B20 by 79%; CP20 by 86%; and CPK20 by 91%; compared to D100. The PM reduction could be due to the molecular structure of these fuels. Comparing CP20 and CPK20, particle formation could be due to the higher molecular weight and boiling point of CP20, which produces more particles than CPK20. This is the same when comparing P20 and B20 as well, where the longer carbon-chain length of pentanol resulted in higher particulate matter emissions compared to butanol [142, 143].

In Table 5-2, the total number concentration (TNC), maximum number concentration (MNC), and median diameter (MND) values are presented. The accumulation mode particles (APs) are significantly lower for blended fuels due to high oxygen content. The lower amount of carbon in butanol leads to there being fewer primary particles to form the accumulation mode particles. For cyclopentanol, this is lower than pentanol and butanol. The reduction of the number of particles for B20 compared to D100 is also in good agreement with previous studies [74, 75]. This reduction is due to the presence of oxygen in the hydroxyl group of the B20 affecting the reduction of soot formation and the improved rate of soot oxidation [41, 77]. Cyclopentanone with the carbonyl group as a ketone showed a significant reduction in particle size distribution and the number of particles. An increase of oxygen content in fuel and a decrease of C-C bonds in the fuels' molecular structure lead to a decrease of soot formation. This was confirmed in previous research [11, 144, 145].

As a conclusion, the ranking for particulate matter emissions was CPK20< CP20< B20< P20< D100. An increase of the oxygen content with the same number of carbons (C5) in the fuel led to significant reductions in particulate emissions. It is the same in the straight-chain alcohols, where an increase of oxygen content from pentanol to butanol led to a reduction of particles.

## 5.3. Summary

This chapter presents the combustion characteristics, engine performance, gaseous emissions and particulate matter characteristics of a diesel engine fuelled with diesel, and diesel blended with 20% by volume of butanol, pentanol, cyclopentanol and cyclopentanone. The following findings can be concluded in comparison with a diesel fuelled engine.

An overview of the results of the combustion analysis indicates the stability of the engine's operation with the tested alternative fuels. Most of the blended oxygenated fuels lead to higher in-cylinder peak pressure, higher heat release rate and longer ignition delay. The ignition delay increased with the reduction of the carbon number. The longer ignition delay of the tested fuels compared with diesel could be due to the high electronegativity of the oxygen atom in molecules that help in reduction of PM emissions.

The increase of the peak heat release rate can be attributed to the lower viscosity of fuels affecting the efficiency of the fuel and air mixing during the ignition delay period. The change in exhaust temperature could be due to a change in the combustion delay. The ISFC for the tested oxygenated fuels is higher compared to the baseline diesel combustion. The ITE at 4 bar IMEP improved due to a faster burning rate and hypothetically, less heat loss to the cylinder walls.

In the gaseous emissions, these fuels lead to higher CO emissions, higher light hydrocarbons, lower total hydrocarbons and higher $NO_x$ emissions. The higher concentration of CO emissions in the exhaust of the blended fuels can be due to the higher heat of the evaporation of these fuels and also their lower cetane number; which can lead to more fuel-air premixing and consequently, a higher number of locally lean fuel-air mixture packets. An increase of oxygen content in fuels affects the increase of combustion pressure and temperature which promotes the formation of $NO_x$ emissions.

The particulate emissions of the blended fuels combustion in the engine decreased significantly for all of the studied fuel blends. This reduction is due to better premixing, the higher fuel oxygen content, and/or improved soot particle oxidation. Also, a lower carbon to hydrogen ratio of straight-chain alcohol fuels can inhibit the formation of particles.

Compared to straight-chain alcohols (B20 & P20), alcohol fuels' molecule with a cyclic structure (CP20), indicated more advantages in the reduction of particulate emissions. Also, in a ketone molecular structure (CPK20), the double bond oxygen to the fuel molecules decreased the $NO_x$ and HCs level and led to a significant reduction of particulate emissions.

In general, a change of the molecular structure of the alternative fuels influences the combustion profile, exhaust gas emissions and particulate matter characteristics. The addition of only one carbon to convert butanol to pentanol; or a change of structure from straight chain to cyclic in pentanol to cyclopentanol; and the addition of double bond oxygen content to cyclopentanol for creating cyclopentanone, indicated the significant impact of emissions' characteristics. As a final conclusion of this chapter, use of the studied fuels (B20, P20, CP20 and CPK20) can provide visible environmental

improvements. The CPK20 and CP20 as cyclic hydrocarbons reduced particulate matters significantly. THC emissions also decreased with combustion of these two cyclic hydrocarbons. These two fuels also showed the best lubrication and tribological behaviour in Chapter 4, too.

# CHAPTER 6. ENHANCING THE LOW TEMPERATURE ACTIVITY OF DIESEL OXIDATION CATALYST BY USING ELECTRICAL HEATING AND ALTERNATIVE FUELS

## 6.1. Introduction

As discussed in Chapter 3, a single cylinder research diesel engine was operated at 2 bar and 4 bar IMEP at a fixed speed of 1500 rpm. Four different blended fuels (B20, P20, CP20 and CPK20) were compared with the baseline diesel (D100). These engine operating conditions are the same as in Chapter 5, with the addition of using the diesel oxidation catalyst (DOC) in this chapter. Also, for the case of the baseline diesel, pure $H_2$ from a gas cylinder was introduced upstream of the DOC at a concentration of 500 ppm, as smaller concentrations are more effective in promoting CO and NO oxidations over a DOC [10]. An efficient aftertreatment heating strategy coupled with the DOC was used to study its interaction with the combustion of alternative fuels in order to identify the potential emissions reduction benefits. This system has a capability to be used in hybrid vehicles. The length of the pipe connecting the engine exhaust manifold to the DOC inlet (Figure 3-9) is approximately 164 cm. The exhaust gas temperature decreases around 80 °C to 90 °C while travelling within this pipe. The electrical heater upstream of the catalyst was used to control the DOC's inlet temperature. There was a negligible (<5°C) difference between the DOC's inlet temperatures while running the engine with different fuels.

The DOC was thermally conditioned in a furnace at 550 °C for 6 hours prior to the testing to limit any possible physisorption or chemisorption effects. Sampling of the exhaust gas was carried out with the FTIR (for gaseous emissions), the HSense (for $H_2$ concentration) and the SMPS (for particle size distribution) before the DOC (bDOC) and after the DOC (aDOC). This chapter is divided into four sections investigating:

i) Effects of alternative fuels' combustion on the DOC's performance without use of any upstream heater (bDOC temperature at 150 °C);

ii) The DOC's light-off when running the engine with different fuels and the effects of the efficient heating strategy on the DOC's performance (bDOC temperature at 350 °C);

iii) Effects of the DOC plus the heater system on particulate matter size distribution.

A summary of the test abbreviations is shown in Table 6-1.

Table 6-1: Engine and aftertreatment operating conditions

| Test abbreviation | Fuel blends with diesel (%v/v) | Engine speed (rpm) | IMEP (bar) | Aftertreatment conditions |
|---|---|---|---|---|
| D100L | Diesel 100% | 1500 | 2 | 1) Heater OFF<br>2) Heater ON<br>3) Light-off |
| B20L | Butanol 20% | 1500 | 2 | |
| P20L | Pentanol 20% | 1500 | 2 | |
| CP20L | Cyclopentanol 20% | 1500 | 2 | |
| CPK20L | Cyclopentanone 20% | 1500 | 2 | |
| D100L+$H_2$ | Diesel 100%+$H_{2,bDOC}$ | 1500 | 2 | |
| D100M | Diesel 100% | 1500 | 4 | 1) Heater OFF<br>2) Heater ON |
| B20M | Butanol 20% | 1500 | 4 | |
| P20M | Pentanol 20% | 1500 | 4 | |
| CP20M | Cyclopentanol 20% | 1500 | 4 | |
| CPK20M | Cyclopentanone 20% | 1500 | 4 | |

As discussed in Chapter 5, oxygenated fuels led to the decrease of THC and the increase of CO emissions. In contrast, $NO_x$ emissions were higher compared to the diesel baseline case. The DOC as an oxidation catalyst can be used to reduce CO and THC.

## 6.2. Results and Discussion

### 6.2.1. Impact of Alternative Fuels' Combustion on the DOC's Catalytic Activity

In this section, the conversion efficiency of the gaseous emissions through the DOC from a diesel engine fuelled with different fuels is investigated. The compositions of the exhaust gases in different test conditions are shown in Figure 6-1 and Figure 6-2. It is concluded that for all the tested fuels, THC decreased using the DOC due to hydrocarbon oxidation, adsorption and condensation. The CO was oxidized to carbon dioxide. The NO increased for all cases; however, the $NO_2$ decreased while the $NO_x$ was constant. It can be hypothesised that most of the $NO_2$ was used as an oxidative reactant to improve CO and THC oxidation efficiency at low temperatures. The use of the oxygenated alternative fuels indicated higher catalytic activity at a lower temperature compared with diesel combustion. It can be seen that higher hydrogen and oxygen content of the fuels increased the rate of CO oxidation over the DOC. The CO conversion efficiency for D100L is 10%, which is increased to 12%, 18.2%, 25% and 24% for B20L, P20L, CP20L and CPK20L, respectively. At 4 bar IMEP, as the exhaust gas temperature increased, the conversion efficiency was improved due to the higher activity of the DOC (D100M = 82.11% < B20M = 85.85% < P20M = 89.11% < CPK20M = 92.2% < CP20M = 93.3%). The addition of 500 ppm of $H_2$ upstream of the DOC, resulted in improved CO conversion efficiency to 39% but worse THC conversion efficiency. The $NO_2$ concentration decreased as well. Hypothetically, the temperature within the DOC was not high enough without the addition of $H_2$ and therefore THC reduction was due to the heavy HC adsorption/condensation on the surface of the monolith channels. After the addition of the $H_2$ and consequently promotion of the exothermic reactions within the DOC, the already adsorbed HC desorbed resulting in a negative conversion efficiency.

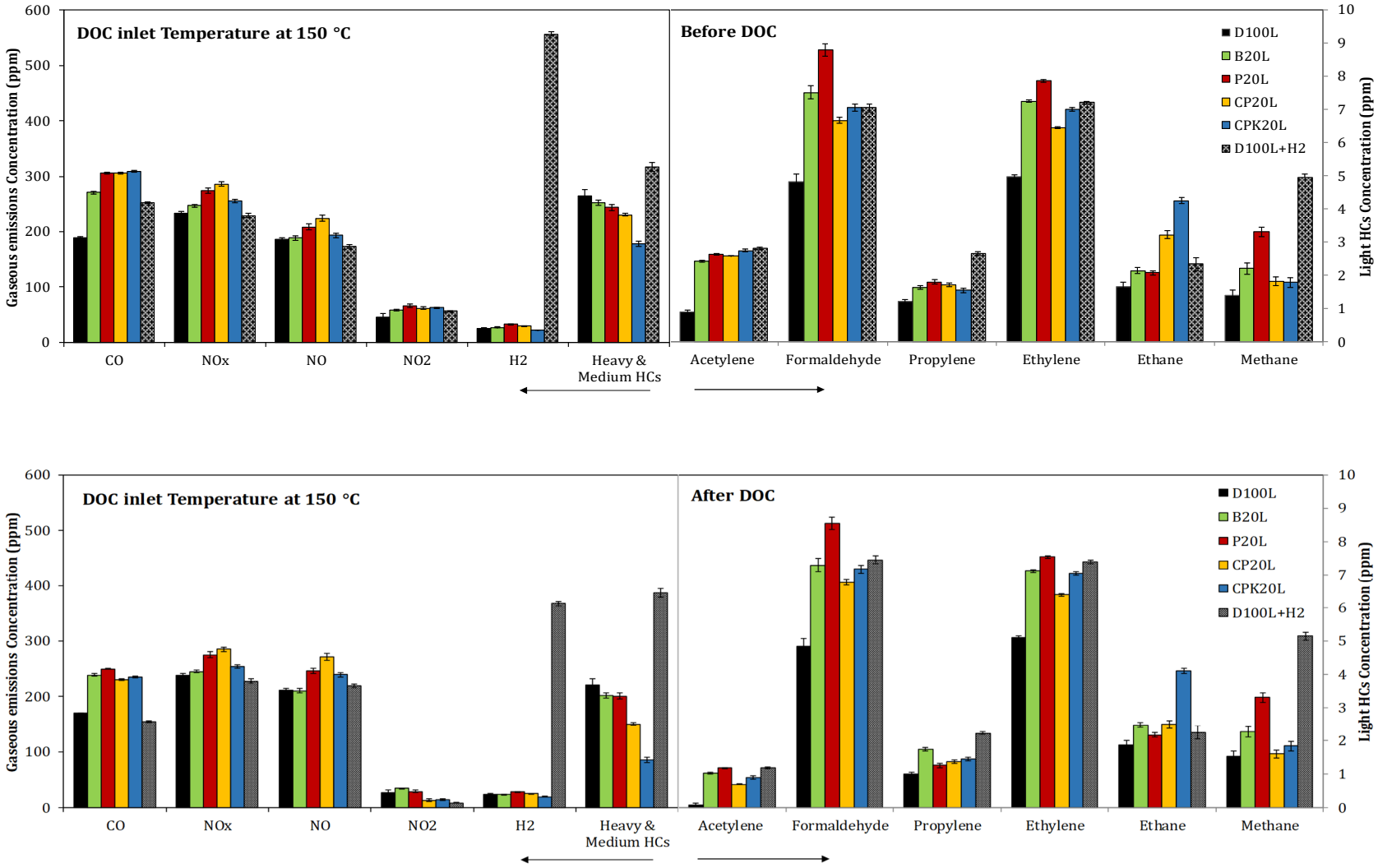



Figure 6-1: Heater OFF-Gaseous emissions' concentration at 2 bar IMEP, bDOC and aDOC

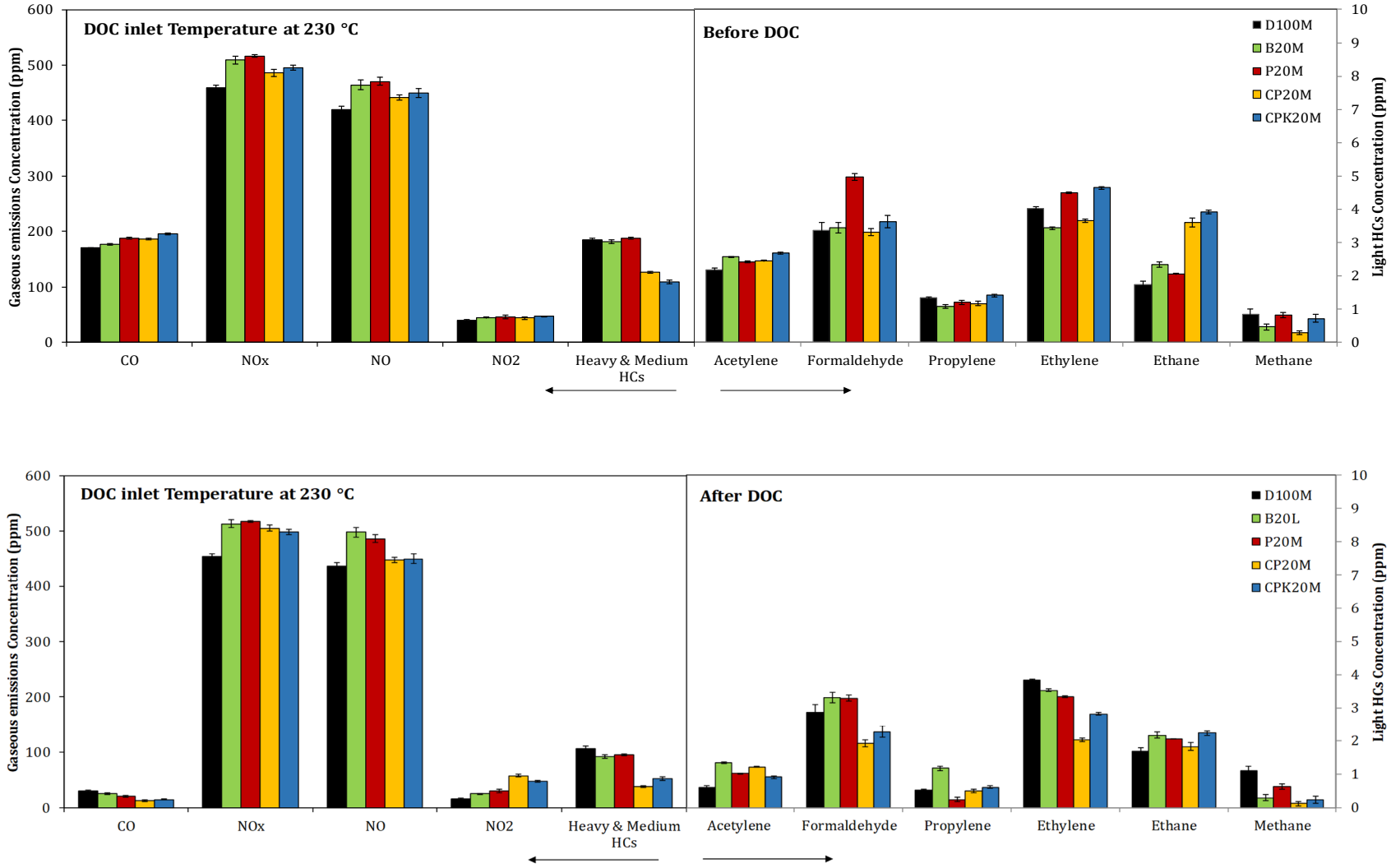



Figure 6-2: Heater OFF-Gaseous emissions' concentration at 4 bar IMEP, bDOC and aDOC

### 6.2.2. Effects of Alternative Fuels' Combustion on DOC Light-off

For this catalyst light-off (T50) study, the catalyst was at exhaust temperature (~150 °C) and then the activity of the DOC was studied while the exhaust gas temperature was increased with a ramp of 5 °C per minute (2 minutes), waiting for one minute at the same temperature. Moreover, the steady state experiments which were explained in detail in Chapter 3 were conducted.

#### 6.2.2.1. CO Conversion in the DOC

Figure 6-3 to Figure 6-8 illustrate CO, THC, NO, $NO_2$ and $H_2$ concentration with respect to the DOC's inlet temperature. Figure 6-9 presents light-off curves. The start of the CO oxidation in the DOC depends on the exhaust gas composition. Generally, by an increase of CO concentration in the exhaust, its light-off is delayed towards a higher temperature. With an increase of temperature, the adsorbed CO on the active sites of the catalyst's surface is released and then catalytic activity improves. The presence of HC can also affect CO oxidation by adsorbing over the catalyst's active sites [10, 36, 75, 146]. At low temperatures, the CO oxidation reaction in the DOC is limited kinetically due to the covered active sites. After the start of oxidation, at high temperatures, the CO is not limited and heat release from the CO oxidation increases the DOC's temperature. So, it is clear that high temperature helps the active sites to oxidize CO emissions. Also, CO could be considered as an inhibitor for other emission species' oxidation. The CO oxidation start earlier than HCs oxidation due to the higher reactivity of CO compared to some of the HC species. This means that catalytic active sites become available for HC oxidation only after CO oxidation is well developed [146, 147]. The $NO_x$ species can also affect the CO oxidation reaction. It was found in the literature that exhaust gases with lower NO concentration show an earlier CO light-off [146]; however, in our studies a difference of

20 ppm in NO concentration had a slight influence in delaying light-off temperature. This means that in this work other factors have a more essential impact on CO light-off temperature than the $NO_x$ species. The competition between CO, HCs and $NO_x$ species at low temperature happens once CO oxidation starts, as before that, CO was adsorbed on the catalyst's active sites.

The B20 and P20 as bio-alcohols decrease the CO light-off temperature by 26 °C (173 °C) and 16 °C (183 °C), respectively, compared with D100 (199 °C). The slightly higher exhaust temperature, and the presence of the hydrogen and oxygen content in the exhaust would make the hydrogen bonded components such as OH increase the oxidation reaction rate of the DOC at lower temperatures [36]. For cyclic fuels, this CO light-off temperature is 188 °C and 191 °C for CP20 and CPK20, respectively. The H/C ratio and also $H_2$ content in the exhaust gas seem to affect the oxidation reaction. There is tough competition between the amount of $NO_x$, HCs, $H_2$ and oxygen contents in the exhaust to oxidise the CO emissions, but it seems that hydrogen and oxygen play a more important role due to the formation of hydrogen bonded structures such as OH which increase the rate of the oxidation reaction. The addition of 500 ppm $H_2$ upstream of the catalyst significantly improved CO oxidation and reduced the light-off temperature by up to 50 °C (149 °C) compared with D100 (199 °C). This is due to an increase of the available active sites for the adsorption of oxygen and other species to promote CO light-off temperature [10, 148]. In previous studies, it was found that the hydrogen exothermic effect is not the only main reason for CO and HCs oxidation at low temperature, also the increase of hydrogen and CO combustion's exothermic effect enables the CO oxidation rate with the increasing temperature [10]. The $H_2$ can lead to the promotion of exothermic reactions and make active sites more available for CO adsorption. Also, it has made NO oxidation possible at the lower temperatures as well and has led to a higher $NO_2$ production [10].

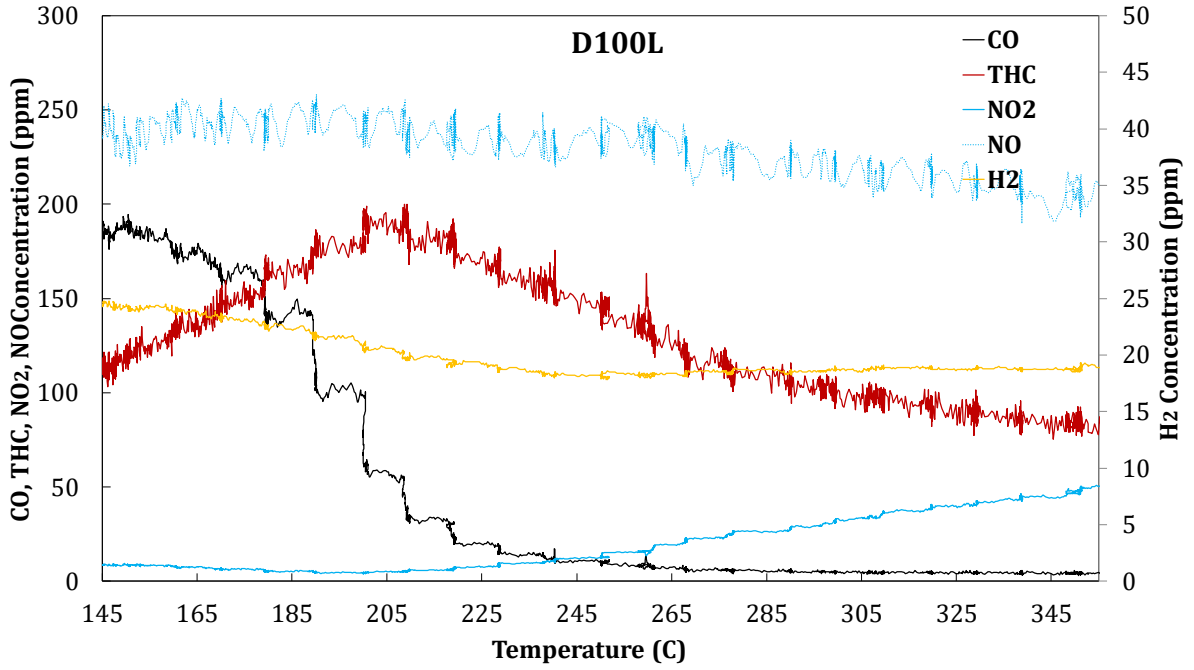



Figure 6-3: Change of aDOC composition in D100L during light-off test

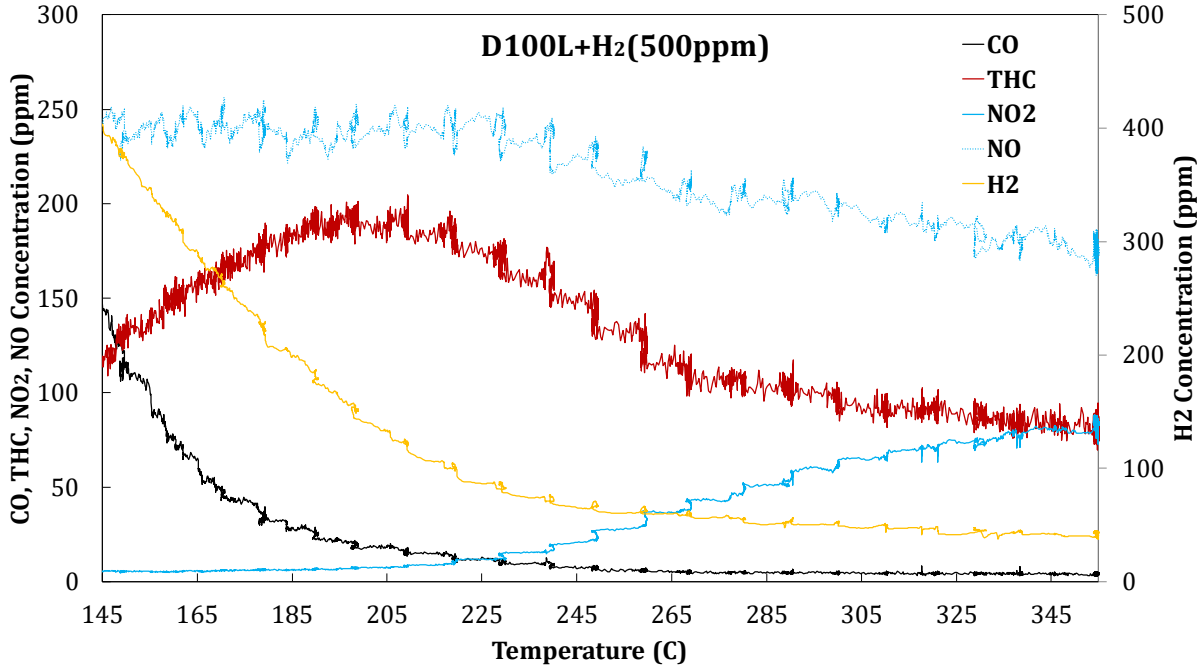



Figure 6-4: Change of aDOC composition in D100L+$H_2$ during light-off test

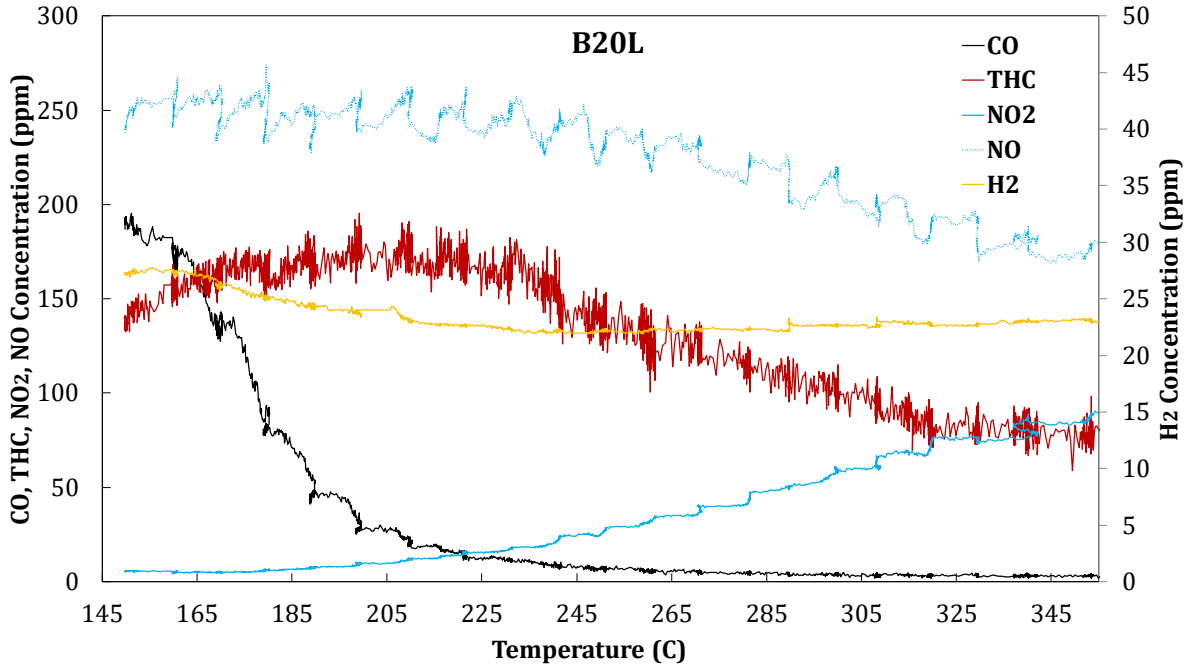



Figure 6-5: Change of aDOC composition in B20L during light-off test

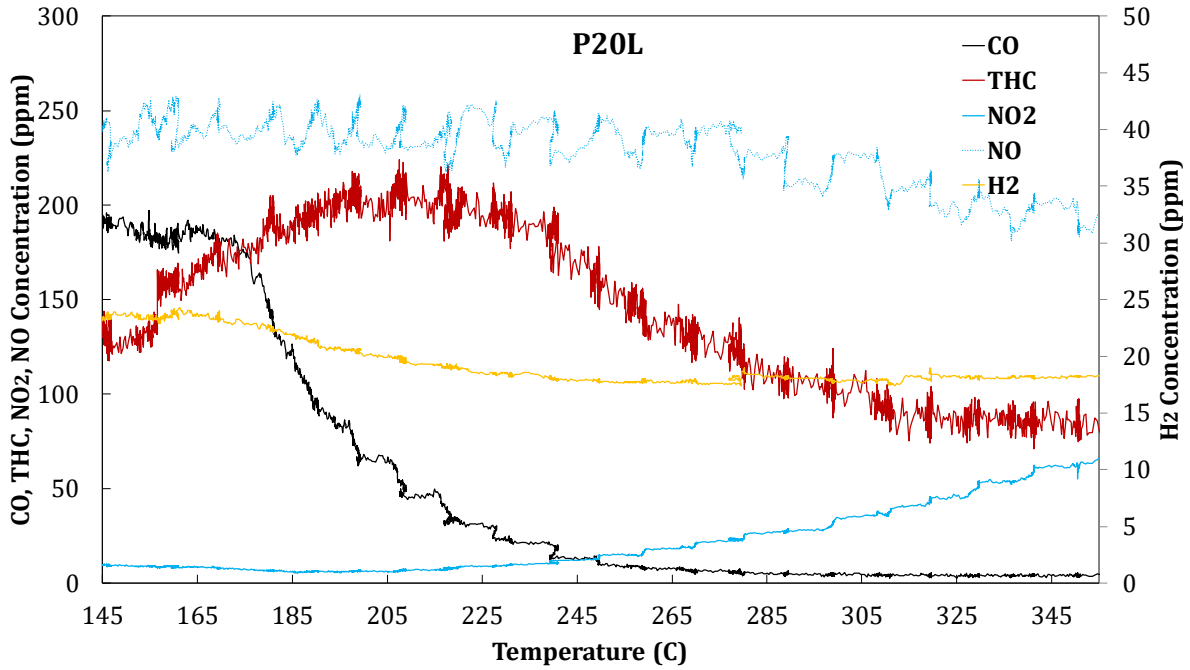



Figure 6-6: Change of aDOC composition in P20L during light-off test

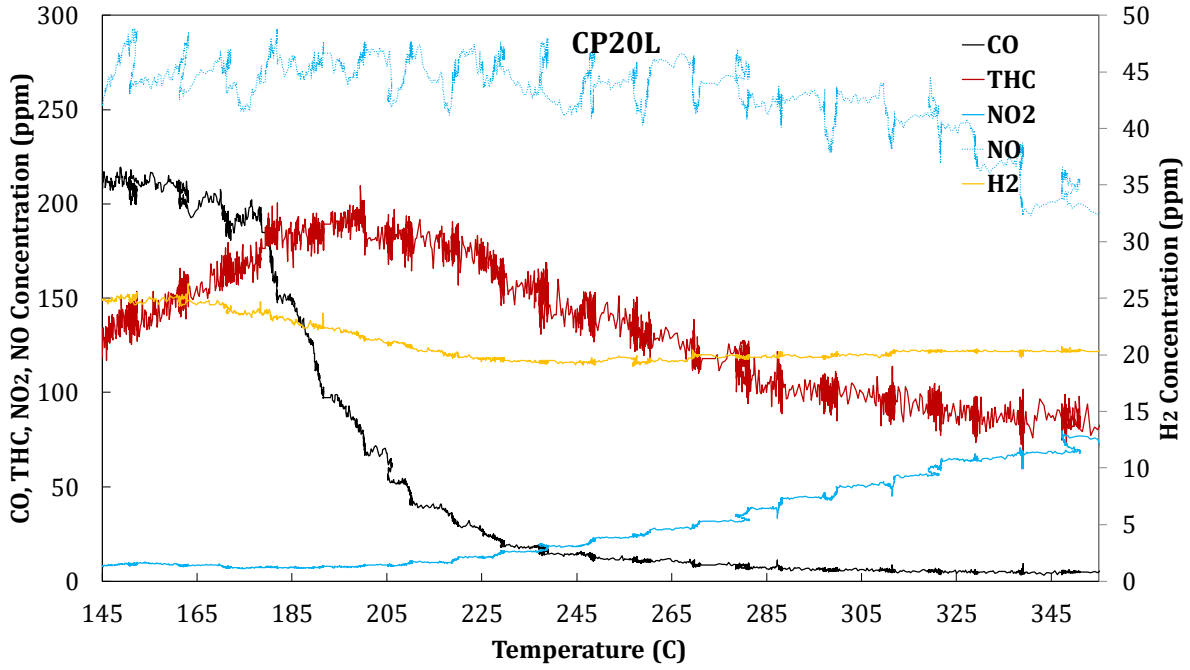



Figure 6-7: Change of aDOC composition in CP20L during light-off test

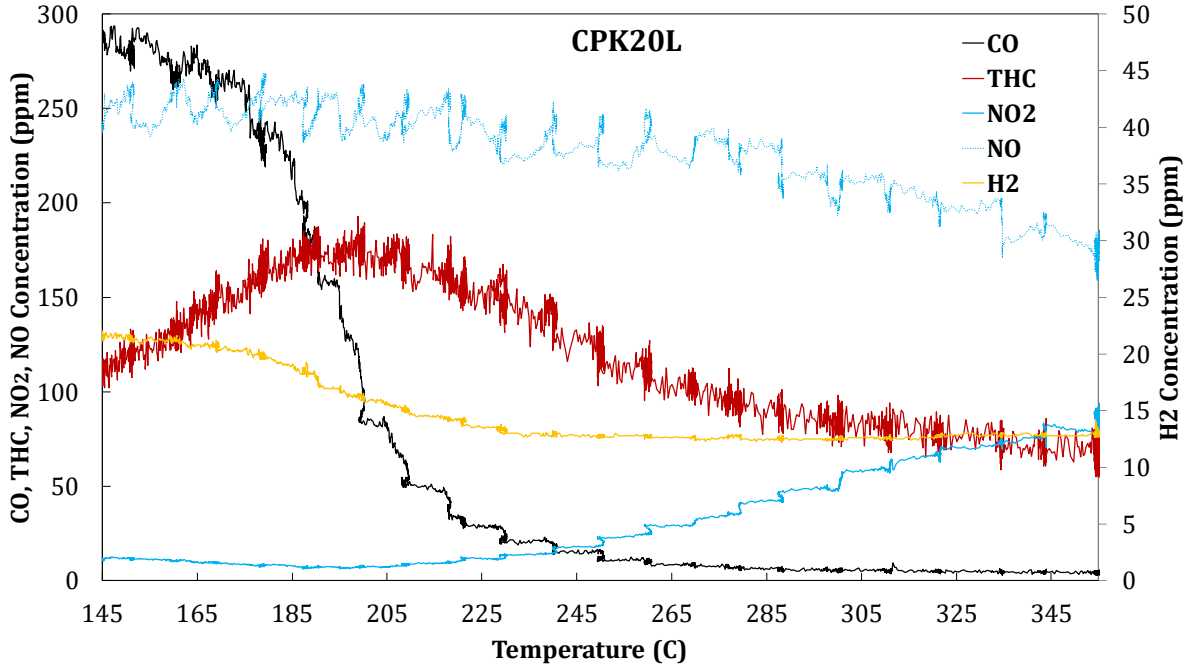



Figure 6-8: Change of aDOC composition in CPK20L during light-off test

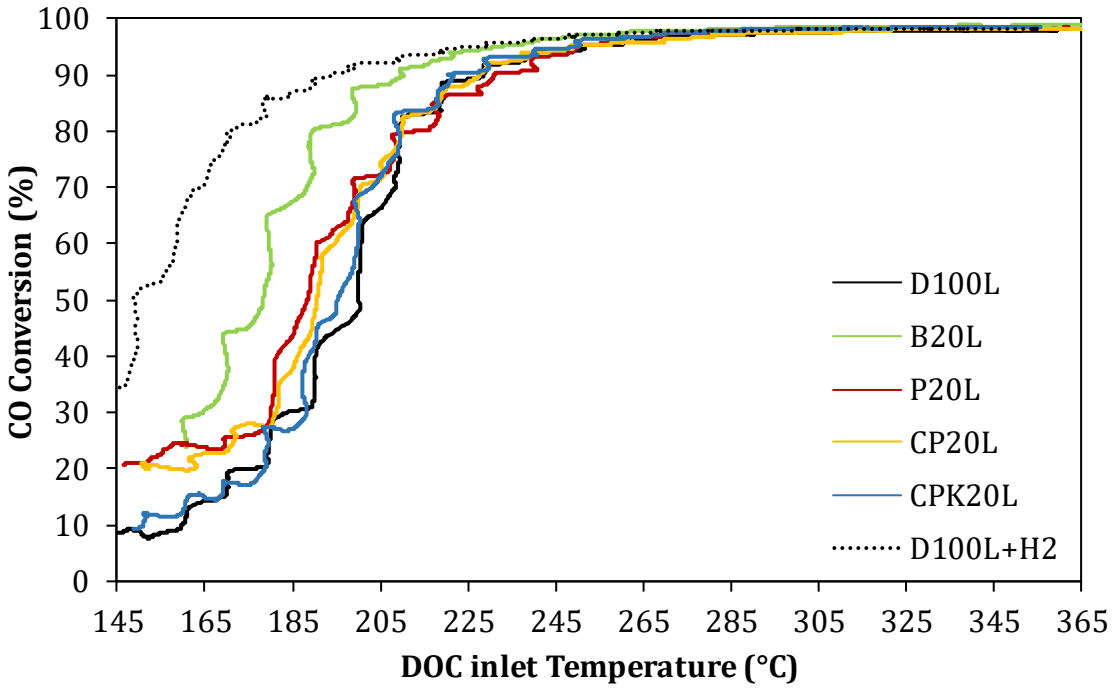



Figure 6-9: CO light-off of the DOC from alternative fuels' combustion

There is a slight link between H/C ratios of fuels molecular structure (Table 4-2 in Chapter 4 - H/C ratio: B20> P20> CP20> D100> CPK20 and O/C: B20> CPK20> CP20> P20> D100) and the $H_2$ amount in exhaust gas (B20 = 31.89 ppm, CP20 = 28.44 ppm, P20 = 27.05 ppm, D100 = 25.21 ppm, CPK20 = 22.21 ppm). These differences are only a few ppms, but the presence of hydrogen and oxygen is hypothesised as one of the reasons for promotion of catalytic activity at a lower temperature, which makes the oxidation reaction easier in the active sites. The order of the starting temperature of CO oxidation is D100+$H_2$, B20, P20, CP20, CPK20 and D100. The overall reasons for the promotion of the catalytic activity at a lower temperature can be hypothesised as: the addition of hydrogen; the presence of oxygen and hydrogen in the exhaust gas; and a higher H/C ratio.

#### 6.2.2.2. THC Conversion in the DOC

The higher conversion for the hydrocarbons at the beginning of the light-offs in Figure 6-10 would be due to the presence of zeolite in the washcoat, which causes trapping (''virtual conversion'') of medium and heavy hydrocarbons at low temperature and releases them in higher temperatures [10, 75, 146, 149]. This higher conversion at the start of light-off in lower temperatures is not considered as the HCs oxidizing because it is due to the ability of zeolites to store HCs. In all of the tested conditions zeolite shows the same behaviour with around 50% conversion efficiency at 145 °C. After the release of the hydrocarbons at a temperature of around 205 °C, the conversion efficiency starts increasing. This point is almost the same temperature that $NO_2$ produced from NO. The different behaviour of the HC light-off is due to the reaction activation energy and rate depending on the fuels' nature, the exhaust hydrocarbon molecular structures and the chain length which affects the adsorption strength [146]. In P20 and CPK20, the reduction in conversion efficiencies could be due to the higher content of heavy and light hydrocarbons, respectively. In P20, heavy and medium hydrocarbons are adsorbed on the zeolites and oxidized as they are released; this is the same process for light hydrocarbons in the CPK20 exhaust. The B20 shows that the amount of HCs which is released is very low compared to other fuels; this could be due to the more active sites presence from proper CO oxidation and HC oxidation even at lower temperatures [75].

As presented in Figure 6-1 and Figure 6-14, conversion of saturated hydrocarbons (methane and ethane) is more difficult due to the low oxidation rate compared to unsaturated hydrocarbons (ethylene, propylene and acetylene), and as reported in the literature [10, 36, 150]. Investigation of hydrocarbon speciation in different temperatures shows that reduction of propylene starts at around 190 °C, formaldehydes

at 170 °C and ethylene from 180 °C; however, there is a slight increase of ethane at around 180 °C and then it starts decreasing at around 200 °C, while methane and acetylene stayed almost constant. So, it can be concluded that incomplete conversion of HCs is due to the presence of different hydrocarbon species where oxidation is limited by mass transfer to the catalyst's active sites [10]. For example, light hydrocarbons have early light-off and are not affected by other emissions' species. Due to their short carbon chains, they are not trapped in zeolites and therefore are more easily oxidized at lower temperature. However, aromatic hydrocarbons oxidise at higher temperatures due to their ring molecular structure and inhabitation from other exhaust species [147]. The DOC's coating affects the hydrocarbon conversion as platinum is the most active metal in oxidation of all the hydrocarbons, except for methane where palladium is preferred [147]. An increase of the DOC's inlet temperature improves the HC oxidation rate [151]. In general, the C-H bond cleavage is a key factor for catalytic oxidation of hydrocarbons, as light hydrocarbons have a strong C-H bond. Oxygen adsorbs on the catalyst's surface to give highly reactive anionic species $O^-$ and $O_2^-$; while superoxide can be formed upon $O_2$ adsorption over metal oxides and zeolites [150]. It was found from the literature that light-off temperatures of heavier hydrocarbons are lower than for the lighter hydrocarbons [150]. This would be the reason that higher light hydrocarbon concentration in CPK20 led to higher T50 compared to other oxygenated tested fuels. The highest HCs' light-off temperature for D100 (275 °C) (Figure 6-10) is due to the higher concentration of heavy hydrocarbons, lower oxygen and hydrogen species in the exhaust, which makes HCs be more difficult to be adsorbed and oxidised.

In the presence of hydrogen, the light-off and oxidation rate of HCs was improved; while the final conversion efficiency of the tested conditions is almost the same. It can be concluded that the effect of hydrogen on HC oxidation is due to the presence of hydrogen

containing active species adsorbed in the catalysts active sites; higher availability of active sites for HC and oxygen; and the exothermic effect of CO and hydrogen [10].

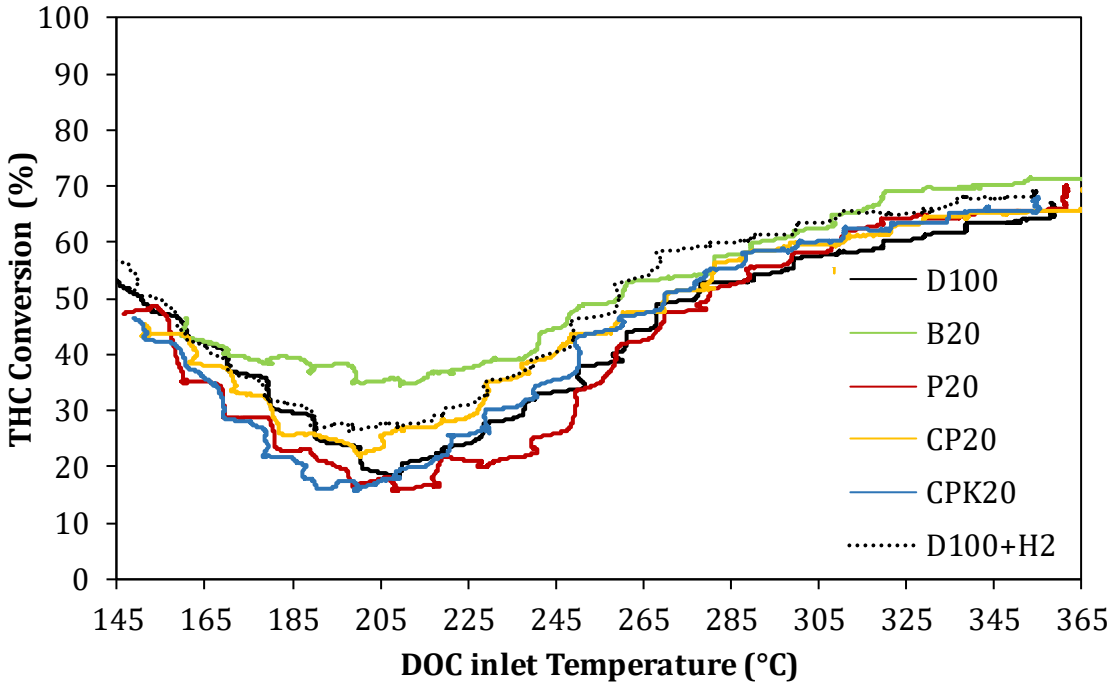



Figure 6-10: THC light-off of the DOC from alternative fuels' combustion

Figure 6-11 summarizes the required DOC inlet temperature for the different exhaust gases of the tested conditions to reach 25%, 50%, 75% and maximum CO conversion efficiency, and 50% of THC conversion efficiency in the DOC. This shows that the exhaust gas with an early start of oxidation is not the condition that will reach to its maximum conversion efficiency. This means that after the start of oxidation, competition between other exhaust species affects its reaction rate. From a combination of Figure 6-9 and Figure 6-11, it has been noticed that once CO oxidation starts, some influence in the THC's conversion efficiency curves occurred due to a change in the oxidation rate as a result of an increase in the HCs' conversion at the same temperatures. As a confirmation for this

hypothesis, Figure 6-3 to Figure 6-8 indicated that in all tested conditions an increase of temperature affects the oxidation performance. After the release of the hydrocarbons from the zeolites, the catalyst's active sites compete for CO oxidation reactions.

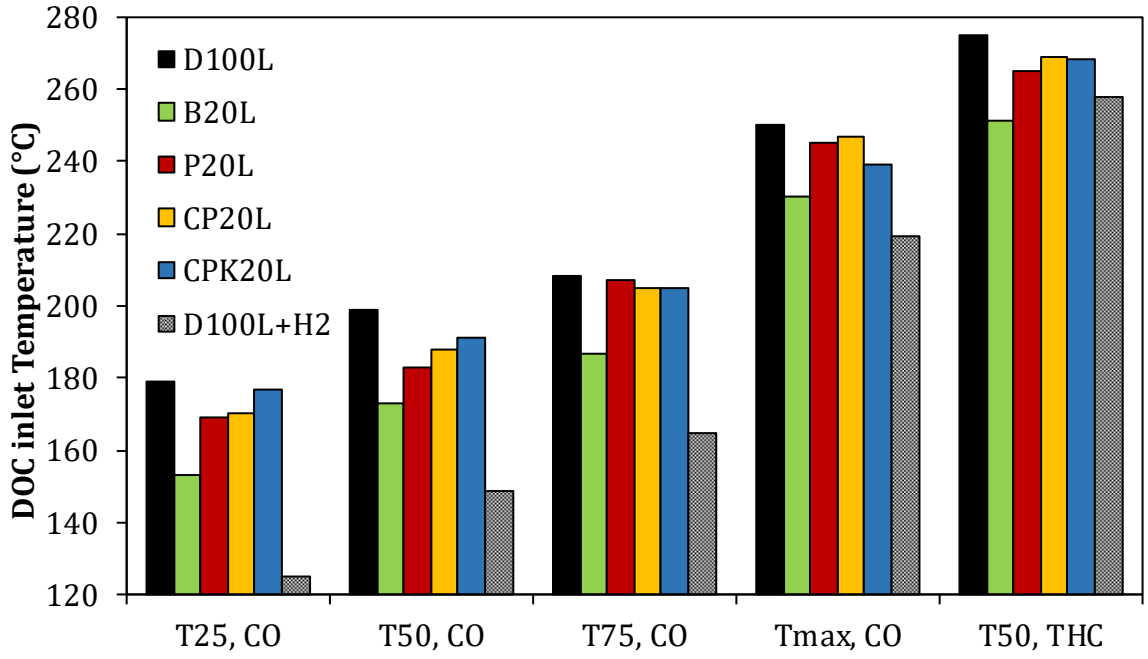



Figure 6-11: DOC inlet temperature required for 25%, 50%, 75% and maximum conversion

#### 6.2.2.3. NO to $NO_2$ Oxidation in the DOC

In addition to oxidation of carbon monoxide and hydrocarbons, the DOC can also oxidise NO to $NO_2$; which is important for higher performance of aftertreatment system components after the DOC, such as $NO_x$ storage (reduction) catalysts (NCR), selective catalytic reduction catalysts (SCR) and diesel particulate filters (DPF). As $NO_2$ oxidizes soot at a temperature around 350 °C, most DPFs are placed after the DOC to facilitate the lower temperature soot oxidation process [152, 153].

As presented in all the tested conditions, total $NO_x$ emissions stay constant through the DOC, but in terms of NO to $NO_2$ oxidation, it would be necessary to investigate the effect of temperature on this oxidation reaction over the DOC. In the exhaust under the tested conditions the DOC promotes the NO to $NO_2$ conversion, which is essential to enhance the low temperature passive soot oxidation process [154, 155]. Also, CO and HCs speciation affects the production of $NO_2$ [10, 146]. The $NO_2$ concentration in the exhaust depends on the type of fuel and engine operating condition. Figure 6-12 illustrates $NO_2/NO_x$ ratios which are CPK20>D100+$H_2$>P20>CP20>B20>D100. This could be affected by the rate of the peroxyl radicals' creation during combustion of these oxygenated fuels [36]. At a specific temperature a simultaneous oxidation of the organic compounds and NO to $NO_2$ occurs [96, 156].

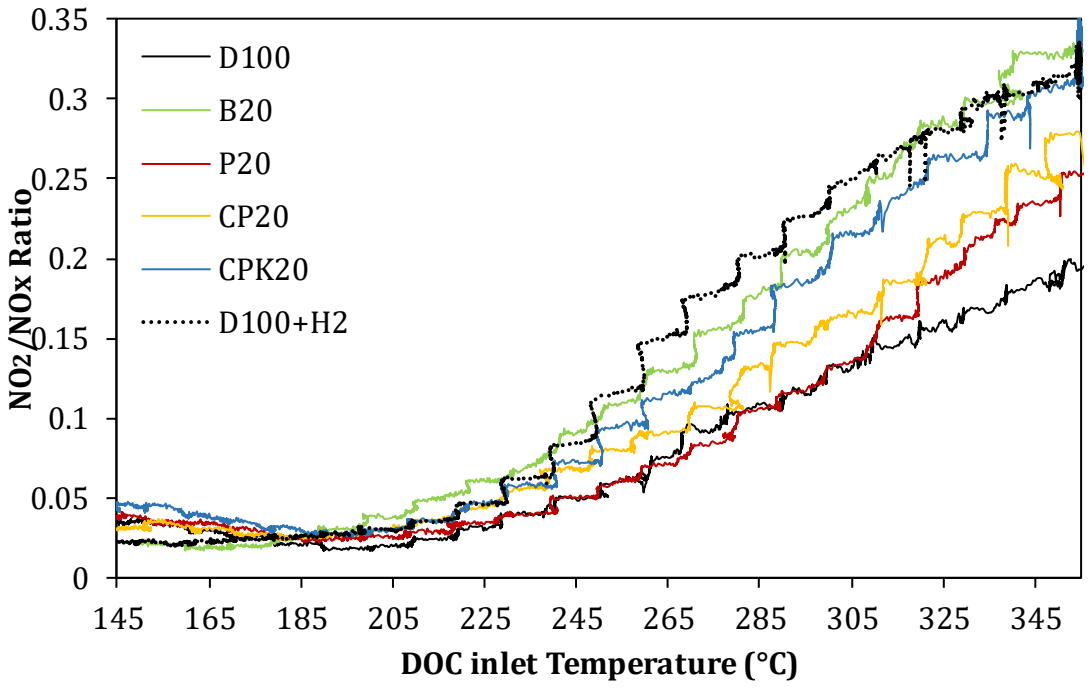



Figure 6-12: $NO_2/NO_x$ ratio in light-off study of alternative fuels' combustion

In addition to the temperature profile, the oxygenated organic compounds such as methanol, acetaldehyde, acetone, ethane and methylamine affect the rate of NO to $NO_2$ conversion. Furthermore, the ratio of HC compounds to NO, the reaction temperature, reaction time and the presence of hydrogen containing compounds affect the NO to $NO_2$ oxidation [157]. The CFD results in the literature indicated that combustion temperature is not the only reason for the increase of $NO_2$ by the addition of $H_2$ in the combustion process. Also, it is found that in-cylinder $HO_2$ enhances the NO to $NO_2$ oxidation in the engine's exhaust. This hypothesis was seen in our alternative fuel combustion and addition of $H_2$ in the exhaust, where the OH in oxygenated fuels and $H_2$ in the exhaust can increase the OH radicals and thus promote formation of $NO_2$ in the exhaust [158].

Based on the literature findings, once the equilibrium is reached, $NO_2$ starts to decrease by an increase of temperature. The NO oxidation to $NO_2$ is limited by kinetics at a lower DOC temperature and by thermodynamics at the DOC's higher temperatures [159]. As presented in the previous section, at lower temperatures $NO_2$ concentration at the DOC's outlet is lower than at the DOC's inlet, due to an increase of NO and a reduction of $NO_2$, while resulting in a small negligible $NO_x$ conversion. With an increase of temperature, CO and HC were reduced and $NO_2$ concentration increased, due to the role of the presence of the CO and HC on $NO_2$ [10, 97, 160, 161]. As presented in Figure 6-12, NO to $NO_2$ reaction started at around 220 °C for all the tested conditions, after complete CO oxidation. The negative conversion efficiency in lower temperature is due to conversion reduction by the HC and the weaker effect of CO adsorption over the catalyst's active sites. The HCs are the main factor in NO to $NO_2$ conversion efficiency, as CO is highly oxidized at this temperature range [10, 132, 154]. Also, after around 350 °C, this conversion efficiency reduced, where $NO_2$ concentration is probably equilibrium limited. After equilibrium, $NO_2$ started decreasing from the increase of temperature. Moreover,

due to the results which show that there is almost the same $NO_x$ concentration bDOC and aDOC for all the tested conditions, it can be concluded that there is no $NO_2$ to $N_2$ reaction in the DOC. Presence of CO and HC affect the $NO_2$ production, this is due to covering catalyst active sites and also presence of any $NO_2$ which was produced from HCs and CO reaction to form $CO_2$ [132, 146, 162]. This shows the important role of CO and HCs to determine $NO_2$ concentration after the DOC which also reported in previous studies [10, 97, 160, 161].

It is essential to optimise $NO_2$ production at the desired temperature to be effective for the DPF's performance. The increase of $NO_2$ after CO and HC light-off could be due to the oxidation of CO and HCs. The $NO_2$ production at a specific range is effective in oxidation of soot particles in which the rate of oxidation reaction is higher than in the case of the oxygen at around 150 °C to 400 °C [155, 163]. The $H_2$ presence and the use of the alternative fuels increase the $NO_2$ concentration compared to diesel combustion. This confirms that a higher concentration of heavy HCs resulted in lower NO conversion which was due to the consumption of $NO_2$ as an oxidiser in the HCs' oxidation reaction [153]. The highest $NO_2$ production in B20 could be due to the presence of oxygenated hydrocarbons. The presence of hydrogen in the exhaust could produce some hydrogen, containing components such as OH and $HO_2$ which promote HC oxidation and also NO to $NO_2$ production. The presence of oxygen in alternative fuels and the higher diffusivity and reactivity of their combustion products species leads to an increase of $NO_2$ production, too [164].

Figure 6-13 shows the $N_2O$ production over the DOC which also was investigated as a harmful greenhouse gas emission, and is responsible for ozone destruction. It can be seen that in medium DOC inlet temperatures before the creation of $NO_2$, the $N_2O$ was

formed in the DOC by a reduction of the $NO_x$ species. The use of alternative fuels and the addition of $H_2$ enhanced $N_2O$ formation. Production of $N_2O$ starts before CO and HC light-off, which could be due to a reduction of the active sites oxidised by NO chemisorption allowing more NO to adsorb, dissociate and form $N_2O$ [10, 165]. In contrast to most of the studies, a previous study shows the advantage of the $N_2O$ on soot oxidation specifically during the in-situ formation of $N_2O$ by the catalyst, during non-selective reduction of $NO_x$ by reaction with $NH_3$, suggesting that surface $N_2O$ (or a surface intermediate in its formation) is the reactive oxidising species [33]. Extensive engine testing is needed to evaluate the extent of soot control together with the associated $NO_x$ reduction over a wide range of operating conditions, and to confirm negligible emissions of $N_2O$.

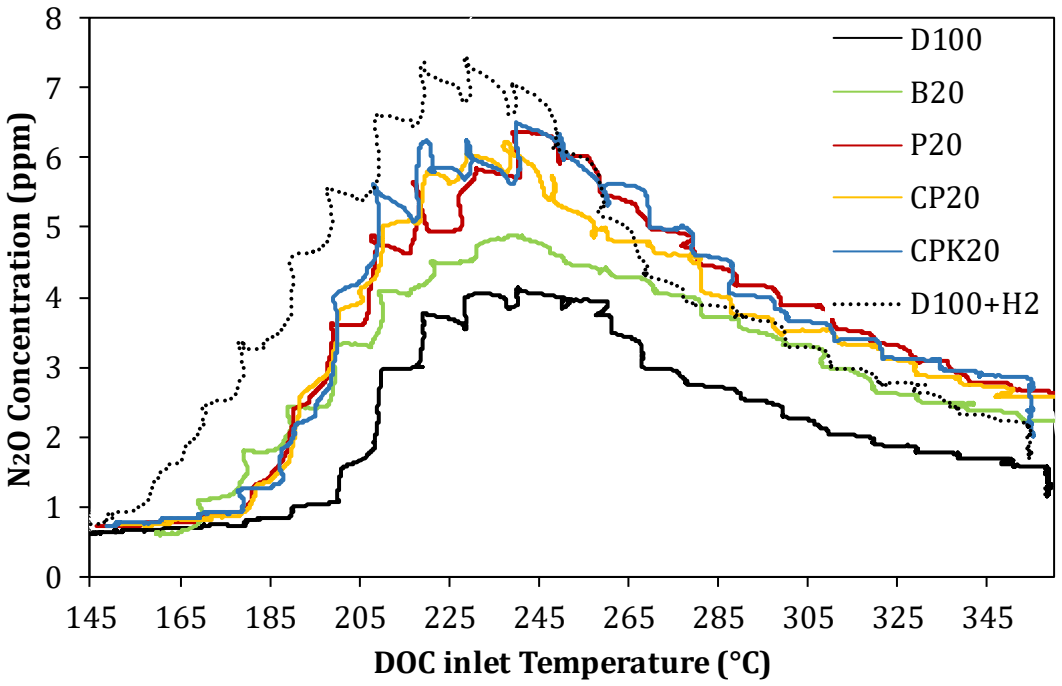



Figure 6-13: $N_2O$ production over the DOC in the exhaust of alternative fuels' combustion

### 6.2.3. Interaction between Efficient Heating Strategy and DOC Activity

Figure 6-14 and Figure 6-15 illustrate the exhaust gas composition upstream and downstream of a catalyst when an electrical heater is running at its highest power. The presence of an electrical heater before the DOC can produce relatively uniform temperature profiles beneficial for improving emissions' conversion and catalyst durability [16]. This heater, which was described in detail in Chapter 3, has a capability to increase exhaust gas temperature before the DOC inlet from 150 °C to approximately 355 °C at 2 bar IMEP and from 230 °C to approximately 415 °C at 4 bar IMEP. The maximum CO and THC conversion efficiencies that were achieved by use of an electrical heater combined with the DOC are almost 99% and 72% for all tested conditions, respectively. This conversion efficiency was around 20% without a heater. The concentration of total $NO_x$ did not change considerably; however, slightly more $NO_2$ was measured in the exhaust gas aDOC due to the catalytic oxidation of NO to $NO_2$. Moreover, the addition of $H_2$ in higher temperature does not have a huge impact on the conversion efficiency as in this temperature, the catalyst passed its light-off temperature.

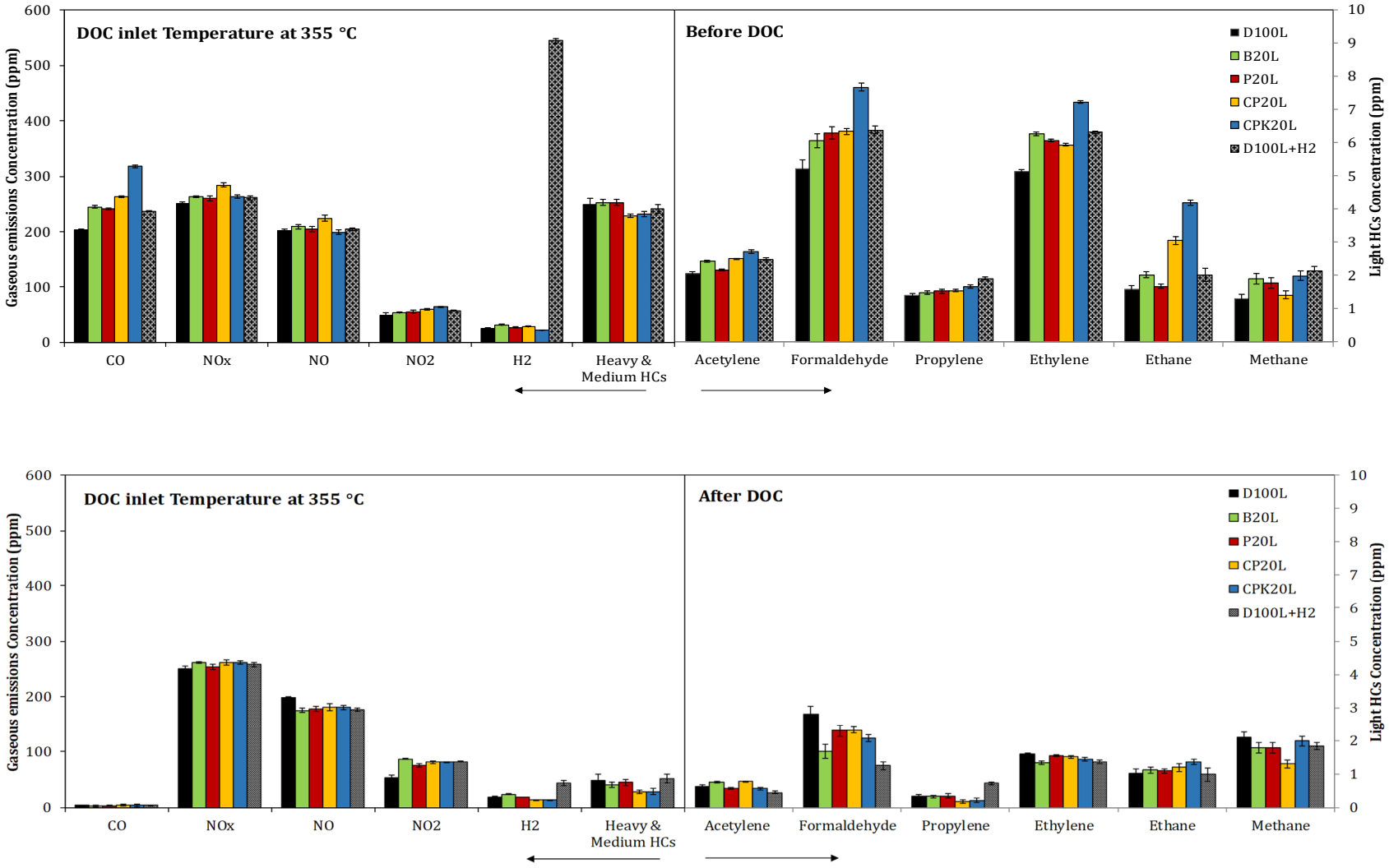



Figure 6-14: Heater ON-Gaseous emissions' concentration at 2 bar IMEP, bDOC and aDOC

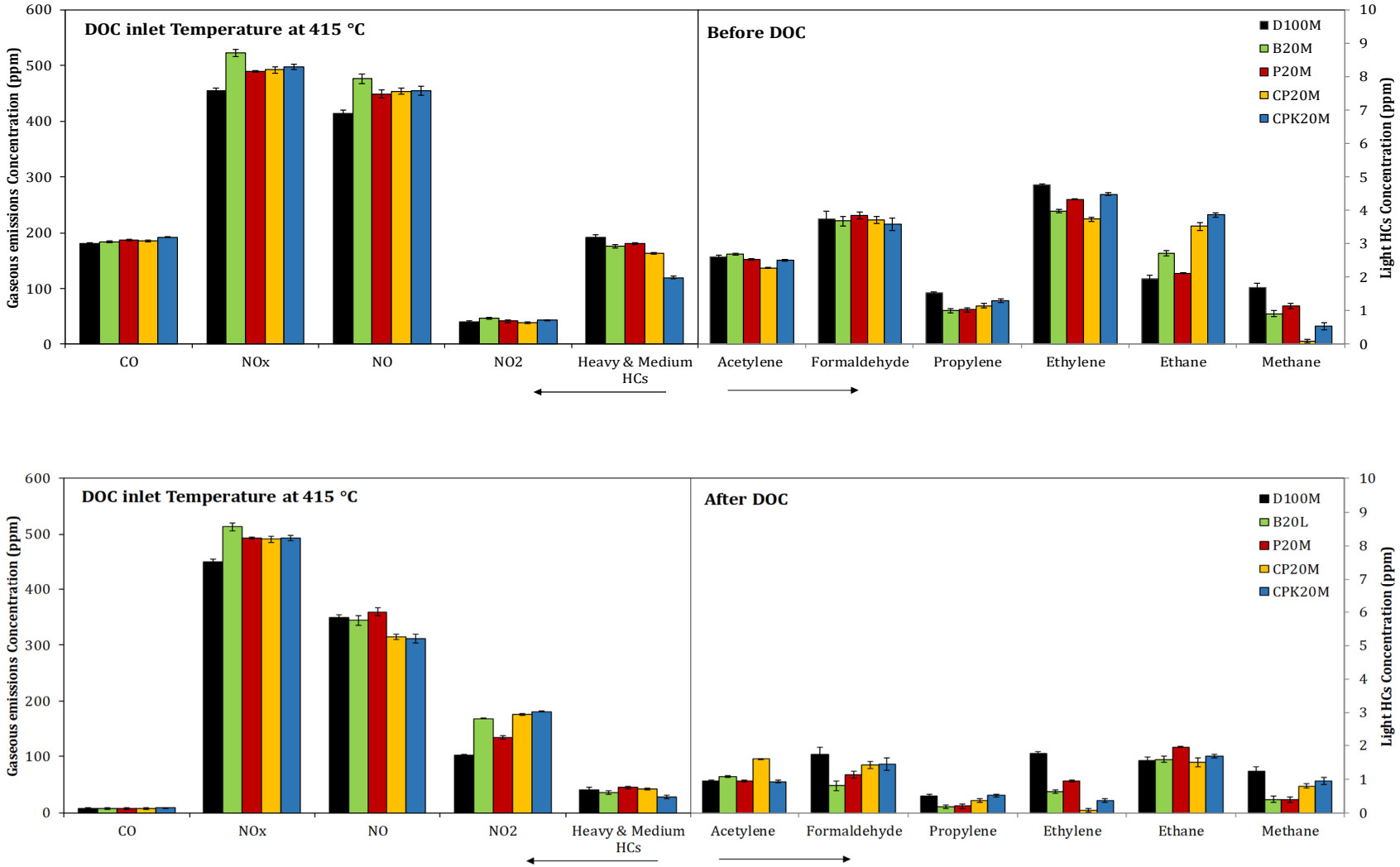



Figure 6-15: Heater ON-Gaseous emissions' concentration at 4 bar IMEP, bDOC and aDOC

### 6.2.4. Effects of Alternative Fuels' Combustion and an Efficiently Heated DOC on Particulate Matter

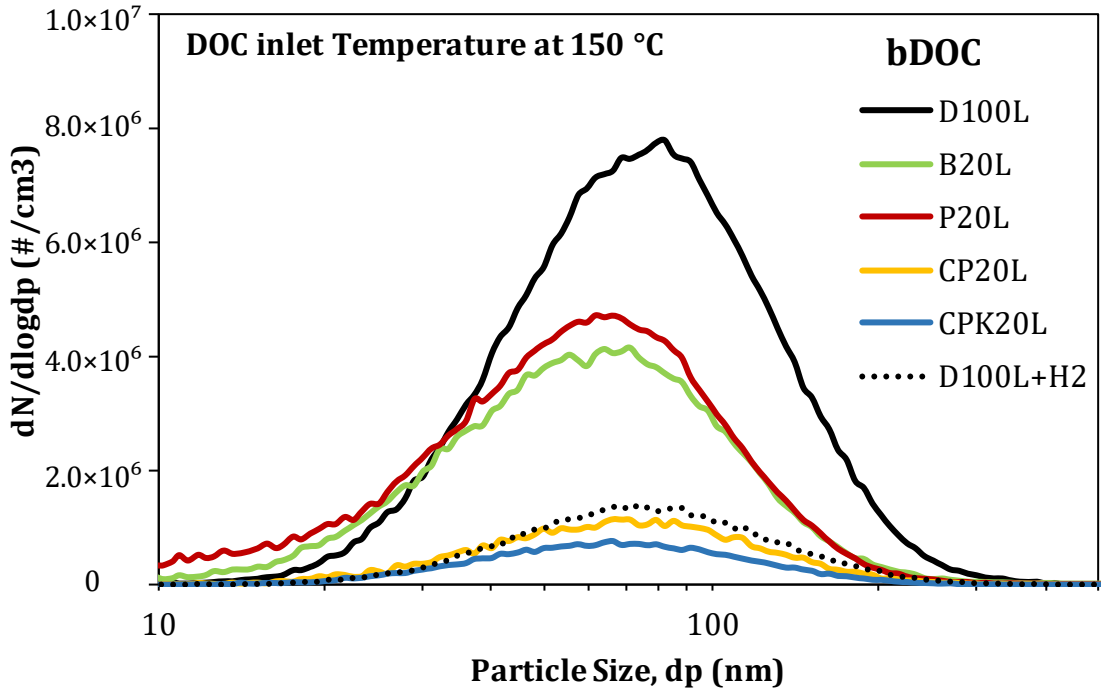
Number concentration and mean diameter of particulate matter emissions from combustion of alternative fuels were lower than in diesel combustion, as discussed in Chapter 5. In this section, particle size distributions measured upstream and downstream of the DOC are presented. This investigation gives an insight regarding the effects of alternative fuels on the DOC's performance for particulate matter reduction at low and high DOC inlet temperatures.

Figure 6-16 to Figure 6-19 illustrate that particulate matter emissions were lower across the whole distribution for alternative fuels. In addition, a small reduction in the median particle diameter was observed (Table 6-2). Particulate matter agglomerates and their primary particles from combustion of alternative fuels are smaller and with a lower fractal dimension which make them easier to be oxidized [75]. The DOC can physically trap some of the particulate matter by desorption and can oxidise volatile and semi-volatile gaseous species that nucleate and /or condense over the surface of soot particles [75].

Compared to D100, the addition of hydrogen upstream of the DOC led to an 80% reduction in total concentration of particulates after the DOC. This could be due to the exothermic reactions within the DOC leading to a significant reduction in particles. As discussed in previous sections, diffusivity and reactivity of exhaust species from combustion of alternative fuels keep the catalytic activity high even at low temperatures. As shown in the figures, when the heater was on, total particle concentration increased upstream and downstream of the DOC compared to the heater-off conditions. This could

be due to the release of accumulated soot particles in the heater and on the exhaust pipes at higher temperatures.

As shown in Table 6-2, at 2 bar IMEP, the total particle removal efficiency by the DOC increased by using the heater. For D100, the total particle removal efficiency was approximately 55% with and without the heater. This remained almost same when hydrogen was added upstream of the DOC. However, in the case of the alternative fuels, as discussed in Chapter 5, it can be seen that the particle removal efficiency using the DOC was almost the same for all fuels and did not depend on the type of fuel.



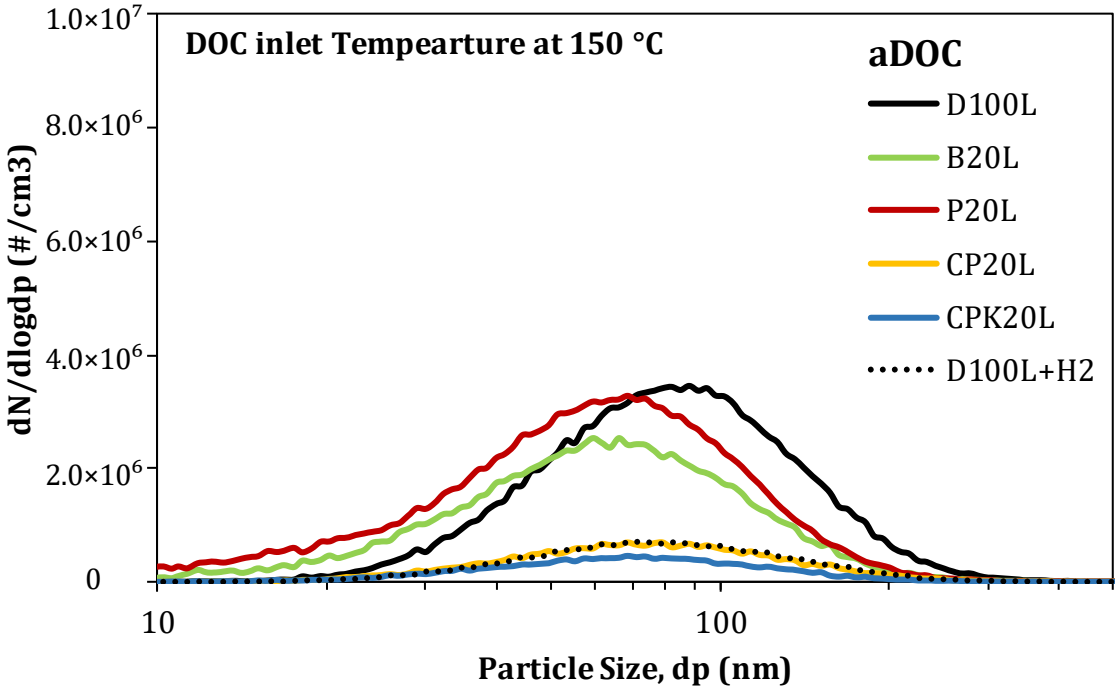




Figure 6-16: Heater OFF-particle size distribution in bDOC and aDOC at 2 bar IMEP

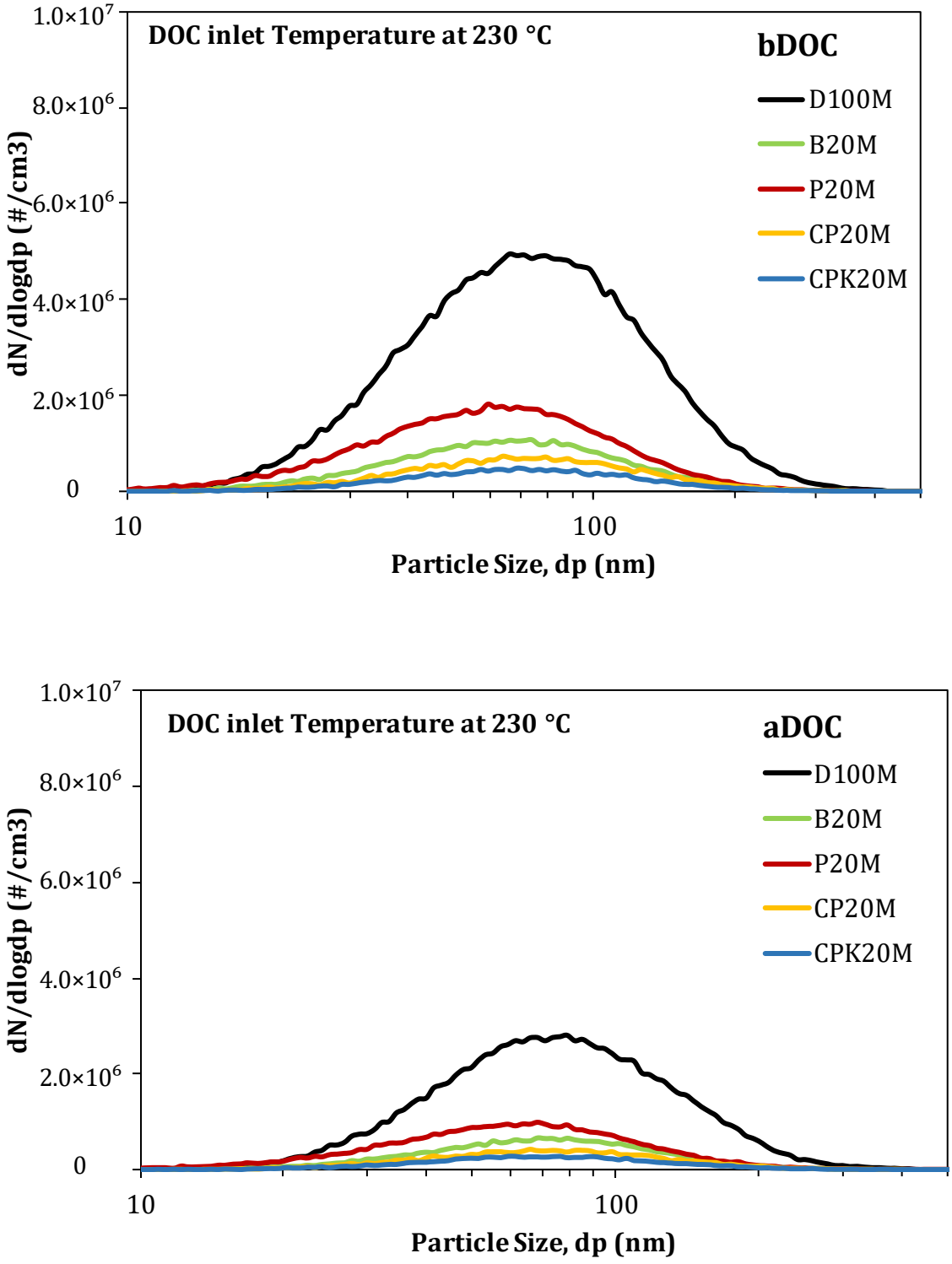
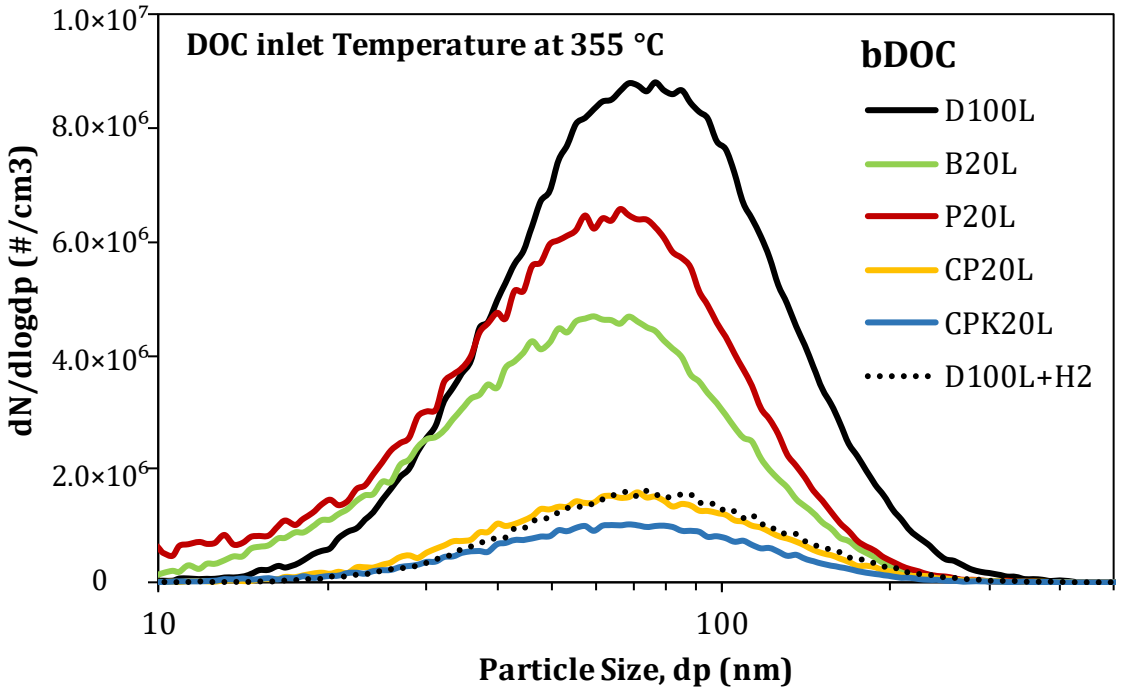



Figure 6-17: Heater OFF-particle size distribution in bDOC and aDOC at 4 bar IMEP



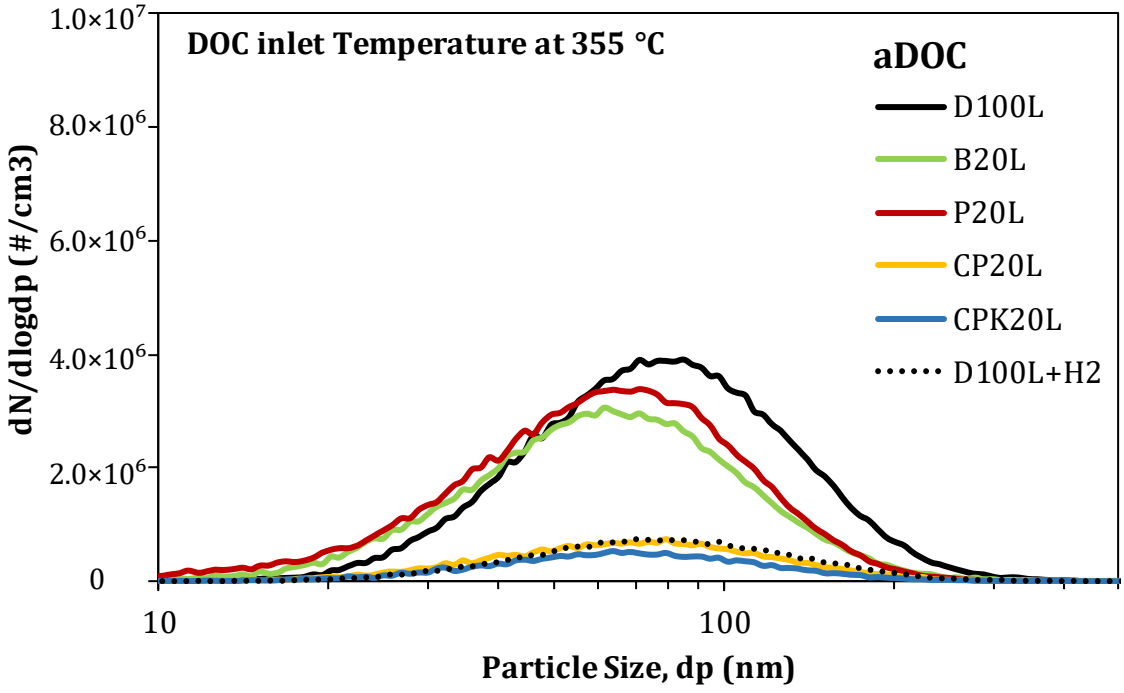
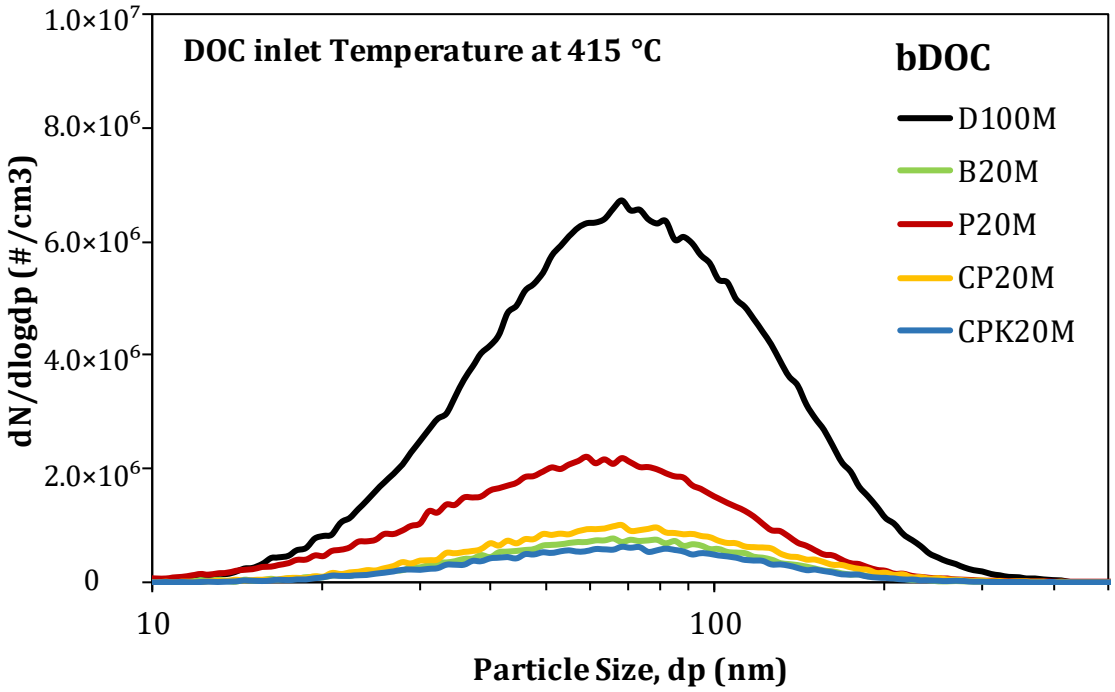




Figure 6-18: Heater ON-Particle size distribution in bDOC and aDOC at 2 bar IMEP



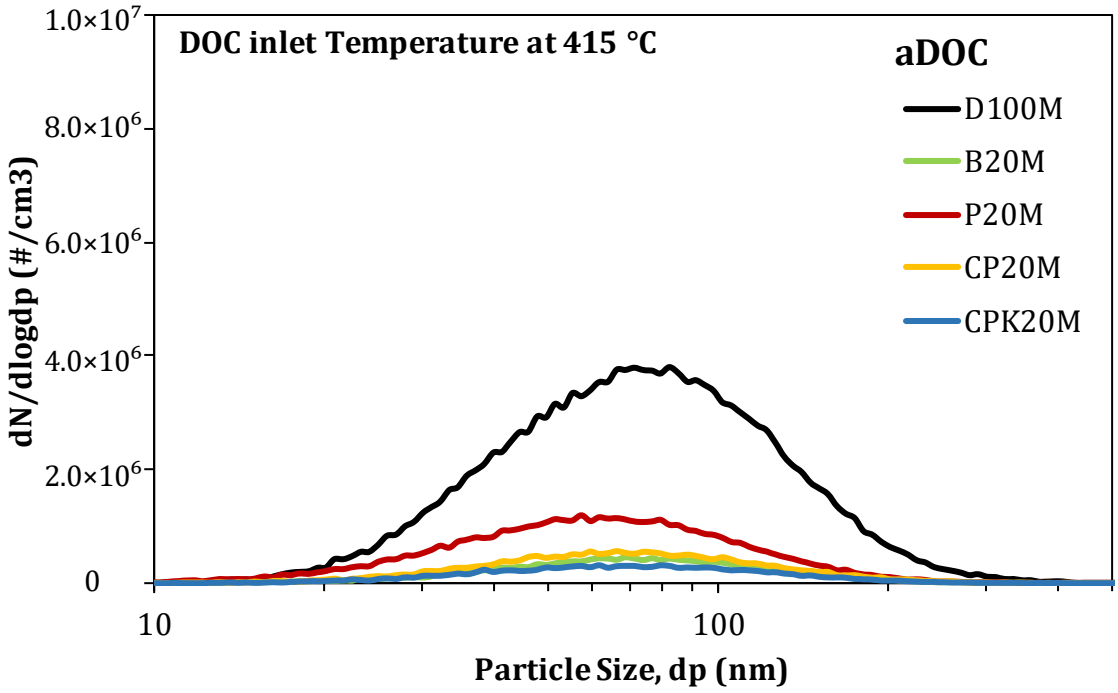




Figure 6-19: Heater ON-particle size distribution in bDOC and aDOC at 4 bar IMEP

Table 6-2: Effects of the DOC on particle size distribution for tested fuels

| Test abbreviation | DOC inlet temp (°C) | Total number concentration (#/cm$^3$) | Maximum number concentration (#/cm$^3$) | Median diameter (nm) |
|---|---|---|---|---|
| D100L-bDOC | Heater OFF 150 °C | $4.48\times10^6$ | $7.79\times10^6$ | 74.23 |
| D100L-aDOC | | $1.93\times10^6$ | $3.47\times10^6$ | 80.99 |
| B20L-bDOC | | $2.25\times10^6$ | $3.67\times10^6$ | 59.73 |
| B20L-aDOC | | $1.32\times10^6$ | $2.23\times10^6$ | 61.55 |
| P20L-bDOC | | $2.90\times10^6$ | $4.72\times10^6$ | 57.91 |
| P20L-aDOC | | $2.00\times10^6$ | $3.28\times10^6$ | 60.26 |
| CP20L-bDOC | | $6.68\times10^5$ | $1.15\times10^6$ | 67.95 |
| CP20L-aDOC | | $4.10\times10^5$ | $7.08\times10^5$ | 72.96 |
| CPK20L-bDOC | | $4.29\times10^5$ | $7.55\times10^5$ | 65.61 |
| CPK20L-aDOC | | $2.55\times10^5$ | $4.58\times10^5$ | 67.92 |
| D100L+H2-bDOC | | $9.56\times10^5$ | $1.26\times10^6$ | 69.26 |
| D100L+H2-aDOC | | $6.25\times10^5$ | $7.49\times10^5$ | 72.28 |
| D100M-bDOC | Heater OFF 230 °C | $3.20\times10^6$ | $4.95\times10^6$ | 71.36 |
| D100M-aDOC | | $1.72\times10^6$ | $2.83\times10^6$ | 73.60 |
| B20M-bDOC | | $6.39\times10^5$ | $1.07\times10^6$ | 64.92 |
| B20M-aDOC | | $3.86\times10^5$ | $6.82\times10^5$ | 69.62 |
| P20M-bDOC | | $1.11\times10^6$ | $1.80\times10^6$ | 59.89 |
| P20M-aDOC | | $5.99\times10^5$ | $9.89\times10^5$ | 60.37 |
| CP20M-bDOC | | $4.37\times10^5$ | $7.40\times10^5$ | 70.10 |
| CP20M-aDOC | | $2.55\times10^5$ | $4.43\times10^5$ | 70.88 |
| CPK20M-bDOC | | $2.79\times10^5$ | $4.89\times10^5$ | 69.55 |
| CPK20M-aDOC | | $1.64\times10^5$ | $2.78\times10^5$ | 69.23 |
| D100L-bDOC | Heater ON 355 °C | $5.26\times10^6$ | $8.81\times10^6$ | 71.44 |
| D100L-aDOC | | $2.25\times10^6$ | $3.90\times10^6$ | 76.87 |
| B20L-bDOC | | $2.63\times10^6$ | $4.13\times10^6$ | 57.54 |
| B20L-aDOC | | $1.55\times10^6$ | $2.70\times10^6$ | 62.27 |
| P20L-bDOC | | $4.05\times10^6$ | $6.57\times10^6$ | 58.23 |
| P20L-aDOC | | $2.03\times10^6$ | $3.38\times10^6$ | 62.25 |
| CP20L-bDOC | | $9.22\times10^5$ | $1.61\times10^6$ | 67.01 |
| CP20L-aDOC | | $4.13\times10^5$ | $7.35\times10^5$ | 69.12 |
| CPK20L-bDOC | | $6.09\times10^5$ | $1.02\times10^6$ | 66.29 |
| CPK20L-aDOC | | $2.83\times10^5$ | $5.19\times10^5$ | 66.65 |
| D100L+$H_2$-bDOC | | $8.87\times10^5$ | $1.60\times10^6$ | 73.63 |
| D100L+$H_2$-aDOC | | $4.29\times10^5$ | $7.49\times10^5$ | 76.36 |
| D100M-bDOC | Heater ON 415 °C | $4.23\times10^6$ | $6.73\times10^6$ | 69.06 |
| D100M-aDOC | | $2.34\times10^6$ | $3.81\times10^6$ | 72.19 |
| B20M-bDOC | | $4.57\times10^5$ | $7.75\times10^5$ | 65.86 |
| B20M-aDOC | | $2.64\times10^5$ | $4.76\times10^5$ | 69.54 |
| P20M-bDOC | | $1.39\times10^6$ | $2.23\times10^6$ | 59.15 |
| P20M-aDOC | | $7.13\times10^5$ | $1.19\times10^6$ | 60.10 |
| CP20M-bDOC | | $6.05\times10^5$ | $1.01\times10^6$ | 67.53 |
| CP20M-aDOC | | $3.23\times10^5$ | $5.53\times10^5$ | 67.45 |
| CPK20M-bDOC | | $3.69\times10^5$ | $6.20\times10^5$ | 66.43 |
| CPK20M-aDOC | | $1.94\times10^5$ | $3.19\times10^5$ | 67.80 |

## 6.3. Summary

In this chapter, the electrically heated DOC activity was investigated experimentally. The heater provides the required thermal energy to activate the catalyst emissions' conversion reactions during engine cold-start. This study was carried out in conjunction with the combustion of alternative fuel blends and small hydrogen addition upstream the DOC in order to improve its light-off activity.

The DOC's light-off activity is highly dependent on the engine's exhaust temperature and composition speciation, which are strongly influenced by the fuel properties used in the engine's combustion. Adsorption of CO and HCs on the catalyst's active sites leads to reducing the conversion efficiency of the DOC, especially at low temperature. It is hypothesised that the formation of OH radicals in the exhaust from oxygenated fuel combustion promotes the rate of oxidation reaction in the DOC. Having earlier CO oxidation at lower temperatures would lead to have more active sites for adsorption.

The potential improvements for DOC's light-off activity using alternative fuels and the addition of hydrogen have been understood. The finding of the studies from this chapter can be used to develop and design more efficient thermal management of aftertreatment systems and also use of cleaner renewable alternative fuels. It was found that the addition of $H_2$ upstream of the DOC and also oxygenated fuel added to diesel reduce the catalyst's light-off temperature by 50 °C. This is due to a combination of a reduction in competitive adsorption, formation of hydrogen containing molecules in the exhaust and the exothermic effect of $H_2$ and CO oxidation through the DOC.

# CHAPTER 7. CONCLUSIONS

The main aim of this research was to reduce a diesel engine's emissions through the use of alternative fuels and thermal management of the aftertreatment system.

The selected alternative fuels (butanol, pentanol, cyclopentanol and cyclopentanone) blended with diesel had not previously been considered as candidates for use in compression ignition engines. Through characterisation of the physical properties of these fuels, particularly lubrication and tribological mechanisms, it was shown that they are suitable alternative candidates for use in conventional direct injection fuelling systems. The aftertreatment system developed in this work incorporates a novel efficient exhaust heating strategy with a potential for use in hybrid electric vehicles. Combined with the use of alternative fuels, the aforementioned heating strategy is aimed at enhancing the low-temperature removal of exhaust emissions.

The results' chapters of this thesis are focused on:

i) Alternative fuels' (bio-alcohols and bio-ketones) physical properties, lubrication and tribology characterisation;
ii) Diesel engines' gaseous and particle emissions' reduction with the use of bio-alcohols and bio-ketones blended with diesel;
iii) A combination of using the alternative fuels and thermal management of the exhaust aftertreatment system for achieving a higher catalytic activity and faster light-off, useful for cold-start.

The main findings from these chapters are presented in the following sections.

## 7.1. Investigation of Lubrication Properties and Tribological Behaviour of Bio-alcohols and Bio-ketones

The density, viscosity, surface tension and calorific value of the 20% (v/v) blends of butanol (B20), pentanol (P20), cyclopentanol (CP20) and cyclopentanone (CPK20) with diesel (D100) fuel were all within the legislative limits. These fuel properties had almost a linear relation with respect to the volumetric concentration of the blended fuels.

The polar species in the alternative oxygenated fuels adsorbed on the metallic surface of the disc (during lubrication tests) and consequently, improved formation of the lubrication film. This led to a reduction of the wear scar diameter and the depth of the worn surfaces. This is an important factor for improving the performance and durability of the fuel injection systems. Cyclopentanone and cyclopentanol blended with diesel showed smaller wear scar sizes compared with other tested fuels. The results showed that blending 20% of cyclopentanol or cyclopentanone with diesel kept the wear scar dimension below the maximum limitations required by the European lubricity standards. This is due to their cyclic structures and oxygen content which led to the formation of the lubrication film. Therefore, polarity of fuel molecules due to the hydrogen bonding capabilities, cyclic structure and presence of oxygen can all influence the lubricity results. This comparison is exactly the same as the following ranking of molecules' polarities: cyclic hydroxyl > hydroxyl l> ketone. Topography measurements and analysis confirmed all the findings from the lubrication analysis. The size of the wear scar is ranked as B20 > P20 > G20 > CP20 > D100 > CPK20. There is no need to use any lubricity enhancer which affects the increase of gaseous emissions. It was confirmed that blending 20% (v/v) of oxygenated fuels with diesel is a promising alternative to neat diesel, considering their

density, surface tension, viscosity, calorific value, lubrication and tribological mechanisms with respect to legislative limits.

## 7.2. Impact of Alternative Fuels on Combustion, Gaseous and Particulate Matter Emissions' Characteristics

The effects of adding alternative fuels with different molecular structures to diesel fuel on combustion, gaseous emissions and particulate matter characteristics were studied. The indicated thermal efficiency at 4 bar IMEP is improved due to faster burning rate and hypothetically less heat loss to the cylinder walls. Blends that contain more oxygenated compounds showed a longer ignition delay compared with diesel, due to the high electronegativity of oxygen atom in the molecules. As a result of a more complete combustion process of these tested fuels caused by the oxygen content, total hydrocarbon concentration decreased compared to the diesel exhaust emissions; whereas the CO and $NO_x$ emissions increased. The higher heat of evaporation of the fuels and also their lower cetane number can lead to more fuel-air premixing and consequently, a higher number of locally lean fuel-air mixture packets. This affects the formation of a higher concentration of CO emissions in the exhaust. An increase of oxygen content in the fuels increased the combustion pressure and temperature which promoted the formation of $NO_x$ emissions.

A higher carbon number of added oxygenated fuels increased the formation of CO emissions. For instance, increasing the carbon chain length from $C_4$ (butanol) to $C_5$ (Pentanol) resulted in a lower oxygen content and H/C, and therefore, higher CO, particulate matter and THC emissions. Using cyclopentanone with double bond oxygen content showed lower THC emissions but higher CO emissions compared to cyclopentanol. Particulate matter emissions from the combustion of the blended fuels

decreased significantly compared to diesel. This reduction is due to better premixing, the higher fuel oxygen content and/or improved soot particle oxidation. Also, lower carbon to hydrogen ratio of straight chain alcohol fuels can inhibit formation of particles.

Using the tested fuels (B20, P20, CP20 and CPK20) as alternative blended fuels can provide considerable environmental improvements. Using CPK20 and CP20 with cyclic hydrocarbons led to the most significant reduction in particulate matter emissions.

## 7.3. Enhancing the Low Temperature Activity of a Diesel Oxidation Catalyst by Using Electrical Heating and Alternative Fuels

This study demonstrated the possibility of improving HC and CO conversion efficiencies in the DOC by using alternative fuels and an efficient catalyst strategy. Various exhaust gas compositions from combustion of alternative fuels highlight the interactions between exhaust gas pollutants in the DOC, by adsorption competition in the catalytic sites of the aftertreatment system. Also, the effects of adding $H_2$ on the DOC's performance were investigated. Even at low exhaust temperatures, the addition of hydrogen improved the CO conversion efficiency. It was found that the addition of $H_2$ upstream of the DOC and also oxygenated fuel added to diesel, reduced catalyst light-off temperature by 50 °C and up to 26 °C, respectively. This is due to the combination of reduction in competitive adsorption, formation of hydrogen containing molecules in the exhaust, and the exothermic effect of $H_2$ and CO oxidation inside the DOC. With regards to the reduction of light-off temperature, the addition of hydrogen had the highest impact, then butanol, pentanol, cyclopentanol and cyclopentanone, compared to diesel as a baseline case study. Among the oxygenated fuels, this could be due to higher oxygen and hydrogen in their molecular structure.

The findings of the studies from this chapter can be used to develop and design more efficient thermal management of an aftertreatment system, and also make use of cleaner, renewable, alternative fuels with potential improvements for a DOC's light-off activity.

## 7.4. Concluding Remarks

All the tested oxygenated fuels show great potential to be used as a blend with diesel fuel in current engines without any additional enhancer additives or any modifications in the engine in terms of fuel characteristics, particularly lubrication and tribological mechanisms. It should be mentioned that as most of the alternative fuels are expensive, further researches need to be done to reduce production pathways of these fuels. These fuels with different molecular structure led to reduction of diesel vehicles' emissions. Interaction between these fuels and a diesel oxidation catalyst significantly improved the DOC's light-off behaviour. Among the studied techniques, the addition of hydrogen upstream of the catalyst has shown great potential in reducing the DOC's light-off temperature. This approach can allow the catalyst to activate the emissions' conversion reactions in cold-start conditions. An efficient heating strategy upstream of the aftertreatment systems showed potential improvement in the catalytic conversions' reactions, which could be used in hybrid electric vehicles.

## 7.5. Future Work

This research indicated some areas that need further investigation:

- In addition to lubrication and tribological studies, corrosion behaviour of the tested fuels with engine fuelling system components' materials (copper, aluminium, stainless steel, etc.) should be studied.

- The use of a higher concentration of bio-alcohols and bio-ketones in fuel blends to investigate their influence on engine-out emissions and performance of aftertreatment systems. A higher concentration of low cetane number fuels requires modification to the engine (geometry, control, etc.) to avoid incomplete combustion. This higher concentration can affect the light-off temperature and also the amount of $NO_2$ production for DPF regeneration.
- A morphological and nano-structural analysis of PM using HR-TEM for the tested conditions in the engine exhaust and also upstream and downstream of aftertreatment system should be carried out.
- In addition to the morphological and nano-structural analysis of PM, thermogravimetric analysis combined with a mass spectrometer (TGA-MS) should be carried out to study the soot oxidation performance and also soot particles' speciation. This analysis can enable further development in the DPF regeneration.
- An efficient heating strategy prior to the DOC can be combined with a DPF and a SCR system with some modifications in an experimental set-up, to investigate their performance regarding the particles and $NO_x$ removal.
- To obtain a more complete view of aftertreatment systems, AVL simulation should be carried out to investigate the effect of the addition of $H_2$ concentration, a change of catalyst properties and also alternative fuel combustion.

# References


1. Forum, W.E. 2016 [cited 2019 01/02/2019]; Available from: https://www.weforum.org/agenda/2016/04/the-number-of-cars-worldwide-is-set-to-double-by-2040.

2. Kalghatgi, G., *Is it really the end of internal combustion engines and petroleum in transport?* Applied Energy, 2018. **225**: p. 965-974.

3. ExxonMobil. *2017 Outlook for Energy: A View to 2040*. [cited 2019 01/02/2019]; Available from: https://cdn.exxonmobil.com/~/media/global/files/outlook-for-energy/2017/2017-outlook-for-energy.pdf.

4. Council, W.E. *Global Transport Scenarios 2050*. [cited 2019 01/02/2019]; Available from: https://www.worldenergy.org/wp-content/uploads/2012/09/wec_transport_scenarios_2050.pdf.

5. Countries, O.o.t.P.E. *World Oil Outlook*. 2013 [cited 2019 01/02/2019]; Available from: https://www.opec.org/opec_web/static_files_project/media/downloads/publications/WOO_2013.pdf.

6. Thomas Knorr, D.E., Oliver Maiwald, Axel Schatz, Rolf Brück *The Electric Heatable Catalyst – An Efficient Measure for Emission Optimization in Mild Hybrid Vehicle Operation Strategies*, in *24th Aachen Colloquium Automobile and Engine Technology 2015* 2015.

7. Pace, L. and M. Presti, *An Alternative Way to Reduce Fuel Consumption During Cold Start: The Electrically Heated Catalyst*. 2011, SAE International.

8. Gao, J., G. Tian, A. Sorniotti, A.E. Karci, and R. Di Palo, *Review of thermal management of catalytic converters to decrease engine emissions during cold start and warm up.* Applied Thermal Engineering, 2019. **147**: p. 177-187.

9. Kong, Y., T. Kozakiewicz, R. Johnson, C. Huffmeyer, J. Huckaby, J. Abel, J. Baurley, and K. Duffield, *Active DPF Regeneration for 2007 Diesel Engines*. 2005, SAE International.

10. Herreros, J.M., S.S. Gill, I. Lefort, A. Tsolakis, P. Millington, and E. Moss, *Enhancing the low temperature oxidation performance over a Pt and a Pt–Pd diesel oxidation catalyst.* Applied Catalysis B: Environmental, 2014. **147**: p. 835-841.

11. M, V.B., M.M. K, and A.P.R. G, *Butanol and pentanol: The promising biofuels for CI engines – A review.* Renewable and Sustainable Energy Reviews, 2017. **78**: p. 1068-1088.

12. Rajesh Kumar, B. and S. Saravanan, *Use of higher alcohol biofuels in diesel engines: A review.* Renewable and Sustainable Energy Reviews, 2016. **60**: p. 84-115.

13. Stone, R., *Introduction to Internal Combustion Engines*. 3rd ed. 1999: McMillan Press, London.

14. Bermúdez, V., J.M. Lujan, B. Pla, and W.G. Linares, *Comparative study of regulated and unregulated gaseous emissions during NEDC in a light-duty diesel engine fuelled with Fischer Tropsch and biodiesel fuels.* Biomass and Bioenergy, 2011. **35**(2): p. 789-798.

15. Payri, F., V.R. Bermúdez, B. Tormos, and W.G. Linares, *Hydrocarbon emissions speciation in diesel and biodiesel exhausts.* Atmospheric Environment, 2009. **43**(6): p. 1273-1279.

16. Hamedi, M.R., *Advanced Thermal Management of Diesel Aftertreatment Systems*, in *Department of Mechanical Engineering*. 2016, The University of Birmingham.

17. Heywood, J., *Internal Combustion Engine Fundamentals*. 1988: McGraw-Hill.

18. Jacobson, M.C., H.-C. Hansson, K.J. Noone, and R.J. Charlson, *Organic atmospheric aerosols: Review and state of the science.* Reviews of Geophysics, 2000. **38**(2): p. 267-294.

19. Tsolakis, A., M. Bogarra, and J. Herreros, *Road Vehicle Technologies and Fuels*, in *Environmental Impacts of Road Vehicles: Past, Present and Future*. 2017, The Royal Society of Chemistry. p. 1-24.

20. Harrison, R.M., A.R. MacKenzie, H. Xu, M.S. Alam, I. Nikolova, J. Zhong, A. Singh, S. Zeraati-Rezaei, C. Stark, D.C.S. Beddows, Z. Liang, R. Xu, and X. Cai, *Diesel exhaust nanoparticles and their behaviour in the atmosphere.* Proceedings of the Royal Society A: Mathematical, Physical and Engineering Sciences, 2018. **474**(2220): p. 20180492.

21. Pui, D.Y.H., S.-C. Chen, and Z. Zuo, *PM2.5 in China: Measurements, sources, visibility and health effects, and mitigation.* Particuology, 2014. **13**: p. 1-26.

22. Mimura, T., T. Ichinose, S. Yamagami, H. Fujishima, Y. Kamei, M. Goto, S. Takada, and M. Matsubara, *Airborne particulate matter (PM2.5) and the prevalence of allergic conjunctivitis in Japan.* Science of The Total Environment, 2014. **487**: p. 493-499.

23. Dockery, D.W., *Health Effects of Fine Particulate Air Pollution: Lines that Connect AU - Pope, C. Arden.* Journal of the Air & Waste Management Association, 2006. **56**(6): p. 709-742.

24. E, J., M. Pham, D. Zhao, Y. Deng, D. Le, W. Zuo, H. Zhu, T. Liu, Q. Peng, and Z. Zhang, *Effect of different technologies on combustion and emissions of the diesel engine fueled with biodiesel: A review.* Renewable and Sustainable Energy Reviews, 2017. **80**(Supplement C): p. 620-647.

25. Hoekman, S.K. and C. Robbins, *Review of the effects of biodiesel on NOx emissions.* Fuel Processing Technology, 2012. **96**: p. 237-249.

26. Bergthorson, J.M. and M.J. Thomson, *A review of the combustion and emissions properties of advanced transportation biofuels and their impact on existing and future engines.* Renewable and Sustainable Energy Reviews, 2015. **42**: p. 1393-1417.

27. Taher Nima, M., M. Mahmoudi, and S. Sajjadivand Seyyede, *Cobalt Catalysts Preparation and Characterization over Alumina Support for Fischer Tropsch Synthesis*, in *Biofuels Engineering*. 2017. p. 51.

28. Hessam Jahangiri, James Bennett, Parvin Mahjoubi, Karen Wilson, and S. Gu, *A review of advanced catalyst development for Fischer–Tropsch synthesis of hydrocarbons from biomass derived syn-gas.* The Royal Society of Chemistry, 2014.

29. Hellier, P., S. Purton, and N. Ladommatos, *Molecular Structure of Photosynthetic Microbial Biofuels for Improved Engine Combustion and Emissions Characteristics.* Frontiers in Bioengineering and Biotechnology, 2015. **3**: p. 49.

30. Hellier, P., M. Talibi, A. Eveleigh, and N. Ladommatos, *An overview of the effects of fuel molecular structure on the combustion and emissions characteristics of compression ignition engines.* Proceedings of the Institution of Mechanical Engineers, Part D: Journal of Automobile Engineering, 2018. **232**(1): p. 90-105.

31. Schönborn, A., N. Ladommatos, J. Williams, R. Allan, and J. Rogerson, *The influence of molecular structure of fatty acid monoalkyl esters on diesel combustion.* Combustion and Flame, 2009. **156**(7): p. 1396-1412.

32. Hellier, P., N. Ladommatos, R. Allan, and J. Rogerson, *Combustion and emissions characteristics of toluene/n-heptane and 1-octene/n-octane binary mixtures in a direct injection compression ignition engine.* Combustion and Flame, 2013. **160**(10): p. 2141-2158.

33. Davies, C., K. Thompson, A. Cooper, S. Golunski, S.H. Taylor, M. Bogarra Macias, O. Doustdar, and A. Tsolakis, *Simultaneous Removal of NOx and Soot Particulate from Diesel Exhaust by In-situ Catalytic Generation and Utilisation of N2O.* Applied Catalysis B: Environmental, 2018.

34. Lapuerta, M., J. Rodriguez-Fernandez, and J.M. Herreros, *Gaseous and Particle Greenhouse Emissions from Road Transport*, in *Environmental Impacts of Road Vehicles: Past, Present and Future*. 2017, The Royal Society of Chemistry. p. 25-45.

35. Gill, S.S., A. Tsolakis, K.D. Dearn, and J. Rodríguez-Fernández, *Combustion characteristics and emissions of Fischer–Tropsch diesel fuels in IC engines.* Progress in Energy and Combustion Science, 2011. **37**(4): p. 503-523.

36. Fayad, M.A., D. Fernández-Rodríguez, J.M. Herreros, M. Lapuerta, and A. Tsolakis, *Interactions between aftertreatment systems architecture and combustion of oxygenated fuels for improved low temperature catalysts activity.* Fuel, 2018. **229**: p. 189-197.

37. Jahangiri, H., A. Osatiashtiani, J.A. Bennett, M.A. Isaacs, S. Gu, A.F. Lee, and K. Wilson, *Zirconia catalysed acetic acid ketonisation for pre-treatment of biomass fast pyrolysis vapours.* Catalysis Science & Technology, 2018. **8**(4): p. 1134-1141.

38. Lapuerta, M., R. García-Contreras, J. Campos-Fernández, and M.P. Dorado, *Stability, Lubricity, Viscosity, and Cold-Flow Properties of Alcohol–Diesel Blends.* Energy & Fuels, 2010. **24**(8): p. 4497-4502.

39. Doustdar, O., M.L. Wyszynski, A. Tsolakis, and H. Mahmoudi, *Bio-Ketones from lignocellulosic biomass: Experimental investigation on fuel properties, combustion and emission characteristics of cyclopentanone blend with diesel in compression ignition engine.* Combustion Engines PTNSS, 2017.

40. Lapuerta, M., J. Rodríguez-Fernández, D. Fernández-Rodríguez, and R. Patiño-Camino, *Cold flow and filterability properties of n-butanol and ethanol blends with diesel and biodiesel fuels.* Fuel, 2018. **224**: p. 552-559.

41. Sukjit, E., J.M. Herreros, K.D. Dearn, R. García-Contreras, and A. Tsolakis, *The effect of the addition of individual methyl esters on the combustion and emissions of ethanol and butanol -diesel blends.* Energy, 2012. **42**(1): p. 364-374.

42. Zeraati Rezaei, S., F. Zhang, H. Xu, A. Ghafourian, J.M. Herreros, and S. Shuai, *Investigation of two-stage split-injection strategies for a Dieseline fuelled PPCI engine.* Fuel, 2013. **107**: p. 299-308.

43. Zeraati-Rezaei, S., Y. Al-Qahtani, and H. Xu, *Investigation of hot-EGR and low pressure injection strategy for a Dieseline fuelled PCI engine.* Fuel, 2017. **207**: p. 165-178.

44. Eslami, F., *Properties, Perfomance and emissions of biofuels in blends with gasoline*, in *School of Engineering*. 2013, The University of Birmingham. p. 139.

45. Holmberg, K., P. Andersson, and A. Erdemir, *Global energy consumption due to friction in passenger cars.* Tribology International, 2012. **47**: p. 221-234.

46. Lapuerta, M., J. Sánchez-Valdepeñas, and E. Sukjit, *Effect of ambient humidity and hygroscopy on the lubricity of diesel fuels.* Wear, 2014. **309**(1–2): p. 200-207.

47. Dearn, K.D., H. Moorcroft, E. Sukjit, P. Poapongsakorn, E.Z. Hu, Y.F. Xu, and X.G. Hu, *The tribology of fructose derived biofuels for DISI gasoline engines.* Fuel, 2018. **224**: p. 226-234.

48. Magı´n Lapuerta, R.G.a.-C., and John R. Agudelo, *Lubricity of Ethanol-Biodiesel-Diesel Fuel Blends.* Energy & Fuels, 2009. **24**: p. 6.

49. Sukjit, E., P. Poapongsakorn, K.D. Dearn, M. Lapuerta, and J. Sánchez-Valdepeñas, *Investigation of the lubrication properties and tribological mechanisms of oxygenated compounds.* Wear, 2017. **376–377, Part A**: p. 836-842.

50. Sukjit, E., K.D. Dearn, and A. Tsolakis, *Interrogating the surface: the effect of blended diesel fuels on lubricity.* SAE Int. J. Fuels Lubr., 2011. **5**(1): p. 154-162.

51. Doustdar, O., M.L. Wyszynski, H. Mahmoudi, and A. Tsolakis, *Enhancing the properties of Fischer-Tropsch fuel produced from syngas over Co/SiO2 catalyst: Lubricity and Calorific Value*, in *IOP Conference Series: Materials Science and Engineering*. 2016. p. 012092.

52. Xu, Y., Q. Wang, X. Hu, C. Li, and X. Zhu, *Characterization of the lubricity of bio-oil/diesel fuel blends by high frequency reciprocating test rig.* Energy, 2010. **35**(1): p. 283-287.

53. Farshad Eslami, Miroslaw Wyszynski, Athanasios Tsolakis, Hongming Xu, Shahrouz Norouzi, and K. Dearn, *Experimental investigation on lubricity of 2,5-dimethylfuran blends.* Combustion Engines. , 2012. **148**(1).

54. Maru, M.M., R.M. Trommer, K.F. Cavalcanti, E.S. Figueiredo, R.F. Silva, and C.A. Achete, *The Stribeck curve as a suitable characterization method of the lubricity of biodiesel and diesel blends.* Energy, 2014. **69**: p. 673-681.

55. Korres, D.M., G. Anastopoulos, E. Lois, A. Alexandridis, H. Sarimveis, and G. Bafas, *A neural network approach to the prediction of diesel fuel lubricity.* Fuel, 2002. **81**(10): p. 1243-1250.

56. Steidley, G.K.a.K.R., *Lubricity of Components of Biodiesel and Petrodiesel. The Origin of Biodiesel Lubricity.* Energy and Fuel American Chemical Society, 2005. **19**: p. 8.

57. Suarez, P.A.Z., B.R. Moser, B.K. Sharma, and S.Z. Erhan, *Comparing the lubricity of biofuels obtained from pyrolysis and alcoholysis of soybean oil and their blends with petroleum diesel.* Fuel, 2009. **88**(6): p. 1143-1147.

58. Sukjit, E. and K.D. Dearn, *Enhancing the lubricity of an environmentally friendly Swedish diesel fuel MK1.* Wear, 2011. **271**(9–10): p. 1772-1777.

59. Hazrat, M.A., M.G. Rasul, and M.M.K. Khan, *Lubricity Improvement of the Ultra-low Sulfur Diesel Fuel with the Biodiesel.* Energy Procedia, 2015. **75**: p. 111-117.

60. Freedman, B. and M.O. Bagby, *Predicting cetane numbers of n-alcohols and methyl esters from their physical properties.* Journal of the American Oil Chemists' Society, 1990. **67**(9): p. 565-571.

61. Lapuerta, M., O. Armas, and R. García-Contreras, *Effect of Ethanol on Blending Stability and Diesel Engine Emissions.* Energy & Fuels, 2009. **23**(9): p. 4343-4354.

62. Cheung, C.S., L. Zhu, and Z. Huang, *Regulated and unregulated emissions from a diesel engine fueled with biodiesel and biodiesel blended with methanol.* Atmospheric Environment, 2009. **43**(32): p. 4865-4872.

63. Rajesh Kumar, B., T. Muthukkumar, V. Krishnamoorthy, and S. Saravanan, *A comparative evaluation and optimization of performance and emission characteristics of a DI diesel engine fueled with n-propanol/diesel, n-butanol/diesel and n-pentanol/diesel blends using response surface methodology.* RSC Advances, 2016. **6**(66): p. 61869-61890.

64. Herreros, J.M., K. Schroer, E. Sukjit, and A. Tsolakis, *Extending the environmental benefits of ethanol–diesel blends through DGE incorporation.* Applied Energy, 2015. **146**: p. 335-343.

65. Hergueta, C., A. Tsolakis, J.M. Herreros, M. Bogarra, E. Price, K. Simmance, A.P.E. York, and D. Thompsett, *Impact of bio-alcohol fuels combustion on particulate matter morphology from efficient gasoline direct injection engines.* Applied Energy, 2018. **230**: p. 794-802.

66. Kumar, S., J.H. Cho, J. Park, and I. Moon, *Advances in diesel–alcohol blends and their effects on the performance and emissions of diesel engines.* Renewable and Sustainable Energy Reviews, 2013. **22**: p. 46-72.

67. Sukjit, E., *Synergistic Effects of Alcohol Based Renewable Fuels: Fuel properties and Emissions*, in *Department of Mechanical Engineering*. 2013, The University of Birmingham.

68. Hellier, P., N. Ladommatos, and T. Yusaf, *The influence of straight vegetable oil fatty acid composition on compression ignition combustion and emissions.* Fuel, 2015. **143**: p. 131-143.

69. Cann, A.F. and J.C. Liao, *Pentanol isomer synthesis in engineered microorganisms.* Applied Microbiology and Biotechnology, 2010. **85**(4): p. 893-899.

70. Campos-Fernández, J., J.M. Arnal, J. Gómez, and M.P. Dorado, *A comparison of performance of higher alcohols/diesel fuel blends in a diesel engine.* Applied Energy, 2012. **95**: p. 267-275.

71. Imdadul, H.K., H.H. Masjuki, M.A. Kalam, N.W.M. Zulkifli, A. Alabdulkarem, M.M. Rashed, Y.H. Teoh, and H.G. How, *Higher alcohol–biodiesel–diesel blends: An approach for improving the performance, emission, and combustion of a light-duty diesel engine.* Energy Conversion and Management, 2016. **111**: p. 174-185.

72. Li, L., J. Wang, Z. Wang, and J. Xiao, *Combustion and emission characteristics of diesel engine fueled with diesel/biodiesel/pentanol fuel blends.* Fuel, 2015. **156**: p. 211-218.

73. Rajesh kumar, B. and S. Saravanan, *Effect of exhaust gas recirculation (EGR) on performance and emissions of a constant speed DI diesel engine fueled with pentanol/diesel blends.* Fuel, 2015. **160**: p. 217-226.

74. Fayad, M.A., A. Tsolakis, D. Fernández-Rodríguez, J.M. Herreros, F.J. Martos, and M. Lapuerta, *Manipulating modern diesel engine particulate emission characteristics through butanol fuel blending and fuel injection strategies for efficient diesel oxidation catalysts.* Applied Energy, 2017. **190**: p. 490-500.

75. Fayad, M.A., J.M. Herreros, F.J. Martos, and A. Tsolakis, *Role of Alternative Fuels on Particulate Matter (PM) Characteristics and Influence of the Diesel Oxidation Catalyst.* Environmental Science & Technology, 2015. **49**(19): p. 11967-11973.

76. Sukjit, E., J.M. Herreros, J. Piaszyk, K.D. Dearn, and A. Tsolakis, *Finding Synergies in Fuels Properties for the Design of Renewable Fuels – Hydroxylated Biodiesel Effects on Butanol-Diesel Blends.* Environmental Science & Technology, 2013. **47**(7): p. 3535-3542.

77. Choi, B. and X. Jiang, *Individual hydrocarbons and particulate matter emission from a turbocharged CRDI diesel engine fueled with n-butanol/diesel blends.* Fuel, 2015. **154**: p. 188-195.

78. Campos-Fernandez, J., J.M. Arnal, J. Gomez, N. Lacalle, and M.P. Dorado, *Performance tests of a diesel engine fueled with pentanol/diesel fuel blends.* Fuel, 2013. **107**: p. 866-872.

79. Xing-cai, L., Y. Jian-guang, Z. Wu-gao, and H. Zhen, *Effect of cetane number improver on heat release rate and emissions of high speed diesel engine fueled with ethanol–diesel blend fuel.* Fuel, 2004. **83**(14): p. 2013-2020.

80. Atmanli, A., *Comparative analyses of diesel–waste oil biodiesel and propanol, n-butanol or 1-pentanol blends in a diesel engine.* Fuel, 2016. **176**: p. 209-215.

81. Eveleigh, A., N. Ladommatos, R. Balachandran, and A. Marca, *Conversion of oxygenated and hydrocarbon molecules to particulate matter using stable isotopes as tracers.* Combustion and Flame, 2014. **161**(11): p. 2966-2974.

82. Eveleigh, A., N. Ladommatos, P. Hellier, and A.-L. Jourdan, *An investigation into the conversion of specific carbon atoms in oleic acid and methyl oleate to particulate matter in a diesel engine and tube reactor.* Fuel, 2015. **153**: p. 604-611.

83. Zhou, C.-W., J.M. Simmie, W.J. Pitz, and H.J. Curran, *Toward the Development of a Fundamentally Based Chemical Model for Cyclopentanone: High-Pressure-Limit Rate Constants for H Atom Abstraction and Fuel Radical Decomposition.* The Journal of Physical Chemistry A, 2016. **120**(36): p. 7037-7044.

84. Koivisto, E., N. Ladommatos, and M. Gold, *Compression Ignition and Exhaust Gas Emissions of Fuel Molecules Which Can Be Produced from Lignocellulosic Biomass: Levulinates, Valeric Esters, and Ketones.* Energy & Fuels, 2015. **29**(9): p. 5875-5884.

85. Yang, Y. and J.E. Dec, *Bio-Ketones: Autoignition Characteristics and Their Potential as Fuels for HCCI Engines.* 2013.

86. Bao, X., Y. Jiang, H. Xu, C. Wang, T. Lattimore, and L. Tang, *Laminar flame characteristics of cyclopentanone at elevated temperatures.* Applied Energy, 2017. **195**: p. 671-680.

87. Lapuerta, M., Á. Ramos, J. Barba, and D. Fernández-Rodríguez, *Cold- and warm-temperature emissions assessment of n-butanol blends in a Euro 6 vehicle.* Applied Energy, 2018. **218**: p. 173-183.

88. Lapuerta, M., J. Rodríguez-Fernández, D. Fernández-Rodríguez, and R. Patiño-Camino, *Modeling viscosity of butanol and ethanol blends with diesel and biodiesel fuels.* Fuel, 2017. **199**: p. 332-338.

89. Lapuerta, M., J. Rodríguez-Fernandez, R. García-Contreras, and M. Bogarra, *Molecular interactions in blends of alcohols with diesel fuels: Effect on stability and distillation.* Fuel, 2015. **139**: p. 171-179.

90. Lapuerta, M., O. Armas, and J. Rodríguez-Fernández, *Effect of biodiesel fuels on diesel engine emissions.* Progress in Energy and Combustion Science, 2008. **34**(2): p. 198-223.

91. Pepiot-Desjardins, P., H. Pitsch, R. Malhotra, S.R. Kirby, and A.L. Boehman, *Structural group analysis for soot reduction tendency of oxygenated fuels.* Combustion and Flame, 2008. **154**(1): p. 191-205.

92. Kalghatgi, G., *Development of Fuel/Engine Systems—The Way Forward to Sustainable Transport.* Engineering, 2019.

93. Twigg, M.V., *Progress and future challenges in controlling automotive exhaust gas emissions.* Applied Catalysis B: Environmental, 2007. **70**(1): p. 2-15.

94. Liu, Q. and J.J. Schauer, *Local-acting Air Pollutant Emissions from Road Vehicles*, in *Environmental Impacts of Road Vehicles: Past, Present and Future*. 2017, The Royal Society of Chemistry. p. 46-85.

95. Herreros, J.M., P. George, M. Umar, and A. Tsolakis, *Enhancing selective catalytic reduction of NOx with alternative reactants/promoters.* Chemical Engineering Journal, 2014. **252**: p. 47-54.

96. Wang, W., J.M. Herreros, A. Tsolakis, and A.P.E. York, *Increased NO2 concentration in the diesel engine exhaust for improved Ag/Al2O3 catalyst NH3-SCR activity.* Chemical Engineering Journal, 2015. **270**: p. 582-589.

97. Katare, S.R., J.E. Patterson, and P.M. Laing, *Diesel Aftertreatment Modeling: A Systems Approach to NOx Control.* Industrial & Engineering Chemistry Research, 2007. **46**(8): p. 2445-2454.

98. Rankovic, N., A. Nicolle, D. Berthout, and P. Da Costa, *Kinetic Modeling Study of the Oxidation of Carbon Monoxide–Hydrogen Mixtures over Pt/Al2O3 and Rh/Al2O3 Catalysts.* The Journal of Physical Chemistry C, 2011. **115**(41): p. 20225-20236.

99. Hamedi, M.R., O. Doustdar, A. Tsolakis, and J. Hartland, *Thermal energy storage system for efficient diesel exhaust aftertreatment at low temperatures.* Applied Energy, 2019. **235**: p. 874-887.

100. Hamedi, M.R., A. Tsolakis, and J.M. Herreros, *Thermal Performance of Diesel Aftertreatment: Material and Insulation CFD Analysis*. 2014, SAE International.

101. Zhang, H., J. Baeyens, G. Cáceres, J. Degrève, and Y. Lv, *Thermal energy storage: Recent developments and practical aspects.* Progress in Energy and Combustion Science, 2016. **53**(Supplement C): p. 1-40.

102. Burch, S.D., T.F. Potter, M.A. Keyser, M.J. Brady, and K.F. Michaels, *Reducing Cold-Start Emissions by Catalytic Converter Thermal Management*. 1995, SAE International.

103. Kim, C.H., M. Paratore, E. Gonze, C. Solbrig, and S. Smith, *Electrically Heated Catalysts for Cold-Start Emissions in Diesel Aftertreatment*. 2012, SAE International.

104. Pfahl, U., A. Schatz, and R. Konieczny, *Advanced Exhaust Gas Thermal Management for Lowest Tailpipe Emissions - Combining Low Emission Engine and Electrically Heated Catalyst*. 2012, SAE International.

105. Socha, L.S. and D.F. Thompson, *Electrically Heated Extruded Metal Converters for Low Emission Vehicles*. 1992, SAE International.

106. Horng, R.-F., H.-M. Chou, and T.-C. Hsu, *Reaction of the electrically-heated catalyst of a four-stroke motorcycle engine under cold-start conditions with additional enrichment of the intake mixture.* Proceedings of the Institution of Mechanical Engineers, Part D: Journal of Automobile Engineering, 2003. **217**(12): p. 1117-1124.

107. PCS, *USV Ultra Shear Viscometer Brochure*. 2016: PCS Instruments.

108. Grunberg, L. and A.H. Nissan, *Mixture Law for Viscosity.* Nature, 1949. **164**: p. 799.

109. Solutions, S.L. *Bubble pressure method for measuring the dynamic surface tension*. 2017 [cited 2019 01/02/2019]; Available from: https://www.sita-lab.com/information-service/basics-about-sita-lab-solutions/surface-tension/bubble-pressure-method/.

110. Standard, A.N., *Standard Test Method for Heat of Combustion of Liquid Hydrocarbon Fuels by Bomb Calorimeter / ASTM D240-02*. 2007, ASTM International United States.

111. Publication, B.S., *Diesel fuel — Assessment of lubricity using the highfrequency reciprocating rig (HFRR)*, in *BS EN ISO 12156-1:2016*. 2016.

112. BSI, *BS EN ISO 12156-1:2006, Diesel Fuel, Assessment of lubricity using the high frequency reciprocationg rig (HFRR) Part 1. Test Method*. 2006.

113. Randolph, A.L., *Methods of Processing Cylinder-Pressure Transducer Signals to Maximize Data Accuracy*. 1990, SAE International.

114. GmbH, V.F.A.-u.M. *HSense, Hydrogen & Helium Mass Spectrometer*. [cited 2019 15/04/2019]; Available from: http://www.vandf.com/en/products/analyzers/hsense/.

115. Abou-Rachid, H., K.E. Marrouni, and S. Kaliaguine, *DFT studies of the hydrogen abstraction from primary alcohols by O2 in relation with cetane number data.* Journal of Molecular Structure: THEOCHEM, 2003. **631**(1): p. 241-250.

116. Yanowitz, J., M.A. Ratcliff, R.L. McCormick, J.D. Taylor, and M.J. Murphy, *Compendium of Experimental Cetane Numbers*. 2017, ; National Renewable Energy Lab. (NREL), Golden, CO (United States). p. Medium: ED; Size: 78 p.

117. Bruce E Pooling, John M. Prausnitz, and J.P. O'connel, *The properties of gases and liquids*. 5th edition ed. 2000, New York USA: McGraw-Hill.

118. Rajesh Kumar, B. and S. Saravanan, *Effects of iso-butanol/diesel and n-pentanol/diesel blends on performance and emissions of a DI diesel engine under premixed LTC (low temperature combustion) mode.* Fuel, 2016. **170**: p. 49-59.

119. Alptekin, E. and M. Canakci, *Determination of the density and the viscosities of biodiesel–diesel fuel blends.* Renewable Energy, 2008. **33**(12): p. 2623-2630.

120. Ali, O.M., R. Mamat, N.R. Abdullah, and A.A. Abdullah, *Analysis of blended fuel properties and engine performance with palm biodiesel–diesel blended fuel.* Renewable Energy, 2016. **86**: p. 59-67.

121. Wei, D.P., H.A. Spikes, and S. Korcek, *The Lubricity of Gasoline.* Tribology Transactions, 1999. **42**(4): p. 813-823.

122. Sukjit, E., M. Tongroon, N. Chollacoop, Y. Yoshimura, P. Poapongsakorn, M. Lapuerta, and K.D. Dearn, *Improvement of the tribological behaviour of palm biodiesel via partial hydrogenation of unsaturated fatty acid methyl esters.* Wear, 2019. **426-427**: p. 813-818.

123. Ophardt, C.E. *Hydrogen Bonding and the Boiling Point of Water*. 2003 [cited 2019 08/04/2019]; Available from: http://chemistry.elmhurst.edu/vchembook/163boilingpt.html.

124. Xu, Y., Y. Peng, K.D. Dearn, X. Zheng, L. Yao, and X. Hu, *Synergistic lubricating behaviors of graphene and MoS2 dispersed in esterified bio-oil for steel/steel contact.* Wear, 2015. **342–343**: p. 297-309.

125. Norouzi, S., F. Eslami, M.L. Wyszynski, and A. Tsolakis, *Corrosion effects of RME in blends with ULSD on aluminium and copper.* Fuel Processing Technology, 2012. **104**: p. 204-210.

126. Habibullah, M., H.H. Masjuki, M.A. Kalam, N.W.M. Zulkifli, B.M. Masum, A. Arslan, and M. Gulzar, *Friction and wear characteristics of Calophyllum inophyllum biodiesel.* Industrial Crops and Products, 2015. **76**: p. 188-197.

127. Li, L., J. Wang, Z. Wang, and H. Liu, *Combustion and emissions of compression ignition in a direct injection diesel engine fueled with pentanol.* Energy, 2015. **80**: p. 575-581.

128. Hellier, P., L. Al-Haj, M. Talibi, S. Purton, and N. Ladommatos, *Combustion and emissions characterization of terpenes with a view to their biological production in cyanobacteria.* Fuel, 2013. **111**: p. 670-688.

129. Anand, K., R.P. Sharma, and P.S. Mehta, *Experimental investigations on combustion, performance and emissions characteristics of neat karanji biodiesel and its methanol blend in a diesel engine.* Biomass and Bioenergy, 2011. **35**(1): p. 533-541.

130. Sharma, A. and S. Murugan, *Combustion, performance and emission characteristics of a DI diesel engine fuelled with non-petroleum fuel: A study on the role of fuel injection timing.* Journal of the Energy Institute, 2015. **88**(4): p. 364-375.

131. Schönborn, A., *Influence of the molecular structure of biofuels on combustion in a compression ignition engine*, in *Department of Mechanical Engineering*. 2009, University College London (UCL).

132. Cordiner, S., V. Mulone, M. Nobile, and V. Rocco, *Impact of biodiesel fuel on engine emissions and Aftertreatment System operation.* Applied Energy, 2016. **164**: p. 972-983.

133. Lapuerta, M., J. Rodríguez-Fernández, and J.R. Agudelo, *Diesel particulate emissions from used cooking oil biodiesel.* Bioresource Technology, 2008. **99**(4): p. 731-740.

134. Lapuerta, M., J.M. Herreros, L.L. Lyons, R. García-Contreras, and Y. Briceño, *Effect of the alcohol type used in the production of waste cooking oil biodiesel on diesel performance and emissions.* Fuel, 2008. **87**(15): p. 3161-3169.

135. Tsolakis, A., A. Megaritis, M.L. Wyszynski, and K. Theinnoi, *Engine performance and emissions of a diesel engine operating on diesel-RME (rapeseed methyl ester) blends with EGR (exhaust gas recirculation).* Energy, 2007. **32**(11): p. 2072-2080.

136. Wei, L., C.S. Cheung, and Z. Huang, *Effect of n-pentanol addition on the combustion, performance and emission characteristics of a direct-injection diesel engine.* Energy, 2014. **70**: p. 172-180.

137. Wei, L., C.S. Cheung, and Z. Ning, *Effects of biodiesel-ethanol and biodiesel-butanol blends on the combustion, performance and emissions of a diesel engine.* Energy, 2018. **155**: p. 957-970.

138. Kim, D., I. Ekoto, W.F. Colban, and P.C. Miles, *In-cylinder CO and UHC Imaging in a Light-Duty Diesel Engine during PPCI Low-Temperature Combustion*. 2008, SAE International.

139. Hellier, P., N. Ladommatos, R. Allan, S. Filip, and J. Rogerson, *The importance of double bond position and cis–trans isomerisation in diesel combustion and emissions.* Fuel, 2013. **105**: p. 477-489.

140. Chen, Z., Z. Wu, J. Liu, and C. Lee, *Combustion and emissions characteristics of high n-butanol/diesel ratio blend in a heavy-duty diesel engine and EGR impact.* Energy Conversion and Management, 2014. **78**: p. 787-795.

141. Pinzi, S., P. Rounce, J.M. Herreros, A. Tsolakis, and M. Pilar Dorado, *The effect of biodiesel fatty acid composition on combustion and diesel engine exhaust emissions.* Fuel, 2013. **104**: p. 170-182.

142. Cataluna, R. and R. da Silva, *Effect of Cetane Number on Specific Fuel Consumption and Particulate Matter and Unburned Hydrocarbon Emissions from Diesel Engines.* Journal of Combustion, 2012. **2012**: p. 6.

143. Hellier, P., N. Ladommatos, R. Allan, and J. Rogerson, *The Influence of Fatty Acid Ester Alcohol Moiety Molecular Structure on Diesel Combustion and Emissions.* Energy & Fuels, 2012. **26**(3): p. 1912-1927.

144. Park, W., S. Park, R.D. Reitz, and E. Kurtz, *The effect of oxygenated fuel properties on diesel spray combustion and soot formation.* Combustion and Flame, 2017. **180**: p. 276-283.

145. Koivisto, E., N. Ladommatos, and M. Gold, *The influence of various oxygenated functional groups in carbonyl and ether compounds on compression ignition and exhaust gas emissions.* Fuel, 2015. **159**: p. 697-711.

146. Lefort, I., J.M. Herreros, and A. Tsolakis, *Reduction of Low Temperature Engine Pollutants by Understanding the Exhaust Species Interactions in a Diesel Oxidation Catalyst.* Environmental Science & Technology, 2014. **48**(4): p. 2361-2367.

147. Patterson, M.J., D.E. Angove, and N.W. Cant, *The effect of carbon monoxide on the oxidation of four C6 to C8 hydrocarbons over platinum, palladium and rhodium.* Applied Catalysis B: Environmental, 2000. **26**(1): p. 47-57.

148. Salomons, S., M. Votsmeier, R.E. Hayes, A. Drochner, H. Vogel, and J. Gieshof, *CO and H2 oxidation on a platinum monolith diesel oxidation catalyst.* Catalysis Today, 2006. **117**(4): p. 491-497.

149. Lafossas, F., Y. Matsuda, A. Mohammadi, A. Morishima, M. Inoue, M. Kalogirou, G. Koltsakis, and Z. Samaras, *Calibration and Validation of a Diesel Oxidation Catalyst Model: from Synthetic Gas Testing to Driving Cycle Applications.* SAE International Journal of Engines, 2011. **4**(1): p. 1586-1606.

150. Diehl, F., J. Barbier, D. Duprez, I. Guibard, and G. Mabilon, *Catalytic oxidation of heavy hydrocarbons over Pt/Al2O3. Influence of the structure of the molecule on its reactivity.* Applied Catalysis B: Environmental, 2010. **95**(3): p. 217-227.

151. Yao, Y.-F.Y., *Oxidation of Alkanes over Noble Metal Catalysts.* Industrial & Engineering Chemistry Product Research and Development, 1980. **19**(3): p. 293-298.

152. Jung, J., S. Song, and K.M. Chun, *Characterization of Catalyzed Soot Oxidation with NO2, NO and O2 using a Lab-Scale Flow Reactor System*. 2008, SAE International.

153. Irani, K., W.S. Epling, and R. Blint, *Effect of hydrocarbon species on no oxidation over diesel oxidation catalysts.* Applied Catalysis B: Environmental, 2009. **92**(3): p. 422-428.

154. Sharma, H. and A. Mhadeshwar, *A detailed microkinetic model for diesel engine emissions oxidation on platinum based diesel oxidation catalysts (DOC).* Applied Catalysis B: Environmental, 2012. **127**: p. 190-204.

155. Tighe, C.J., M.V. Twigg, A.N. Hayhurst, and J.S. Dennis, *The kinetics of oxidation of Diesel soots by NO2.* Combustion and Flame, 2012. **159**(1): p. 77-90.

156. Chong, J.J., A. Tsolakis, S.S. Gill, K. Theinnoi, and S.E. Golunski, *Enhancing the NO2/NOx ratio in compression ignition engines by hydrogen and reformate combustion, for improved aftertreatment performance.* International Journal of Hydrogen Energy, 2010. **35**(16): p. 8723-8732.

157. Hjuler, K., P. Glarborg, and K. Dam-Johansen, *Mutually Promoted Thermal Oxidation of Nitric Oxide and Organic Compounds.* Industrial & Engineering Chemistry Research, 1995. **34**(5): p. 1882-1888.

158. Lilik, G.K., H. Zhang, J.M. Herreros, D.C. Haworth, and A.L. Boehman, *Hydrogen assisted diesel combustion.* International Journal of Hydrogen Energy, 2010. **35**(9): p. 4382-4398.

159. Olsson, L., B. Westerberg, H. Persson, E. Fridell, M. Skoglundh, and B. Andersson, *A Kinetic Study of Oxygen Adsorption/Desorption and NO Oxidation over Pt/Al2O3 Catalysts.* The Journal of Physical Chemistry B, 1999. **103**(47): p. 10433-10439.

160. Boubnov, A., S. Dahl, E. Johnson, A.P. Molina, S.B. Simonsen, F.M. Cano, S. Helveg, L.J. Lemus-Yegres, and J.-D. Grunwaldt, *Structure–activity relationships of Pt/Al2O3 catalysts for CO and NO oxidation at diesel exhaust conditions.* Applied Catalysis B: Environmental, 2012. **126**: p. 315-325.

161. Hauff, K., U. Tuttlies, G. Eigenberger, and U. Nieken, *Platinum oxide formation and reduction during NO oxidation on a diesel oxidation catalyst – Experimental results.* Applied Catalysis B: Environmental, 2012. **123-124**: p. 107-116.

162. Wang, T.J., S.W. Baek, and J.-H. Lee, *Kinetic Parameter Estimation of a Diesel Oxidation Catalyst under Actual Vehicle Operating Conditions.* Industrial & Engineering Chemistry Research, 2008. **47**(8): p. 2528-2537.

163. Shrivastava, M., A. Nguyen, Z. Zheng, H.-W. Wu, and H.S. Jung, *Kinetics of Soot Oxidation by NO2.* Environmental Science & Technology, 2010. **44**(12): p. 4796-4801.

164. Thomas, J.F., S.A. Lewis, B.G. Bunting, J.M. Storey, R.L. Graves, and P.W. Park, *Hydrocarbon Selective Catalytic Reduction Using a Silver-Alumina Catalyst with Light Alcohols and Other Reductants*. 2005, SAE International.

165. Yang, J.-I. and H. Jung, *The effect of temperature on NOx reduction by H2 in the presence of excess oxygen on a Pt/Al2O3 monolithic catalyst.* Chemical Engineering Journal, 2009. **146**(1): p. 11-15.